

**CHARACTERIZATION OF *P. AERUGINOSA* MAJOR AND MINOR  
PILINS**

**STRUCTURAL AND FUNCTIONAL CHARACTERIZATION OF  
*PSEUDOMONAS AERUGINOSA* MAJOR AND MINOR PILINS**

By

**YLAN NGUYEN, B.Sc.**

A Thesis Submitted to the School of Graduate Studies in Partial Fulfillment  
of the Requirements for the Degree

Doctor of Philosophy

McMaster University © Copyright by Ylan Nguyen, April 2015

McMaster University DOCTOR OF PHILOSOPHY (2015)  
Hamilton, Ontario (Biochemistry and Biomedical Sciences)

TITLE: Structural and functional characterization of *Pseudomonas aeruginosa* major and minor pilins

AUTHOR: Ylan Nguyen, B.Sc. (McMaster University)

SUPERVISOR: Dr. Lori L. Burrows

NUMBER OF PAGES: xv, 194

## **LAY ABSTRACT**

*Pseudomonas aeruginosa* is a bacterium that can take advantage of a weakened immune system to cause lethal infections. The first step of infection involves attachment to the host using long sticky fibres called type IV pili. Each fibre is composed primarily of a single protein, the major pilin, but also contains low abundance proteins called minor pilins. Without these proteins, the bacteria can't attach and cause infections, making pilins excellent vaccine candidates. This study focused on the characterization of major and minor pilins to understand the diversity of these proteins and how these differences might affect pilus assembly. We show that the molecular structure of the major pilin differs between strains although the core architecture is the same, and that the minor pilins are required for initiation of pilus assembly. This work furthers our understanding of the structures and functions of pilin proteins, and provides information helpful for the development of vaccines.

## **ABSTRACT**

Type IV pili (T4P) are long, fibrous surface appendages involved in attachment, motility, biofilm formation and DNA uptake that are expressed by bacteria and archaea. They are an important virulence factor for a number of bacteria, including *Pseudomonas aeruginosa*, an opportunistic pathogen that is a common cause of nosocomial infections. T4P are composed mainly of monomers of the major pilin subunit, PilA, although several low abundance proteins called minor pilins are also present. These surface-exposed proteins are potential vaccine candidates, although a more complete understanding of their diversity and function is required for the rational development of a pilus-based vaccine. There are five distinct groups of *P. aeruginosa* major pilins, which vary based on their sequence and their associated accessory proteins, and two distinct sets of minor pilins, although the roles of the latter in pilus biology are poorly understood. This study focuses on the structural characterization of major and minor pilins and functional implications for pilus assembly and disassembly dynamics. The structural analysis of major pilins from groups III and V revealed specific differences in pilin structure that may affect subunit interactions within the pilus fibre and interactions with their specific accessory proteins and minor pilins. The minor pilins PilVWX were shown to form a putative subcomplex with the adhesin and anti-retraction protein PilY1, which is proposed to prime pilus assembly and thus traffic PilY1 to

the bacterial surface. High resolution X-ray crystal structures of the minor pilins FimU and PilE were solved and functional characterization suggested that FimU and PilE are necessary for efficient pilus assembly to stably connect the priming subcomplex to the major pilin subunits. Together, this work has increased our understanding of pilin diversity and defined a concrete role for the minor pilins in pilus assembly.

## **ACKNOWLEDGEMENTS**

I would like to sincerely thank my supervisor Dr. Lori Burrows for guiding me and supporting me throughout all these years. I would not be the scientist and person I am today without you as my mentor. You've taught me to critically analyze my data, to look at the bigger picture and to not get married to my hypothesis. Thank you for encouraging me to do something new and scary everyday to push my limits and grow. I appreciate all the reminders to relax and that as a perfectionist I am probably harder on myself than I need to be.

I would also like to thank Dr. Murray Junop for taking me on as an undergraduate thesis student and inspiring me to continue with graduate research. You've been way beyond a collaborator to me but more a co-supervisor, always available and willing to help me understand my proteins and to suggest new ideas to try. I wouldn't have all these crystal structures in my thesis without you. I'd also like to thank you for all the general conversations about life and science, that there is more to life than what is within the walls of the lab.

To Dr. Justin Nodwell, thank you for being on my committee all these years and putting up with the alphabet soup. You have challenged me to better explain my data and ideas. Thank you for pushing me past my limits to become a stronger person and better scientist.

Thank you to the members of the Junop lab who have helped me over the years. Sean, you took a chance on me as an undergrad and trained me well for graduate studies. I am grateful for that experience. Sean and Seiji, thank you for taking the time to solve these pilin structures and to teach me along the way. Thank you Mac for tutoring me and helping me understand crystallography.

Thank you to all the past and present members of the Burrows lab. I couldn't have asked for better people to work with everyday. You've all supported me on those bad science days and celebrated with me on the good days. I am lucky to call you all my friends. Hanjeong, thank you so much for everything you've done for me, I wouldn't be here without you. Your love and support has truly been invaluable. To Uyen, Sara and Ryan, thank you for all the talks and for the adventures both inside and out of the lab. To the H-Os: to the moon and back, to the moon and back. I'd like to also thank all the students I have had the privilege of supervising, thank you for working so hard and living up to my standards.

I have to thank my wonderful family for their love and support over this long journey. I couldn't have done it without your constant encouragement and strength. Lastly, to my friends and those who have prayed for me from near and far, thank you for walking with me throughout this journey.

## TABLE OF CONTENTS

<b>LAY ABSTRACT</b> .....	<b>iii</b>
<b>ABSTRACT</b> .....	<b>iv</b>
<b>ACKNOWLEDGEMENTS</b> .....	<b>vi</b>
<b>TABLE OF CONTENTS</b> .....	<b>viii</b>
<b>LIST OF FIGURES</b> .....	<b>xi</b>
<b>LIST OF TABLES</b> .....	<b>xiii</b>
<b>LIST OF ABBREVIATIONS</b> .....	<b>xiv</b>
<b>CHAPTER ONE - Introduction</b> .....	<b>1</b>
<b>Preface</b> .....	<b>2</b>
<b>Overview</b> .....	<b>3</b>
<b>Classification of type IV pili</b> .....	<b>4</b>
<b>Twitching motility</b> .....	<b>5</b>
The T4P assembly system.....	6
<b>Major pilins</b> .....	<b>7</b>
Processing of major pilins.....	8
Structure of pilins.....	9
The N-terminal $\alpha$ -helix.....	12
The $\beta$ -sheet.....	13
The $\alpha\beta$ -loop.....	14
The D-region.....	15
<i>P. aeruginosa</i> pilin diversity.....	18
<b>The pilus fibre</b> .....	<b>22</b>
Pilus models.....	22
The mechanism of pilus assembly.....	25
<b>Minor pilins</b> .....	<b>29</b>
Minor pilin diversity.....	30
Function of <i>P. aeruginosa</i> minor pilins in pilus assembly.....	31
Other function of minor pilins.....	34
The pilus-associated protein, PilY1.....	37
<b>Hypothesis and research aims</b> .....	<b>39</b>
<b>CHAPTER TWO – Structural characterization of novel <i>Pseudomonas aeruginosa</i> type IV pilins</b> .....	<b>42</b>
<b>Preface</b> .....	<b>43</b>
<b>Title page and author list</b> .....	<b>44</b>
<b>Abstract</b> .....	<b>45</b>
<b>Introduction</b> .....	<b>46</b>
<b>Results and Discussion</b> .....	<b>51</b>
Structure of group V Pa110594 PilA.....	51
Comparison of PilA <sub>0594</sub> with T4a and T4b pilins.....	59

Implications for pilus structure .....	62
Sequence and structural homology with group III PA14 PilA .....	65
<b>Conclusions</b> .....	<b>68</b>
<b>Materials and methods</b> .....	<b>69</b>
Expression and purification of recombinant PilA <sub>0594</sub> .....	69
Crystallization and X-ray diffraction data collection .....	71
PilA <sub>0594</sub> X-ray crystal structure determination and refinement .....	71
Electron microscopy of <i>P. aeruginosa</i> Pa110594.....	72
PilA <sub>0594</sub> pilus models .....	73
PilA <sub>PA14</sub> model .....	73
PDB accession codes.....	73
<b>Acknowledgements</b> .....	<b>74</b>

<b>CHAPTER THREE – <i>Pseudomonas aeruginosa</i> minor pilins prime type IVa pilus assembly and promote surface display of the PilY1 adhesin</b> .....	<b>75</b>
<b>Preface</b> .....	<b>76</b>
<b>Title page and author list</b> .....	<b>77</b>
<b>Abstract</b> .....	<b>78</b>
<b>Introduction</b> .....	<b>79</b>
<b>Experimental procedures</b> .....	<b>84</b>
Strains and growth conditions.....	84
Generation of mutants and complementation constructs .....	85
Isolation of sheared surface proteins, SDS-PAGE analysis .....	85
Western blot analysis of sheared surface fractions .....	86
Interaction of FimU with PilA and minor pilins .....	86
Expression and purification of FimU, PilV and PilX .....	87
Structure determination .....	89
<b>Results</b> .....	<b>91</b>
PilVWX and PilY1 are dependent on one another for incorporation into pili .....	91
FimU interacts with the major pilin and specific minor pilins.....	93
High resolution crystal structure of FimU.....	93
FimU is structurally similar to T2S minor pseudopilin GspH.....	95
Type IVa pilus assembly can be primed by minor pseudopilins ....	98
A subset of minor components can prime assembly .....	102
<b>Discussion</b> .....	<b>103</b>
Identification of a putative minor pilin-PilY1 complex.....	103
The putative connector subunit, FimU .....	106
Minor subunits prime pilus assembly.....	108
Minor subunits are part of the pilus filament .....	109
Minor pseudopilins cannot replace minor pilins when retraction is active .....	110
<b>Acknowledgements</b> .....	<b>112</b>

<b>CHAPTER FOUR – Structural and functional studies of the</b>	
<i>Pseudomonas aeruginosa</i> minor pilin, PilE .....	<b>113</b>
<b>Preface</b> .....	<b>114</b>
<b>Title page and author list</b> .....	<b>115</b>
<b>Abstract</b> .....	<b>116</b>
<b>Introduction</b> .....	<b>117</b>
<b>Experimental procedures</b> .....	<b>121</b>
Bacterial strains and plasmids .....	121
Bacterial adenylate cyclase two-hybrid assay .....	122
Protein expression and purification.....	123
Crystallization and structure determination.....	124
Construction of fluorescently tagged PilE .....	125
Twitching motility assay .....	125
Sheared surface protein preparation .....	126
Intracellular PilE protein levels.....	127
Fluorescence microscopy .....	127
<b>Results</b> .....	<b>128</b>
PilE interacts with major and minor pilins .....	128
The high-resolution crystal structure of PilE reveals characteristic pilin architecture.....	129
Comparison of PilE and PilX <sub>Nm</sub> structures .....	133
PilV <sub>Nm</sub> is predicted to be structurally similar to PilE .....	135
PilE incorporation into pili is necessary for function.....	137
<b>Discussion</b> .....	<b>141</b>
<b>Acknowledgements</b> .....	<b>145</b>
<b>CHAPTER FIVE – Summary and Conclusions</b> .....	<b>150</b>
<b>Summary of findings</b> .....	<b>151</b>
Structure of PilA <sub>0594</sub> .....	151
Role of minor pilins in pilus assembly .....	154
<b>Future directions</b> .....	<b>156</b>
PilA-accessory protein interactions.....	156
Minor pilin-PilY1 interaction studies .....	157
Surface localization of PilY1 .....	158
<b>Significance and Conclusions</b> .....	<b>160</b>
<b>REFERENCES</b> .....	<b>161</b>

## LIST OF FIGURES

<b>CHAPTER ONE - Introduction</b> .....	<b>1</b>
Figure 1.1 Polar T4P of <i>P. aeruginosa</i> .....	4
Figure 1.2 Simplified model of the <i>P. aeruginosa</i> T4P system .....	7
Figure 1.3 Protein sequence alignment of conserved N-termini of T4P major pilins .....	8
Figure 1.4 Structure of T4P major pilins.....	11
Figure 1.5 Pilin diversity in <i>P. aeruginosa</i> .....	19
Figure 1.6 T4aP and T4bP fibre models .....	24
Figure 1.7 Structure of T2S major pseudopilin and pseudopilus model .....	27
Figure 1.8 Genetic organization of minor pilins and minor pseudopilins in <i>P. aeruginosa</i> .....	29
<b>CHAPTER TWO – Structural characterization of novel <i>Pseudomonas aeruginosa</i> type IV pilins</b> .....	<b>42</b>
Figure 2.1 Pilin modification and assembly systems in <i>P. aeruginosa</i> .....	49
Figure 2.2 Structure of <i>P. aeruginosa</i> PilA <sub>0594</sub> .....	54
Figure 2.3 B-factor analysis of PilA <sub>0594</sub> structures .....	57
Figure 2.4 Comparison of PilA <sub>0594</sub> with T4a and T4b pilins .....	61
Figure 2.5 Comparison of T4aP and T4bP-based 0594 pilus homology models .....	63
Figure 2.6 Comparison of group III and group V pilins.....	66
<b>CHAPTER THREE – <i>Pseudomonas aeruginosa</i> minor pilins prime type IVa pilus assembly and promote surface display of the PilY1 adhesin</b> .....	<b>75</b>
Figure 3.1 Gene organization of T4P and T2S minor components.....	82
Figure 3.2 Incorporation of minor pilins into pili .....	92
Figure 3.3 Interaction of FimU with major pilin and minor pilins.....	94
Figure 3.4 Crystal structure of FimU <sub>Δ1-28</sub> .....	96
Figure 3.5 Structural comparison of FimU and T2S pseudopilin GspH .....	97
Figure 3.6 Pilus assembly in the absence of minor components .....	101
Figure 3.7 Model of pilus assembly.....	103
Figure 3.8 Comparison of loops in FimU, PilH <sub>Nm</sub> , and EpsH .....	107
<b>CHAPTER FOUR – Structural and functional studies of the <i>Pseudomonas aeruginosa</i> minor pilin, PilE</b> .....	<b>113</b>
Figure 4.1 Interactions of PilE with minor pilins and PilA .....	129
Figure 4.2 X-ray crystal structure of PilE <sub>Δ1-28</sub> .....	131
Figure 4.3 Comparison of PilE <sub>Δ1-28</sub> with <i>N. meningitidis</i> PilX <sub>Nm</sub> .....	134

Figure 4.4	Complementation of <i>pilE</i> with PilE mCherry .....	138
Figure 4.5	Pilus assembly by PilE mCherry in a retraction-deficient background .....	140
Figure S4.1	Sequence alignment of PilE with PilX <sub>Nm</sub> and PilV <sub>Nm</sub> .....	146

## LIST OF TABLES

<b>CHAPTER TWO – Structural characterization of novel <i>Pseudomonas aeruginosa</i> type IV pilins .....</b>	<b>42</b>
Table 2.1 0594 PilA crystallographic and data refinement statistics...	52
<b>CHAPTER THREE – <i>Pseudomonas aeruginosa</i> minor pilins prime type IVa pilus assembly and promote surface display of the PilY1 adhesin .....</b>	<b>75</b>
Table 3.1 Data collection and refinement statistics.....	90
<b>CHAPTER FOUR – Structural and functional studies of the <i>Pseudomonas aeruginosa</i> minor pilin, PilE .....</b>	<b>113</b>
Table 4.1 Strains and plasmids used in this study.....	147
Table 4.2 PilE data collection and refinement statistics.....	149

## LIST OF ABBREVIATIONS

A	absorbance
Ala	alanine
Ap	ampicillin
BCIP	5-bromo-4-chloro-3-indolylphosphate
C-terminal	carboxyl-terminal
CTD	C-terminal domain
Cys	cysteine
DSL	disulphide bonded loop
DNA	deoxyribonucleic acid
DXMS	hydrogen/deuterium exchange mass spectrometry
EM	electron microscopy
g	gravity
GC	gonococcal
Gm	gentamicin
Glu	glutamic acid
Gly	glycine
h	hour(s)
IgG	immunoglobulin G
IPTG	isopropyl $\beta$ -D-thiogalactopyranoside
K	Kelvin
kb	kilobase
kDa	kilodaltons
kV	kilovolts
LB	Luria-Bertani medium
LDAO	lauryldimethylamine-oxide
Leu	leucine
LES	Liverpool epidemic strain
Met	methionine
min	minute(s)
MS	mass spectrometry
N-terminal	amino-terminal
NBT	nitro-blue tetrazolium
NMR	Nuclear magnetic resonance
NTD	N-terminal domain
OD	optical density

ORF	open reading frame
PCR	polymerase chain reaction
PDB	Protein Data Bank
PEG	polyethylene glycol
pH	power of hydrogen
Phe	phenylalanine
Pro	proline
RMSD	root mean square deviation
s	second
SAD	single-wavelength anomalous dispersion
SDS	sodium dodecyl sulfate
SeMet	selenomethionine
T2S	type II secretion
T4P	type IV pili/pilus
T4aP	type IV a pili/pilus
T4bP	type IV b pili/pilus
TCP	toxin-coregulated pili/pilus
TEV	tobacco etch virus
tRNA	transfer ribonucleic acid
Val	valine

# **CHAPTER ONE**

## **Introduction**

**Preface:**

Chapter One consists of parts adapted from the following publication:

**Giltner, CL, Nguyen Y and Burrows LL.** 2012. Type IV pilin proteins: versatile molecular modules. *Microbiol. Mol. Biol. Rev.* 76:740-772.

Sections and figures used here were written and made primarily by Y.N. and L.L.B.

Copyright © American Society for Microbiology, *Microbiology and Molecular Biology Reviews*, volume 76, 2012, 740-772, DOI: 10.1128/MMBR.00035-12

## Overview

Type IV pili (T4P) are long, thin protein fibers and are among the most widespread multi-functional prokaryotic surface structures (19, 141) (Figure 1.1). They are expressed by gram-negative bacteria such as *Pseudomonas aeruginosa* (179), *Neisseria meningitidis* (165) and *Vibrio cholerae* (174); gram-positive bacteria such as *Clostridium perfringens* (175); as well as archaeal species such as *Methanococcus maripaludis* (128). T4P are involved in a variety of functions, including attachment to surfaces (68, 153, 155), flagella-independent twitching motility (25, 122, 160), biofilm formation (134), phage adsorption (24), DNA uptake (63, 166) and electron transfer (151).

Type IV pili are an important virulence factor for bacteria (49) including *P. aeruginosa*, an opportunistic pathogen and common cause of nosocomial infections (22, 115). *P. aeruginosa* is a cause of chronic infections in the lungs of cystic fibrosis patients, contributing to their mortality (116, 126). As surface exposed proteins, the pilin subunits are excellent vaccine candidates, although a full understanding of their diversity is necessary for the rational development of a broadly protective pilus-based vaccine. This thesis explores the structural diversity of pilin subunits and the related functional implications for pilus assembly and disassembly dynamics of *P. aeruginosa* T4P.



**Figure 1.1. Polar T4P of *P. aeruginosa*.** The pole of a hyperpilated strain of *P. aeruginosa* visualized by transmission electron microscopy. *P. aeruginosa* has a single polar flagellum (closed arrow) and single pilus fibres (open arrow) and bundled pili. Scale bar represents 0.5  $\mu\text{m}$ . Image courtesy of Poney Chiang.

### **Classification of type IV pili**

There are two classes of T4P: type IVa (T4aP) and type IVb (T4bP) (168). The T4aP class is widely distributed among plant, animal and human pathogens such as *Pseudomonas*, *Dichelobacter* and *Neisseria* while T4bP are found mainly in enteric bacteria such as enteropathogenic *E. coli*, *Salmonella typhi* and *Vibrio cholerae* (49, 141). T4b pili include the Flp or Tad subclass of T4P, first identified in *Aggregatibacter actinomycetemcomitans* and found in other gram-negatives (85). Pili in

gram-positive bacteria such as *Clostridia* have features of both T4aP and T4bP, suggesting both may have evolved from a common gram-positive precursor (121). Interestingly, *P. aeruginosa* is currently the only species in which T4aP, T4bP and Tad systems are encoded by a single strain (18, 37, 52); however, the T4aP system is the best characterized to date.

Members of the two subclasses were initially separated based on size and sequence of their major pilin proteins (49, 168); however, each subclass is now appreciated to have characteristic differences in the architecture and complexity of their respective pilus assembly machineries (14, 30). The T4aP subclass has been extensively characterized in *Pseudomonas*, *Neisseria*, *Thermus*, and *Myxococcus*, the predominant genera used as model systems due to their tractability and for the first two, medical significance (30, 123). The T4aP of *P. aeruginosa* are the focus of this thesis.

### **Twitching motility**

T4P were initially described as flexible microbial surface fibers capable of mediating flagellar-independent motility, called twitching motility (104, 136). This form of motility, associated mainly with the T4aP class, typically occurs on moist surfaces and involves the repeated extension, surface attachment and retraction of T4P, which moves the cell toward the point of pilus attachment (25). Twitching motility typically occurs in groups

of cells, called a “raft”, although individual twitching cells have been observed. Optical tweezer measurements on single cells suggested the retraction forces exerted by one T4P exceeds 100 pN, making their molecular motors among the strongest yet identified (117).

### *The T4P assembly system*

The regulation, assembly and disassembly of surface pili in *P. aeruginosa* involves over 50 genes (81). A subset of proteins involved in the T4P system are depicted in Figure 1.2. T4P are composed of thousands of copies of a single protein, called the major pilin PilA. The pilins are initially translated as pre-pilins and are processed into mature pilins by a dedicated peptidase (PilD) prior to assembly (133). The major pilin subunits do not spontaneously assemble but are polymerized into a fibre in the periplasm using energy provided by the cytoplasmic extension ATPase PilB (180) and extrude through the outer membrane via a PilQ secretin pore (20). T4aP are unique in their ability to retract back into the cell through their depolymerisation at the base of the filament, powered by the retraction ATPase PilT, a process that drives twitching motility (180). The outer membrane secretin and the inner membrane motor subcomplexes are connected through the alignment subcomplex (106). Mutants lacking *pilB* are non-piliated (131), while mutants lacking *pilT* are hyperpiliated (180), showing that pilus extension and retraction are

independent processes.

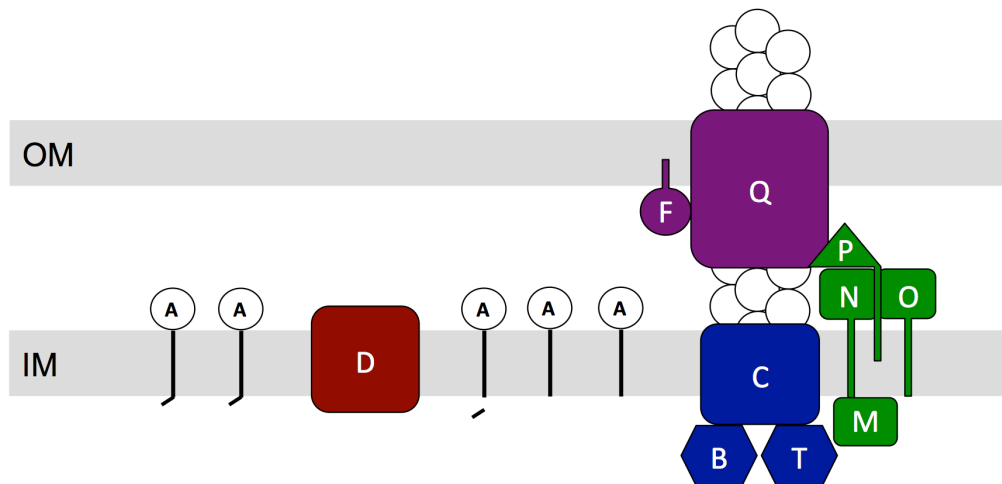


**Figure 1.2. Simplified model of the *P. aeruginosa* T4P system.** PilA subunits are expressed as pre-pilins and processed by the pre-pilin peptidase PilD (red). The mature pilins are polymerized and depolymerized by the inner membrane motor subcomplex (blue) and exit the cell through the outer membrane secretin subcomplex (purple). The inner membrane and outer membrane subcomplexes are connected through the alignment subcomplex (green). Figure adapted from (107).

### Major pilins

The major pilin subunits are small 15-20 kDa proteins that assemble into strong micrometre length fibres that mediate a number of diverse functions (59). The understanding of these proteins and how they polymerize is vital to understand the diversity of T4P functions, and to design therapeutics against these virulence factors.

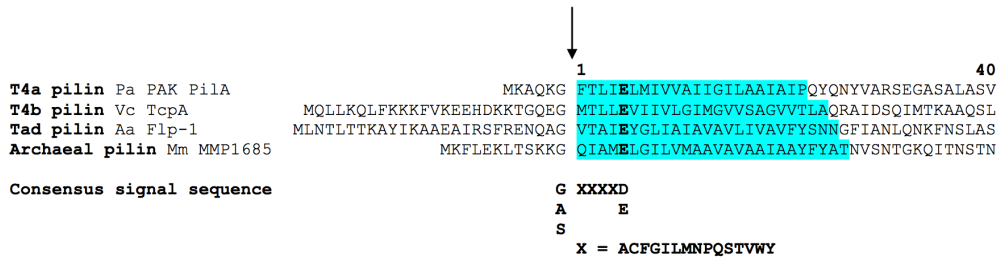


**Figure 1.3. Protein sequence alignment of conserved N-termini of T4P major pilins.** Multiple sequence alignment of the first 40 amino acids of representative T4a, T4b, Tad and archaeal mature major pilins with their basic leader peptides. Pilin proteins share the type III signal sequence, which is cleaved between the Gly-1 and Phe1 residues, although the +1 residue can vary. The consensus signal sequence used by the PilFind algorithm (79) to identify putative type IV pilin proteins is shown below the alignment. The highly conserved Glu5 residue is shown in bold. The transmembrane segments, as predicted by Geneious Pro v5.0.3 (Biomatters Ltd.) using TMHMM, are highlighted in cyan. Pa, *P. aeruginosa*; Vc, *V. cholerae*; Aa, *Aggregatibacter (Actinobacillus) actinomycetemcomitans*; Mm, *Methanococcus maripaludis*. Figure adapted from (66).

### *Processing of major pilins*

T4P pre-pilins are inserted into the inner membrane by the Sec system, resulting in their orientation with the N-termini embedded in the membrane and the C-terminal domains in the periplasm (10, 62). Pilins are characterized by a highly conserved, hydrophobic N-terminal segment preceded by a positively-charged type III signal sequence (171), which differs from type I and type II signal sequences by its cleavage on the

cytoplasmic side of the inner membrane (Figure 1.3) (167). Pre-pilins are not competent for assembly until the leader sequence is cleaved, resulting in mature pilins (167). The recently developed PilFind and FlaFind algorithms exploit this characteristic type III signal sequence motif to identify putative pilin-encoding genes in bacterial and archaeal genomes (79, 171).

Among the key features that distinguishes T4a and T4b pilins are their leader sequences. T4a leader sequences are typically short (6-7 residues) while the T4bP class have longer leader peptides (15-30 residues) (49). Cleavage is mediated by a dedicated aspartyl pre-pilin peptidase, which cleaves after a conserved Gly residue (133)(Figure 1.3), although Ala substitutions at this position are permissive (167). In T4a pilins, the first residue of the mature protein (at position +1) is usually a Phe, which is subsequently methylated by the same bifunctional pre-pilin peptidase enzyme (133, 169, 170). The methylated N-terminal residue of the mature T4b pilin is variable (Val, Leu or Met), which differentiates it from T4a pilins (49).

### *Structures of pilins*

Although the N-terminus of pilins with the characteristic type III signal sequence is well conserved across species, the rest of the protein is highly variable in sequence. Despite the sequence divergence, the

structures of pilins solved by X-ray crystallography and NMR spectroscopy reveal a common fold important for their assembly into pili (49).

Ironically, despite the high level of sequence conservation in the N-terminal segment of pilins and its critical importance to their function, it is frequently removed to facilitate structure determination. To date, there are seventeen major pilin structures of which only five are full-length structures, all from the T4a subclass (12, 15, 50, 51, 69, 71, 90, 94, 111, 129, 138, 144, 149, 150, 187). Truncation of the N-terminus does not appear to affect the pilin structure as the full-length and truncated *P. aeruginosa* PAK pilins were essentially structurally identical, with a root mean square deviation of 0.69 Å over all atoms (50).

From these structures, it is clear that type IV pilins have a characteristic architecture resembling a lollipop or ladle, with a long N-terminal  $\alpha$ -helix, the top half of which packs against the back of the C-terminal domain and a 4-7 stranded antiparallel  $\beta$ -sheet with loops of various sizes and configuration (Figure 1.4). Most T4 pilins have a disulphide bond that connects the C-terminus to the  $\beta$ -sheet, encompassing a region known as the disulphide-bonded loop (DSL) or D-region (49). The loop connecting the N-terminal  $\alpha$ -helix and the  $\beta$ -sheet – known as the  $\alpha\beta$ -loop – and the D-region vary between pilin structures, likely since they are exposed and involved in interactions between pilin subunits in the pilus fibre and therefore contribute significantly to the

structural diversity associated with these proteins. In support of specific inter-subunit interactions along the filament, heterologous expression of one pilin in a strain expressing another does not result in fibres of mixed composition (140).

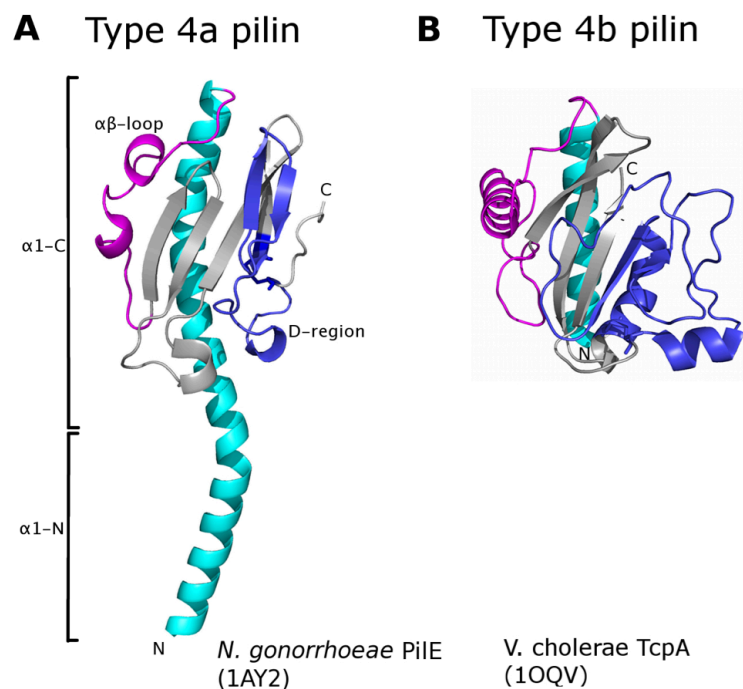


**Figure 1.4. Structure of T4 major pilins.** Type IV pilins have a conserved structural fold characterized by a long N-terminal  $\alpha$ -helix (cyan) connected to a core  $\beta$ -sheet (gray). Variable regions include the  $\alpha\beta$ -loop (magenta) that connects the  $\alpha$ -helix and  $\beta$ -sheet as well as the D-region (blue) that is formed by a disulphide bond between two cysteine residues in most T4 pilins. Full-length T4a pilin structure represented by *N. gonorrhoeae* PilE (Protein Data Bank [PDB] code 1AY2) (A) and truncated T4b pilin structure represented by *V. cholerae* TcpA (PDB code 1OQV) (B) showing the difference in protein folding. Figures were prepared using MacPymol (DeLano Scientific). Figure adapted from (66).

### *The N-terminal $\alpha$ -helix*

The long N-terminal  $\alpha$ -helix can be subdivided into two segments:  $\alpha$ 1-N (residues ~ 1-28) and  $\alpha$ 1-C (residues ~29-52).  $\alpha$ 1-N extends from the C-terminal head domain and is mainly hydrophobic, embedding the pilin in the inner membrane prior to assembly. This segment also forms the central core of the assembled pilus fibre and interacts with other pilin subunits. The only charged residue in this region, a conserved Glu5, interacts with the positively charged N-terminus of the preceding pilin monomer in the pilus fibre, suggested to ensure proper helical registration between subunits during assembly (51). The importance of this residue was demonstrated in *N. gonorrhoeae* and *P. aeruginosa* where mutations of Glu5 prevented pilus assembly (1, 167).  $\alpha$ 1-C is amphipathic and packs against the back of the  $\beta$ -sheet to make up the globular C-terminal head domain.

The full-length structures of *P. aeruginosa* PAK PilA, *N. gonorrhoeae* PilE, and *Dichelobacter nodosus* FimA (50, 51, 69, 138) show that there is a shallow S-shaped curvature in the N-terminal helix of T4a pilins. Highly conserved Pro22 and Gly/Pro42 (Gly41 for *D. nodosus* FimA) residues introduce kinks in the  $\alpha$ -helix. The resulting curvature is thought to control the extent of inter-subunit packing, thereby contributing to the flexibility of the pilus fibre and possibly the dynamics of its disassembly (28, 50, 110, 138). Interestingly, the atypical T4a major pilin

of *Geobacter sulfurreducens* is short, only 61 residues compared to ~ 150 residues for other T4a pilins, 50 of which comprise  $\alpha 1$ , while the remainder are part of a short flexible C-terminal segment (150). The *G. sulfurreducens* pilin has Pro22 but has an Asn residue at position 42, and therefore lacks the S-shaped curve present in other T4a pilins. However, no interactions that might increase rigidity are predicted between the flexible C-terminal regions. Instead, the predicted *G. sulfurreducens* pilus fibre has exposed regions of clustered aromatic residues that are important for electron transfer along these nanowires (150, 176).

The T4b pilins lack the characteristic Pro or Gly residues (15, 50, 94, 149, 187), although a full-length structure has yet to be solved. The flexibility of T4bP is likely due predominantly to the presence of bulkier head groups on the surface of the pilus that have limited inter-subunit interactions, leaving gaps between them that expose parts of the N-terminal alpha helix to the solvent (110).

### *The $\beta$ -sheet*

The  $\beta$ -sheet of T4 pilins is a highly conserved feature that makes up the majority of the C-terminal head of the protein. In T4a pilins, the  $\beta$ -sheet is composed of four antiparallel  $\beta$ -strands with nearest neighbour connectivity (12, 50, 51, 69, 71, 90, 138). In the T4b pilins, the antiparallel  $\beta$ -sheet is composed of five to seven non-continuous  $\beta$ -strands for *V*.

*cholerae* TcpA and *S. typhi* PilS or a mixture of parallel and antiparallel  $\beta$ -strands for enteropathogenic *E. coli* BfpA (15, 50, 94, 111, 149, 187).

Similarly, the recently determined structure of the major pilin PilA1 from gram-positive bacterium *C. difficile* has non-nearest neighbour connectivity in its four-stranded antiparallel  $\beta$ -sheet, making it more similar to T4b pilins than T4a (144).

The loops between the  $\beta$ -strands of the C-terminal head domain vary in length, with shorter loops forming  $\beta$ -turn motifs, although they generally lack defined secondary structure. These loop regions are predicted to participate in subunit-subunit interactions within the pilus (48, 49, 51). Interestingly, the  $\beta$ -sheet loops of *C. difficile* PilA1 form a secondary two-stranded antiparallel  $\beta$ -sheet oriented at  $90^\circ$  to the central  $\beta$ -sheet; this feature is thought to replace the stabilizing disulphide bond of gram-negative T4 pilins (see below) (144).

### *The $\alpha\beta$ -loop*

Connecting the conserved N-terminal  $\alpha$ -helix and  $\beta$ -sheet is a hypervariable loop region, referred to as the  $\alpha\beta$ -loop in type IV pilin structures. This region is involved in subunit interactions within the pilus fibre (49). Since the  $\alpha\beta$ -loop is partially surface exposed, sequence differences in this region can alter the surface topology and chemistry of the pilus fibre (48), conferring strain and species specificity.

The  $\alpha\beta$ -loop can contain a minor  $\beta$ -sheet, as seen in the pilin of *P. aeruginosa* strain PAK; have helical character like those of *N. gonorrhoeae* and *P. aeruginosa* K122-4; or be irregular in structure like that of *D. nodosus* FimA (12, 50, 51, 69, 71, 90, 138). The  $\alpha\beta$ -loops of both *P. aeruginosa* K122-4 PilA and *D. nodosus* FimA contain disulphide bonds which connect the  $\alpha\beta$ -loop to  $\beta$ 2 (69, 90). In the pilin from *N. gonorrhoeae*, the  $\alpha\beta$ -loop is a site of post-translational modification with glycosylation at Ser63 and phosphoethanolamide or phosphocholine at Ser68, which alter the pilus surface and contribute to immune evasion (50, 51, 61, 72, 138).

Most T4b pilin structures have a prominent  $\alpha$ -helix in the  $\alpha\beta$ -loop that is oriented at  $\sim 90^\circ$  relative to  $\alpha$ 1 (50, 149) (15, 187). The  $\alpha$ -helix of T4b pilin CofA from enterotoxigenic *E. coli* is shorter than other T4b pilins and is preceded by a  $3_{10}$  helix (94).

### *The D-region*

The second hypervariable region associated with T4 pilins is at the C-terminal end, referred to as the D-region or disulphide-bonded loop (DSL). The name describes the segment captured by a disulphide bond between two highly conserved Cys that connects the C-terminus to the core  $\beta$ -sheet of the protein. Like the  $\alpha\beta$ -loop, the D-region is involved in intersubunit interactions along the pilus fibre (48, 49) but also has

important functional roles (see below). However, some major T4 pilins lack a C-terminal disulphide bond. Besides the additional  $\beta$ -sheet in the gram-positive pilin PilA1 from *C. difficile* that is thought to confer a similar level of stability (144), the gram-negative T4a pilin FimA of *D. nodosus* has a structure similar to other T4a pilins even in the absence of a C-terminal disulphide, stabilized by a network of non-covalent bonds (69).

In *P. aeruginosa*, the length of the D-region can vary from 12-29 residues (101). Similar sizes, typically less than 30 residues, are evident in other T4a pilin proteins (49). The D-region of T4a pilins typically starts at the end of the last  $\beta$ -strand of the core  $\beta$ -sheet and extends downwards before looping back up to form the disulphide bond. In *Neisseria* and *Pseudomonas* pilins, this loop has a two  $\beta$ -turns, two consecutive type I turns for *Neisseria* PilE and a type I turn followed by a type II turn for *Pseudomonas* PilA, implicated in receptor binding (below). With a D-region of 29 residues, *N. gonorrhoeae* PilE has an additional  $\beta$ -hairpin at the beginning of the D-region (138).

The T4b pilins have a much larger D-region at an average of 55 residues (49). The connectivity is different, with the disulphide bond loop starting within the core  $\beta$ -sheet and encompassing at least one of the  $\beta$ -strands (50). There are also two  $\alpha$ -helices within the D-region of T4b pilins. Specific point mutations in the D-region of *V. cholerae* TcpA prevented

bundling between pilus fibres suggesting they are important for lateral pilus-pilus interactions (84, 111).

The D-region plays an important structural role in pilin biology. Some reports suggested that mutating the Cys residues had a negative impact on pilin stability (111, 190) although in *P. aeruginosa*, this result could be due to poor recognition of mutant proteins by the antibody, since the DSL epitope is highly immunogenic (70). However, preventing the formation of a disulphide bond through mutation of either the Cys residues or the disulphide bond isomerases prevented pilus assembly (173, 190). The D-regions are involved in subunit-subunit interactions within the pilus fibre (see below) and thus may be important for fibre stability. Interestingly, treatment of both T4aP and T4bP with reducing agents completely disintegrated assembled pili, supporting this idea (109).

The D-region of *P. aeruginosa* has also been implicated as an adhesin, since D-region specific antibodies blocked attachment to a variety of different surfaces (71, 105). Its adhesiveness was attributed to surface-main chain interactions, to account for a common functional phenotype despite high sequence variability in this region (71). Given that antibodies to this segment were able to block function of T4P, a number of studies have investigated the vaccine potential of the D-region (31-33, 86, 87). These vaccines generated pilus specific antibodies that were cross-reactive with multiple strains, which provided protection from *P.*

*aeruginosa* challenge (32, 86). However, these studies were performed using data mainly from one group of pilin alleles (below).

### *P. aeruginosa* pilin diversity

Besides the structural diversity between major pilins of different subclasses and species, there is also a considerable amount of intraspecies pilin diversity. Each *P. aeruginosa* strain encodes one of five groups of phylogenetically distinct major pilins (PilA) between the *pilB* gene and a conserved *tRNA<sup>Thr</sup>* gene (101). The five groups (I-V) are distinguished by their pilin sequence, size, and length of the D-region, as well as the presence – or in the case of group II, the absence – of specific accessory protein genes, downstream of the pilin gene (101) (Figure 1.5). An understanding of this diversity is crucial for the development of a broadly protective pilus-based vaccine.

Most T4P studies, including structural characterizations, have used the common *P. aeruginosa* laboratory strains, PAK and PAO1, both of which are group II strains (12, 50, 71, 90). These pilin genes are more likely to be found in environmental strains than in strains infecting cystic fibrosis patients (101). Group II expresses the smallest pilins of the five (mature proteins of 143-148 residues) with the smallest D-region, and is the only one that lacks accessory genes (101). This group may represent an exception to the pilin repertoire of *P. aeruginosa*.

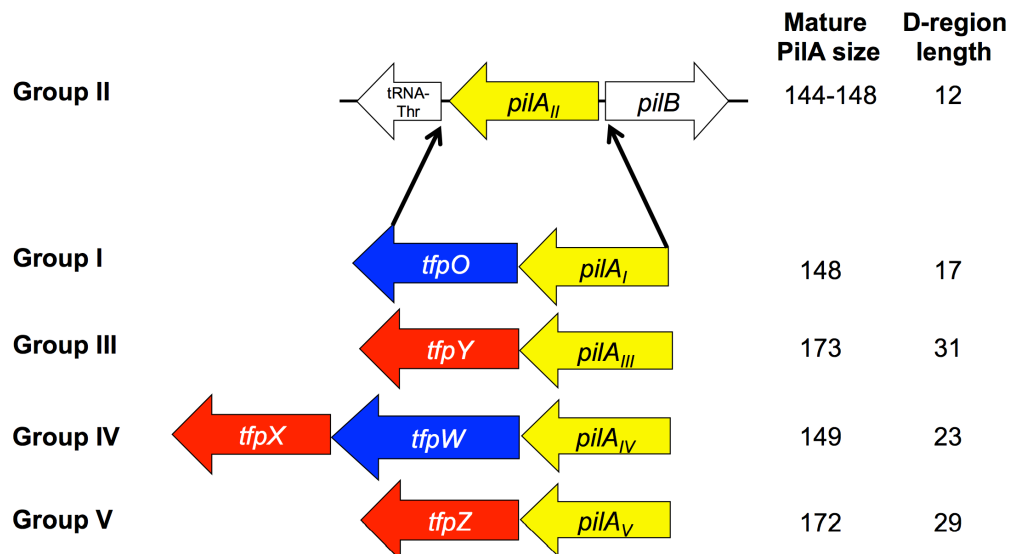


**Figure 1.5. Pilin diversity in *P. aeruginosa*.** The five groups of *P. aeruginosa* pilin alleles (yellow) and their associated accessory genes colored based on functional similarity of their protein products. *tfpO* and *tfpW* (blue) encode glycosyltransferases whereas *tfpX*, *tfpY* and *tfpZ* (red) encode membrane proteins involved in pilus assembly dynamics. The pilin proteins vary in size and length of the D-region between groups. Figure adapted from (101).

The other four pilin groups are associated with specific accessory proteins, although the roles of only two of these have been unambiguously identified. Group I strains – which include the Liverpool epidemic strain (LES) and the well-characterized strain 1244 – encode a 148 residue mature pilin with a D-region of 17 amino acids (40, 41, 139). Group I strains have an additional open reading frame (ORF) downstream of *pilA*, which encodes a protein originally named PilO (38, 164). To avoid confusion with the assembly protein called PilO –encoded by the

*pilMNOPQ* operon – the accessory protein was subsequently renamed TfpO (type four pilus protein O) (101). TfpO is a glycosyltransferase that post-translationally modifies the C-terminal Ser148 residue of group I pilins with an O-antigen subunit, although it can glycosylate other pilins that contain the requisite recognition elements (38, 39, 147). This modification modestly increases the virulence of group I strains, providing a possible explanation for the predominance of group I strains in cystic fibrosis patients (101, 163, 178).

Group IV strains also have glycosylated pilins. This group includes *P. aeruginosa* strains PA7 and Pa5196 that express mature pilins of 149 residues with a D-region of 23 amino acids (100, 101). Interestingly, this group has two accessory genes: *tfpW*, which encodes the glycosyltransferase, and *tfpX*, which encodes a predicted membrane protein similar to TfpY and TfpZ (below) (101). TfpW post-translationally modifies group IV pilins at several positions on the each subunit, including Thr64 and Thr66 in the predicted  $\alpha\beta$ -loop, with  $\alpha$ 1, 5 linked D-arabinofuranose homopolymers, chemically identical to those found in the *Mycobacterium tuberculosis* and *M. leprae* cell wall polymers lipoarabinomannan and arabinogalactan (100, 178).

Early studies of pilin diversity identified a single strain of *P. aeruginosa*, G7, with an unusual pilin sequence unlike those of group I and II pilins (164). This strain encoded a mature pilin of 173 residues with

a D-region of 31 residues, and was classified as group III (164). A putative ORF downstream of *pilA* was also identified, and later named *tfpY* (101, 164). Additional strains of group III were identified in a comprehensive analysis of environmental and clinical *P. aeruginosa* strains (101), and include PA14, the most frequently isolated clone of *P. aeruginosa* in the world (181) and a popular tool for virulence studies.

Group V strains encode a slightly smaller sized mature pilin of 172 residues with a 29-residue D-region. The downstream accessory gene encodes TfpZ, approximately 50% similar each to TfpX (group IV) and TfpY (group III), although the function of these proteins is currently unknown. Group III and V pilins are the largest among *P. aeruginosa* pilins and also the most sequence divergent compared to those of group II, at ~ 45 % sequence similarity (11, 100). The similarity is concentrated within the conserved N-terminal transmembrane segment. This high sequence divergence in the C-terminal head group makes it difficult to generate high-confidence structure models based on the structures of group II pilins. Complementation of a group II *pilA* mutant strain of PAO1 with the group III or V pilin gene alone restored less twitching motility than the wild-type group II pilin. However, provision of both the heterologous pilin and its associated accessory protein increased twitching motility without changing total pilin pools (11). Poor complementation of twitching motility by heterologous pilins was hypothesized to be the result of a slower rate of

assembly initiation, causing an imbalance between pilus assembly and retraction in the absence of the accessory proteins. From these data, the accessory proteins were suggested to affect pilus retraction dynamics, although their exact mechanism of action remains unclear (11).

### **The pilus fibre**

Pilin subunits are assembled into a pilus fibre on the periplasmic face of the inner membrane and extend out of the cell through a secretin pore. The internal diameter of the secretin varies between the T4a and T4b systems, with the T4b secretin able to support extrusion of a larger pilus (46, 159). Although the mechanism of pilin polymerization is unclear, structural modeling of the pilus fibre may provide helpful information about how the subunits fit together and help elucidate the mechanism. The differences between T4a and T4b pilins subunits reflect the differences in their respective pilus models; however, all models agree the pilins are assembled in a helical manner.

### *Pilus models*

Early pilus models suggested that T4aP were polymerized into a one-start helix five with pilin subunits per turn (71, 138). However, subsequent studies suggested that four subunits per turn would result in less steric hindrance and expose the D-region at the pilus tip to promote

adhesion (51, 71). Based on studies in which a 2.3 Å crystal structure of *N. gonorrhoeae* PilE was modelled into a 12.5 Å cryo-electron microscopy (EM) reconstruction of the pilus, there are ~3.6 pilin subunits per turn in a three-start, left-handed helix, which can be alternately viewed as a right-handed one- or four-start helix (51) (Figure 1.6). This fibre model has a diameter of ~60 Å, which would match the ~65 Å diameter opening estimated for the PilQ secretin (20, 45, 46).

In this model, the pilin subunits are tightly packed by electrostatic and hydrophobic interactions between the N-terminal  $\alpha$ -helices buried in the core (51). The N-terminal aromatic Phe1 is involved in interactions in the four-start helix, with conserved Tyr24 and Tyr27 forming a stabilizing arrangement of aromatic residues (109). The C-terminal globular head domains participate in additional stabilizing interactions on the outside of the pilus (51). In a left-handed three-start helix, there are polar interactions between the D-region of one subunit and the  $\alpha\beta$ -loop of the adjacent subunit (51). Interactions between the loops of the  $\beta$ -sheets of adjacent subunits in the four-start right-handed view are also predicted to contribute to pilus stability (51). Together, these interactions stabilize the T4aP fibre, contributing to its ability to withstand changes in temperature and treatment with 6M urea (109), and over 100 pN of force (117).

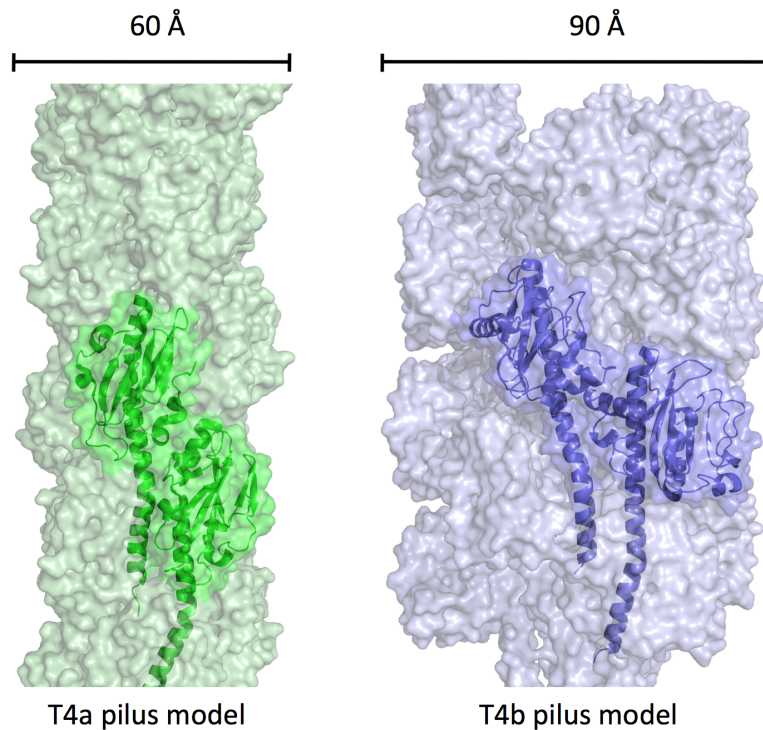


**Figure 1.6. T4aP and T4bP fibre models.** Fibre models derived from docking high-resolution pilin structures to low-resolution EM data. The T4aP model of the *N. gonorrhoeae* pilus (51) (left, PDB: 2HIL) has an approximate diameter of 60 Å, with tight packing of the pilin subunits. The T4bP model of *V. cholerae* pilus (110) (kindly provided by Dr. Lisa Craig) has a larger diameter at 90 Å due to looser packing of the subunits. Figures were prepared using MacPymol (DeLano Scientific). Figure adapted from (66).

T4bP are less stable than T4aP in their ability to resist proteolysis, thermal and chemical denaturation (109), likely due to a more loosely packed pilus fibre with limited interactions among the bulkier head groups (50, 109, 110) (Figure 1.6). Currently available T4b pilin structures are

truncated (15, 50, 94, 111, 149, 187) so in order to generate a pseudo atomic resolution T4bP model, a full-length T4b pilin structure was modeled by combining the 1.3 Å X-ray crystal structure of truncated *V. cholerae* TcpA pilin with the  $\alpha$ 1-N segment from full-length *P. aeruginosa* PAK pilin (109, 110). Fibre models of T4bP have been generated fitting the pilin structure into negative stain TEM reconstructions. The models are organized as a left-handed three-start helix also viewed as a right-handed one-start helix, similar to T4aP (50, 109, 110). This fibre model is 90 Å in diameter, although T4b secretin opening has been reported to be ~70 Å (159).

In the one-start model, hydrophobic interactions between N-terminal  $\alpha$ -helices form the core of the T4bP with Glu5 interacting with the N-terminus of an adjacent pilin like in T4aP (109, 110). This T4bP model of *V. cholerae* pili is supported by hydrogen/deuterium exchange mass spectrometry (DXMS) experiments, which identified areas of pili that are solvent-exposed (110). The globular C-terminal head groups barely contact each other in the T4bP model, leaving inter-subunit gaps exposing parts of the N-terminal alpha helix to the solvent and the D-region available to mediate pilus-pilus bundling (109, 110).

#### *The mechanism of pilus assembly*

The N-terminal  $\alpha$ 1-N helices of pilins alternately embed them in the

membrane or form the inner core of the pilus, stabilized by hydrophobic interactions. How pilin subunits are extracted from the membrane for pilus assembly and how assembly is initiated remain among several unanswered questions in the field.

Some clues are provided by studies of the evolutionarily related type II secretion (T2S) system, which express pilin-like proteins called pseudopilins, with the characteristic type III signal sequence for processing by a pre-pilin peptidase (132, 146). The major pseudopilins share the T4 pilin-fold, although instead of a DSL, major pseudopilins have a calcium-binding site that is integral to their function in protein secretion (95) (Figure 1.7). Based on their similarity to T4 pilins, the T2S major pseudopilins are thought to form a short pilus-like polymer, called the pseudopilus, that extends across the periplasm to facilitate the selective secretion of exoproteins (132, 145). In support of this hypothesis, overexpression of the major pseudopilin results in long T4P-like fibres that can mediate adhesion (55, 158, 177). Models of the T2S pseudopilus were generated with low-resolution EM images, conformational restraints and molecular modeling, and closely resemble a T4aP fibre, as a one-start right-handed helix (34, 35) (Figure 1.7).

Recently, a set of four additional pilin-like proteins, called the minor pseudopilins, was implicated in initiating *Klebsiella oxytoca* pseudopilus assembly (43). The minor pseudopilins, called PulHIJK, have the

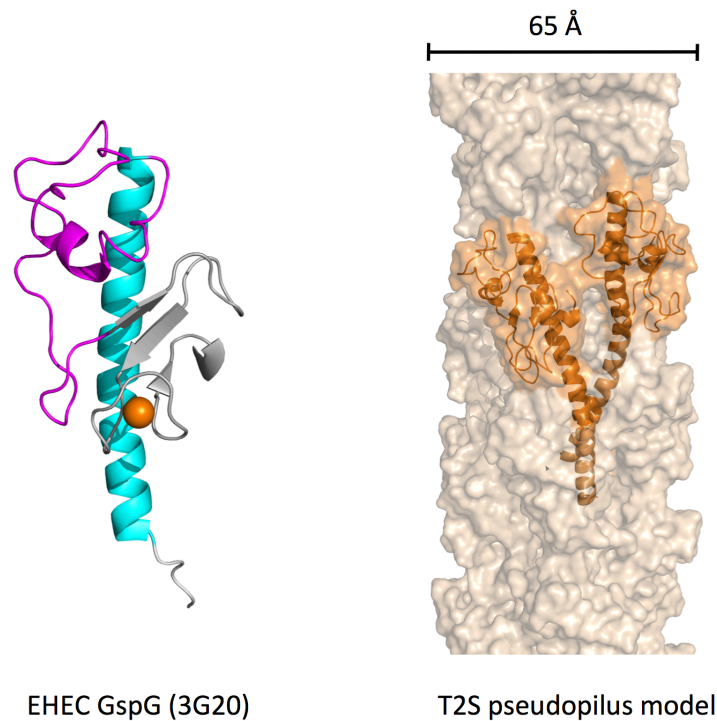


**Figure 1.7. Structure of T2S major pseudopilin and pseudopilus model.** The major pseudopilins, represented by EHEC GspG (PDB 3G20) left, maintain a T4 pilin-like fold with an N-terminal  $\alpha$ -helix connected to a core  $\beta$ -sheet through a variable  $\alpha\beta$ -loop. The D-region of major pseudopilins is stabilized by a calcium-binding motif (calcium ion depicted in orange). The T2S pseudopilus model (kindly provided by Dr. Olivera Francetic, right) resembles the T4aP model with a one-start right-handed helix. Figure adapted from (66).

characteristic hydrophobic N-terminus of major (pseudo)pilins with the type III signal peptide for cleavage, and are required for protein secretion (146, 158). In the absence of the minor pseudopilins, only rare pseudopili were observed by immunofluorescence microscopy, but assembly was restored by providing Pull and PulJ (43). These minor pseudopilins

interact in the membrane with PulK, resulting in a predicted 1 nm vertical displacement relative to one another. Their interaction was predicted in molecular dynamics simulations to cause membrane deformation (43), hypothesized to reduce the energy barrier required for initiation of pseudopilus assembly (43).

The fourth minor pseudopilin PulH was not required for pseudopilus assembly (43) although its homologues have been shown to interact with Pull and PulJ homologues (54, 99) plus the major pseudopilin (99, 113), suggesting it connects them (54, 99). The structure of pseudopilin EpsH (Extracellular protein secretion) from *V. cholerae* has been solved; it was modeled at the top of the pseudopilus containing only major subunits with no steric clashes, supporting its role as a putative connector (189).

There are several pieces of data that support the formation of a minor pseudopilin complex. The C-terminal domains of EpsI and EpsJ from *V. vulnificus* were crystallized as a dimer (188). Furthermore, in the T2S (General secretion pathway, Gsp) system of enterotoxigenic *E. coli*, the C-terminal domains of the minor pseudopilins GspI-GspJ-GspK co-crystallized as a heterotrimeric complex (96). This large complex is hypothesized to be at the tip of pseudopilus (96), supporting a role in initiation of pseudopilus assembly, although there is no evidence for their presence in polymerized fibres (177).

## Minor pilins

Homologues of each of the GspHIJK minor pseudopilins belonging to the T4P system were identified in *P. aeruginosa* in the mid-1990s (6-8). These pilin-like proteins, named FimU, PilV, PilW and PilX, are referred to as minor pilins due to their low abundance. They are encoded in a single operon (17) sharing synteny with the minor pseudopilins and have the characteristic hydrophobic N-terminal  $\alpha$ -helix preceded by a type III signal sequence (6-8) (Figure 1.8). Like the major pilin subunit PilA, they are processed by the pre-pilin peptidase PilD (65) and are embedded in the inner membrane by their hydrophobic N-terminal transmembrane regions with their C-terminal domains in the periplasm (6-8, 154).

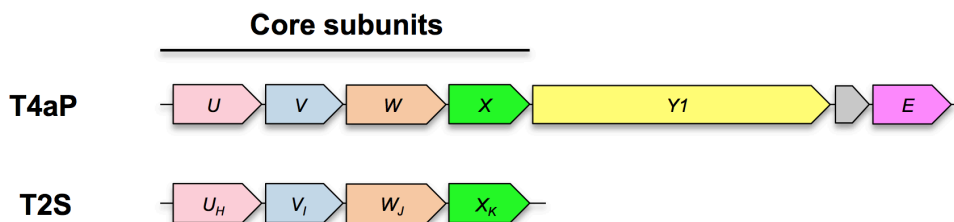


**Figure 1.8. Genetic organization of minor pilins and minor pseudopilins in *P. aeruginosa*.** The T4aP minor pilins FimU-PilVWXE are encoded on a polycistronic operon with the gene for PilY1, a non-pilin protein. FimU-PilVWX share homology with the T2S minor pseudopilins XcpUVWX (known as Gsp/Pul/EpsHIJK in other organisms) suggesting they are ‘core’ subunits and may share common function. PilE is a ‘non-core’ minor subunit and does not have an equivalent in the T2S system, suggesting it is T4P specific.

Since FimU, PilV, PilW and PilX-like proteins are common to both T2S and T4aP systems, they have been designated 'core' components (66). *P. aeruginosa* has an additional minor pilin, PilE, which is considered a 'non-core' minor pilin since it lacks an equivalent in the T2S system (66). PilE is the minor pilin most similar to the major pilin PilA at 38% sequence similarity, and is encoded in the same operon as the other minor pilins (17, 154).

#### *Minor pilin diversity*

In *P. aeruginosa*, the genes encoding the major pilin and minor pilins were shown to be part of a single ~36 kb pilin island (67). Interestingly, strains belonging to pilin groups I, II and IV have similar minor pilins, while groups III and V strains, which have related pilins and accessory proteins, have a set of identical minor pilins that are divergent from those of the other three groups (67). These findings suggest that minor pilins have co-evolved with the major pilin, a hypothesis that is supported by functional differences. Cross-complementation of group II minor pilin mutants with the heterologous minor pilins from group III only partially restores twitching motility and surface piliation, except in the case of PilX, where twitching motility and surface piliation could not be restored (67). However, co-introduction of PilX<sub>III</sub> into a recombinant group III strain

expressing group II minor pilins restored twitching motility, suggesting that PilX may be a group specific factor (67).

#### *Function of P. aeruginosa minor pilins in pilus assembly*

PilE and PilV minor pilins were originally identified in mutant screens for strains that were resistant to pilus-specific phages and deficient in twitching motility (7, 154). The genes for FimU, PilW and PilX were subsequently identified by sequencing the region of the chromosome surrounding *pilV* (6, 8). Mutants lacking any of the individual minor pilins were unable to twitch and lacked surface piliation, suggesting a role in pilus biogenesis (6-8, 154).

To determine if minor pilins are absolutely required for pilus assembly, mutants were made in a *pilT* background where retraction is abolished, thus any pili assembled are trapped on the surface where they can be quantified (65). In the absence of retraction, the minor pilin mutants produced some surface pili, suggesting the minor subunits were dispensable for pilus assembly (65). However, the level of piliation was reduced compared to the *pilT* control, suggesting that the minor pilins are involved in optimizing assembly of the pilus (65). In contrast, *Neisseria* core minor pilins were suggested to oppose PilT-mediated pilus retraction, as piliation appeared to be restored to the levels commensurate with the *pilT* control in minor pilin-*pilT* double mutants (36, 184).

Deletion of the entire minor pilin operon in a retraction-deficient background resulted in wild-type levels of surface piliation suggesting the minor pilins are not required for pilus assembly (73). Similarly, in the absence of the positive regulator of the minor pilin operon, AlgR, a few pili were assembled in a retraction-deficient strain, supporting a role for the minor pilins in optimizing pilus assembly (65, 67).

Given the similarity of the minor pilins to the major pilin subunit, it was hypothesized the minor pilins may interact with PilA and be incorporated into the pilus, or potentially form their own unique fibre (154). Radiolabeling experiments showed the minor pilins PilV, PilW and PilX were found only in the membrane fraction and not in the sheared surface fraction, suggesting they are not incorporated into the pilus (6, 7). More recently, immunogold labeling of the pilus with minor pilin specific antibodies showed the presence of all the minor pilins in the pilus fibre (65). This result is consistent with the observation of *N. gonorrhoeae* and *N. meningitidis* minor pilins in the surface pilus fractions (2, 74, 183, 184). However, a recent study suggests that 'non-core' minor pilins from *N. meningitidis*, PilX<sub>Nm</sub> and PilV<sub>Nm</sub>, function from within the periplasm (80). Although some protein was incorporated into pili, they proposed that the functional pool is likely in the periplasm since blocking incorporation of either protein into surface pili through fusion of each to a large fluorescent mCherry protein did not impair function (80).

The minor pilins were suggested to form one or more complexes, similar to their T2S equivalents (65). Analysis of protein stability in the absence of individual minor pilins suggested a potential interaction between PilW with FimU, PilV and PilX as well as an interaction between FimU and PilE (65). The stoichiometry of the minor pilins also appears to be important, as overexpression of FimU and PilX caused the expression of short pili, although the strains were still able to twitch (65).

Interestingly, a similar phenotype was observed with overexpression of XcpX, the homologue of PilX in the T2S system of *P. aeruginosa*, where increased levels of XcpX led to decreased lengths of the pseudopilus (56). XcpX and its homologues in both T2S and T4aP systems lack the Glu5 residue that is conserved among other T4 pilins and T2S pseudopilins. Mutation of the Thr5 of XcpX to Glu5, caused a decrease in pseudopilus assembly, suggesting the uncharged properties of this position are important for function (56). In the T2S model of pseudopilus assembly, the absence of a charged residue at position 5 is thought to facilitate extraction from the membrane and thus allow for the formation of a staggered pseudohelical arrangement of the minor pseudopilins in the membrane (43).

Taken together, although the role of the minor pilins in *P. aeruginosa* pilus assembly is still unclear, the available data and the homology to T2S minor pseudopilins suggest that the *P. aeruginosa* minor

pilins may form a complex that initiates pilus assembly (65, 66).

Interestingly, minor pilins in *E. coli* K-12 were recently shown to prime heterologous *K. oxytoca* pseudopilus assembly in the absence of minor pseudopilins, suggesting a conserved function in the two systems (44).

#### *Other functions of minor pilins*

Apart from pilus biogenesis, the core *P. aeruginosa* minor pilins PilW and PilX have been implicated in repression of swarming motility, a flagellar-dependent motility occurring on semisolid media (98). Their proposed role involves modulating the levels of the secondary messenger molecule cyclic-di-GMP – a global regulator of biofilm formation – produced by the diguanylate cyclase, SadC (98). PilV, PilW and PilX have also been implicated in activation of surface-associated virulence through their association with the mechanosensory protein, PilY1 (161).

Interestingly, these behaviours appear to be independent of pilus assembly and PilD processing, as mutation of the type III signal cleavage site in PilX did not affect the protein's regulatory function (98, 161).

Together, these data suggest the minor pilins, particularly PilV, PilW and PilX – likely through their association with the mechanosensor PilY1 – can function within the periplasm in complex regulatory networks, although the mechanisms involved are poorly understood.

Although *P. aeruginosa* non-core minor pilin PilE appears to function with the core minor pilins in pilus assembly, it may have additional functions, similar to the non-core minor pilins in *Neisseria*. In *N. meningitidis*, minor pilin PilX<sub>Nm</sub> (called PilL in *N. gonorrhoeae*) is encoded with the core minor pilins, similar to the arrangement in *P. aeruginosa* (184). PilX<sub>Nm</sub> was found in sheared pilus fractions and was proposed to antagonize retraction, promoting bacterial cell-cell aggregation (74, 75), and to cause conformational changes in the pilus fibre that are important for T4P-mediated signalling to the host (26). The crystal structure of truncated PilX<sub>Nm</sub> has been solved (75), and remains one of the few minor pilin structures available. It has the typical T4aP fold with an extended N-terminal  $\alpha$ -helix connected to a four-stranded anti-parallel  $\beta$ -sheet (75). The disulphide bond loop encompasses 18 residues that form a C-terminal hook-like loop that was suggested to function by interacting with similar features on adjacent, anti-parallel pili (75).

The structure of ComP, another 'non-core' minor pilin in *N. meningitidis*, has been solved by NMR spectroscopy (42). Like PilX<sub>Nm</sub>, it has the conserved T4a pilin architecture, with an N-terminal  $\alpha$ -helix connected to a four-stranded antiparallel  $\beta$ -sheet (42). ComP is incorporated into pili and is required for competence in *Neisseria* (27, 186), binding directly to DNA containing *Neisseria*-specific uptake

sequences via an electropositive region extending across the surface-exposed  $\beta$ -sheet region (42).

The *N. gonorrhoeae* minor pilin PilV (PilV<sub>Ng</sub>) shares 36% sequence identity with PilE and has also been identified in sheared pilus fractions, although it is encoded separately from the other minor pilins (183). PilV<sub>Ng</sub> is essential for pilus attachment to host cells, as it promotes the functional display of the putative T4aP adhesins PilC1/PilC2, homologs of PilY1 (see below) (6, 183). In contrast, PilV from *N. meningitidis* (PilV<sub>Nm</sub>) is not required for pilus attachment, although it is involved in host cell receptor recruitment (47), reshaping the host cell plasma membrane to help the bacteria resist shear stress (124) and to promote invasion of endothelial and epithelial cells (172).

Recently, Imhaus and colleagues showed that the *N. meningitidis* type IV pilus-specific effects on competence, attachment, aggregation and plasma membrane reshaping could be modulated by adjusting the levels of piliation by manipulation of PilB levels (80). These results suggested that instead of functioning as components of the pilus as previously suggested, non-core minor pilins PilX<sub>Nm</sub> and PilV<sub>Nm</sub> modulate pilus assembly levels from within the periplasm (80). In general, the function and mechanism of the non-core minor pilins remains poorly understood, and warrants further research.

*The pilus-associated protein, PilY1*

The *P. aeruginosa* minor pilins are encoded by a polycistronic operon (17). Embedded toward the end of the operon is the gene for *pilY1*, coding for a large 125 kDa non-pilin protein (6). PilY1 has been implicated in pilus assembly, anti-retraction, and attachment, as well as non-T4P related functions (6, 23, 73, 82, 97, 114, 135, 161).

Like the other members of the operon, mutants lacking PilY1 failed to twitch and were devoid of surface pili, suggest a role for PilY1 in pilus biogenesis (6, 23, 73). In the absence of retraction, *pilY1* mutants had some surface pili, although the levels were less than the *pilT* mutant control (73). Those data suggest that like the minor pilins, PilY1 is dispensable for pilus assembly. Instead, PilY1 was proposed to stabilize the pilus, preventing its retraction (73). Although PilY1 is not a pilin, it was predicted to have a potential pre-pilin peptidase cleavage site at its N-terminus (108) and was observed in surface fractions (6, 73, 135). Interestingly, the presence of PilY1 in the sheared surface protein fraction is dependent on one or more of the minor pilins encoded in the *fimU-pilVWXY1E* operon, suggesting an association with the minor pilins (73). However, the localization of PilY1 is controversial, since PilY1 has also been suggested to be a secreted protein, as an 88 kDa fragment of PilY1 was observed in outer membrane vesicles and in extracellular protein fractions (23).

The C-terminal domain (CTD) of PilY1 is homologous to the CTD of *Neisseria* PilC (6), a protein proposed to be a T4aP tip adhesin (152). Like, PilY1, mutants lacking PilC are non-piliated, PilC has been detected in surface pilus fractions, and its incorporation into the pilus requires the minor pilins (184). PilC has also been implicated in opposing pilus retraction (185). It is hypothesized that the CTDs of these proteins are involved in antagonizing retraction in a calcium-dependent manner, while the NTDs are involved in attachment (135). There are two variants of PilC encoded at different locations in the *Neisseria* chromosome, PilC1 and PilC2. In *N. gonorrhoeae*, PilC1 and PilC2 are functionally interchangeable in terms of piliation and attachment; however, in *N. meningitidis*, only PilC1 is able to mediate attachment (125, 127). The reason why *Neisseria* has two PilC variants is unclear.

The crystal structure of the CTD of PilY1 was solved and revealed a broken  $\beta$ -propeller fold and novel type of calcium-binding site (135). The calcium-binding site was implicated in regulation of pilus retraction; a point mutant mimicking the calcium-bound state was impaired for retraction, while release of the calcium ion was suggested to be required for PilT-mediated retraction (135). It was suggested that binding to a surface through the NTD of PilY1 could signal release of the calcium ion, allowing retraction of the pilus fibre for twitching motility to occur (135).

PilY1 has been shown to interact with host cell basolateral surfaces as a T4P-associated adhesin (73). In addition to the calcium-binding site in the CTD, PilY1 has a second calcium-binding site in the NTD, both of which are important for PilY1-mediated integrin binding. Since those binding experiments were performed with a purified fragment of PilY1, the requirement for T4aP in this phenotype is unknown (82).

Similar to PilW and PilX, PilY1 is involved in repression of *P. aeruginosa* swarming motility and surface-activated virulence (97, 161). PilY1 was proposed to act as a putative mechanosensor of surface contact via a von Willebrand factor A-like domain in its NTD (161). Interestingly, PilY1 was reported to be present in surface fractions in the absence of T4aP, although the T4P assembly machinery appears to be important for its export (114). How PilY1 is presented on the cell surface, and whether there are different pilus-associated and pilus-free forms remains unknown.

### **Hypothesis and research aims**

The expression of major and minor pilin proteins on the surface and their importance in T4P function make these proteins ideal vaccine candidates. However, understanding of the diversity associated with these proteins is crucial for the rational design of a pilus-based vaccine. There are five distinct groups of *P. aeruginosa* major pilins, which vary based on

their sequence and accessory proteins, and two sets of minor pilins, whose roles in type IV pilus biology are poorly understood. Cross-complementation of a group II *pilA* mutant with heterologous group III or V pilin genes resulted in less twitching motility than with the cognate group II gene (11) suggesting important functional differences. The overarching hypothesis of this work is that differences in the structures and interactions of *P. aeruginosa* major and minor pilins contribute to their assembly and disassembly dynamics.

The specific research aims of this thesis are:

**1. Assess the structural diversity of *P. aeruginosa* major pilins to better understand the role of the accessory proteins**

Since the sequence of the pilins from groups III and V predicts larger proteins, it is possible that the pilins have a different size and/or shape than that of the group II pilins, leading to reduced assembly rates in cross-complementation experiments, and therefore fewer (or shorter) pili on the surface. These structural differences may require specific accessory proteins to modulate pilus retraction dynamics for efficient function. This idea is investigated in chapter 2.

**2. Investigate the potential interactions between the minor pilins FimU-PilVWXE and the putative adhesin PilY1, and address their potential role in *P. aeruginosa* T4a pilus assembly**

There may also be some specificity between the major and minor pilins during fibre assembly that is disrupted upon complementation with heterologous pilins. The minor pilins and PilY1 are involved in pilus assembly in an unknown manner; however, based on the similarity of minor pilins to the T2S minor pseudopilins, they are predicted to interact and to prime pilus assembly. This hypothesis is explored in chapter 3.

**3. Characterize the structure and putative connector function of non-core minor pilin PilE**

The non-core minor pilin PilE is associated with core minor pilins and PilY1, and is incorporated into pili (65). However, recent data in *Neisseria* suggests the non-core minor pilins may function from the periplasm (80). This controversy will be addressed in chapter 4.

# **CHAPTER TWO**

## **Structural characterization of novel *Pseudomonas aeruginosa* type IV pilins**

## **Preface**

Chapter Two consists of the following publication:

**Nguyen Y, Jackson, SG, Aidoo, F, Junop, M, Burrows LL. 2010.**

Structural characterization of novel *Pseudomonas aeruginosa* type IV pilins. J Mol Biol 395:491-503.

Attributions: Y.N. cloned, expressed, purified and crystallized the protein. F.A. helped with protein expression and purification. S.G.J. and M.J. collected diffraction data. S.G.J. solved the structure. Y.N., M.J. and L.L.B. designed the experiments. Y.N., S.G.J., M.J. and L.L.B wrote the manuscript.

Reprinted from Journal of Molecular Biology, 395, Nguyen Y, Jackson, SG, Aidoo, F, Junop, M, Burrows LL, Structural characterization of novel *Pseudomonas aeruginosa* type IV pilins, 491-503, Copyright 2010, with permission from Elsevier.

**Structural characterization of novel *Pseudomonas aeruginosa* type  
IV pilins**

Ylan Nguyen, Sean G. Jackson, Francisca Aidoo, Murray Junop and Lori  
L. Burrows\*

Department of Biochemistry and Biomedical Sciences and the Michael G.  
DeGroote Institute for Infectious Diseases Research, McMaster University,  
1200 Main St. W., Hamilton, ON, L8N 3Z5, Canada

\* To whom correspondence should be addressed: [burrowl@mcmaster.ca](mailto:burrowl@mcmaster.ca)

Running title: Novel *P. aeruginosa* type IV pilins

## Abstract

*Pseudomonas aeruginosa* type IV pili, composed of PilA subunits, are used for attachment and twitching motility on surfaces. *P. aeruginosa* strains express one of five phylogenetically distinct PilA proteins, four of which are associated with accessory proteins that are involved either in pilin post-translational modification or in modulation of pilus retraction dynamics. Full understanding of pilin diversity is crucial for the development of a broadly protective pilus-based vaccine. Here, we report the 1.6-Å X-ray crystal structure of a N-terminally truncated form of the novel PilA from strain Pa110594 (group V), which represents the first non-group II pilin structure solved. Although it maintains the typical T4a pilin fold, with a long N-terminal  $\alpha$ -helix and four-stranded antiparallel  $\beta$ -sheet connected to the C-terminus by a disulfide-bonded loop, the presence of an extra helix in the  $\alpha\beta$ -loop and a disulfide-bonded loop with helical character gives the structure T4b pilin characteristics. Despite the presence of T4b features, the structure of PilA from strain Pa110594 is most similar to the *Neisseria gonorrhoeae* pilin and is also predicted to assemble into a fiber similar to the GC pilus, based on our comparative pilus modeling. Interactions between surface-exposed areas of the pilin are suggested to contribute to pilus fiber stability. The non-synonymous sequence changes between group III and V pilins are clustered in the same surface-exposed areas, possibly having an effect on accessory

protein interactions. However, based on our high-confidence model of group III PilA<sub>PA14</sub>, compensatory changes allow for maintenance of a similar shape.

## **Introduction**

A wide range of bacteria express type IV pili (T4P), which are long protein fibers involved in a diverse array of functions ranging from attachment to and twitching motility on living and nonliving surfaces to competence for DNA uptake and electron transfer (49, 141). T4P are required for virulence by a number of pathogenic species including *Pseudomonas aeruginosa*, an opportunistic pathogen of plants, animals and humans. Each fiber is composed of thousands of subunits of the major pilin protein, whose assembly and disassembly at the inner membrane result in pilus extension and retraction, leading to twitching motility (118). Two subclasses of T4P have been identified, T4aP and T4bP, which differ in several respects. The major pilins of the two subtypes have limited sequence identity, different lengths of the leader peptide (type IVa pilins have ~6 residue leaders, type IVb pilins have ~15-30) as well as the mature protein (type IVb are larger), and disparate identity of the N-methylated N-terminal residue of the mature subunit (Phe in type IVa, varies in type IVb) (49, 141). The differences in the major subunits are mirrored in the architecture of their respective assembly

systems, where type IVa pilins are assembled by complex systems encoded across the genome of the host organism while type IVb assembly systems are composed of fewer components that are typically encoded in single gene clusters, often located on plasmids (141). The T4aP subclass is found in a broad range of bacterial species including *P. aeruginosa* and *Neisseria* spp., while the T4bP have a more restricted distribution, typically in genera such as *Salmonella* and *Vibrio* and pathogenic *Escherichia coli* species that colonize the mammalian gastrointestinal tract (48, 49, 141).

Structures of pilins from both subclasses have been solved (12, 50, 51, 71, 90, 138, 149, 187) and reveal a similar overall architecture. Both have a long, hydrophobic N-terminal  $\alpha$ -helix, subdivided into  $\alpha$ 1-N and  $\alpha$ 1-C.  $\alpha$ 1-N retains individual subunits in the inner membrane until assembly, when it forms the core of the assembled pilus fiber, while  $\alpha$ 1-C is embedded in a C-terminal  $\beta$ -sheet and loop domain that forms the exterior surface of the pilus (48). There is a characteristic disulfide-bonded loop (DSL), often called the D-region, located in the C-terminal regions of both pilin subclasses, which anchors the C-terminus to the  $\beta$ -sheet and is important for function (70). The hydrophobic  $\alpha$ 1-N region of the mature pilin is typically truncated for structural work to improve solubility, as it is highly conserved between species and previous studies have shown that full length and truncated structures of individual pilins are superimposable (50, 71). Despite their general similarities, examination of T4aP and T4bP

pilin structures currently available shows that they have distinct folds that arise primarily from differences in the numbers and topology of  $\beta$ -strands in the C-terminus (48).

A limited number of structures are also available for proteins related to the T4 pilins (9, 75, 93, 96, 188, 189). Minor pilins are pilin-like proteins sharing the conserved N-terminal leader peptide and hydrophobic  $\alpha$ 1-N helix and are required for expression of surface-exposed pilus fibers (6-8, 154) or in the case of PilX, a minor pilin from *Neisseria meningitidis*, for specific fiber properties (74). The evolutionarily-related type II secretion system's pseudopilins and minor pseudopilins, involved in transport of proteins through the outer membrane, also have a conserved N-terminal leader and  $\alpha$ 1-N hydrophobic region (145). The structures of the major pseudopilins PulG (93) and XcpT (9) (from *Klebsiella* and *Pseudomonas*, respectively), and the minor pseudopilins EpsH (189) (from *Vibrio cholerae*), EpsI and EpsJ (188) (from *Vibrio vulnificus*) and GspK, GspI and GspJ (96) (from *E. coli*), confirmed that they share a common architecture with the type IV pilins, although differences that may relate to specific functions are present.

*P. aeruginosa* strains express one of five phylogenetically distinct T4aP PilA alleles, three of which were identified only recently (101). The five PilA proteins differ in their overall sequences and length, the size of the key C-terminal DSL (70); and the association of the pilin gene with

specific downstream accessory genes involved in pilin post-translational modification (38, 100, 178) or modulation of pilus assembly (11) (Figure 2.1). Structures are available only for *P. aeruginosa* group II pilins (12, 50, 71, 90), which are the smallest among the five groups and the only ones lacking associated accessory proteins, making them the exception in the *P. aeruginosa* pilin repertoire (101).

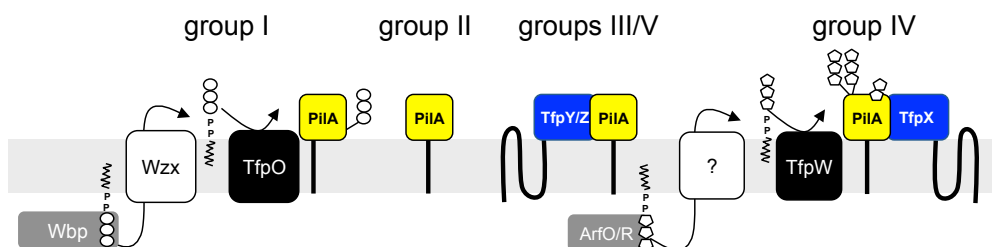


**Figure 2.1. Pilin modification and assembly systems in *P.***

**aeruginosa.** Group I pilins are glycosylated by TfpO on the C-terminal Ser with an O antigen unit synthesized by the LPS machinery. Group II pilins have no accessory proteins. Group III and V pilins each have a specific accessory protein that promotes their assembly: TfpY for group III and TfpZ for group V. Group IV pilins are glycosylated at several positions by TfpW with mono-, di- and trisaccharides of D-arabinofuranose synthesized by the ArfO/R proteins (Harvey and Burrows, unpublished data). Group IV pilins have a TfpX accessory protein that is similar to TfpY and TfpZ.

Phylogenetic analysis suggested that groups III, IV and V pilins are members of a separate family that diverges from the branch containing groups I and II (101). Group III and V pilins are 43.5% identical with one

another over 144 residues in their C-terminal domains but show much lower identity to group I, II, and IV pilins in that region. Pairwise comparisons revealed 17.2% identity between the C-termini of pilins from groups I and III, 26% between groups II and III, and 23.4% between groups III and IV. Similar values are obtained when group V pilins are used as the comparator. Introduction of group III or V alleles of *pilA* into the common group II laboratory strain PAO1 lacking its own *pilA* gene led to poor recovery of motility unless the associated accessory gene was co-introduced (11). Inactivation of the *tfpY* accessory gene in the group III strain PA14 caused a marked decrease in surface piliation and motility without affecting pilin levels in the cell, suggesting that pilus assembly was impaired in its absence.

Together, the bioinformatic and functional data led us to hypothesize that *P. aeruginosa* group III and V pilins might have an unusual architecture compared with the known structures of group II pilins, leading to their requirement for accessory factors to facilitate the pilus assembly process. To test this hypothesis, we initiated a study to determine the structures of group III and V pilins for comparison with the existing group II structures. Here, we report the X-ray crystal structure of an  $\alpha$ 1-N-truncated form of the novel pilin from Pa110594 (group V), the first example of this subfamily of *P. aeruginosa* T4a pilins, revealing some T4b-like characteristics. The pronounced sequence similarity between

group III and V pilins allowed us to generate a high-confidence model of the group III pilin from strain PA14, the world's most widespread clone of *P. aeruginosa* (181). Comparison of the group III and V pilins shows that the majority of the nonconservative substitutions between the two are clustered in surface-exposed regions corresponding to potential intermolecular interfaces in the assembled pilus fiber.

## **Results and discussion**

### **Structure of group V Pa110594 PilA**

The structure of PilA from strain Pa110594 (abbreviated PilA<sub>0594</sub>) was solved by X-ray crystallography to determine if the group V pilins were unlike other T4a pilins whose structures are currently available. The mature pilin was made soluble as in Ref. (71) by truncating  $\alpha$ 1-N (corresponding to the first 28 N-terminal amino acids). The purified PilA<sub>0594</sub> protein crystallized readily in two crystal forms belonging to different space groups: needle shaped, from space group P2<sub>1</sub>2<sub>1</sub>2<sub>1</sub> and diamond shaped, from space group P4<sub>1</sub>2<sub>1</sub>2. Initially, a native data set from a diamond-shaped crystal was collected to 1.8 Å on a home source. Attempts to solve the structure by molecular replacement using existing structures of pilin and pilin-like proteins were unsuccessful, suggesting that the PilA<sub>0594</sub> structure differed significantly. A single-wavelength anomalous dispersion (SAD) data set was then collected from a

selenomethionine (SeMet)-labeled diamond-shaped crystal. This structure was solved and subsequently used as a search model in molecular replacement to solve the structure of the native protein (Table 2.1).

**Table 2.1. 0594 PilA crystallographic and data refinement statistics**

	<b>Native 0594 PilA</b>	<b>SeMet-0594 PilA</b>
<i>Data collection</i>		
Beamline	NSLS X12C	NSLS X12C
Wavelength	1.1000	0.9793
Space Group	P2 <sub>1</sub> 2 <sub>1</sub> 2 <sub>1</sub>	P4 <sub>1</sub> 2 <sub>1</sub> 2
Unit- cell parameters (Å)		
<i>a</i> , <i>b</i> , <i>c</i> (Å)	29.46, 44.87, 88.91	63.06, 63.06, 67.74
$\alpha = \beta = \gamma$ (°)	90.0	90.0
No. of molecules in asymmetric unit	1	1
Resolution range (Å) <sup>a</sup>	50 – 1.6 (1.63 – 1.6)	50 – 1.55 (1.58-1.55)
Unique reflections	16 182	20 404
Data Redundancy <sup>a</sup>	6.9 (6.5)	14.5 (14.7)
Completeness (%) <sup>a</sup>	99.4 (96.7)	99.9 (100)
<i>I</i> / $\sigma$ ( <i>I</i> ) <sup>a</sup>	31.5 (11.7)	33.9 (10.6)
R <sub>merge</sub> (%) <sup>a</sup>	5.8 (17.0)	6.8 (29.4)
<i>Model and Refinement</i>		
Resolution range (Å) <sup>a</sup>	27.96 - 1.60 (1.65 - 1.60)	29.84 – 1.55 (1.59 - 1.55)
R <sub>work</sub> (%)	18.0	17.7
R <sub>free</sub> (%)	20.3	20.9
No. of reflections	16 094	20 149
No. of amino acid residues/atoms	150/1068	150/1093
No. of waters	224	282
r.m.s.d bond lengths (Å)	0.02	0.02
r.m.s.d bond angles (°)	1.9	1.4
Average B factor (Å <sup>2</sup> )	10.4	13.6
Ramachandran plot statistics (%) <sup>b</sup>		
Favored regions	89.8	90.9
Allowed regions	10.2	9.1
<sup>a</sup> Values in parentheses represent the highest resolution shell.		
<sup>b</sup> Ramachandran values are from the program PROCHECK (103)		

Although PilA<sub>0594</sub> has limited sequence identity to the group II pilin from PAK (Figure 2.2A), similar secondary-structure elements are seen in comparable orientations. The structure of PilA<sub>0594</sub> has the same general architecture as other type IVa pilins (Figure 2.2) with a long N-terminal  $\alpha$ -helix, a four-stranded antiparallel  $\beta$ -sheet, and the characteristic DSL linking the C-terminus to the  $\beta$ -sheet. Pro42 introduces a kink in the  $\alpha$ 1-C helix, suggesting that the S-shaped helix found in full-length pilins that promotes flexibility in the pilus fiber is a conserved feature in this protein (28, 49, 110). However, there are some notable differences. The  $\alpha\beta$ -loop connecting the N-terminal  $\alpha$ -helix to the  $\beta$ -sheet domain contains an  $\alpha$ -helix ( $\alpha$ 2) (Figure 2.2b and c), a feature reminiscent of T4b pilins (below). Within the four-stranded antiparallel  $\beta$ -sheet,  $\beta$ 3 and  $\beta$ 4 are longer and twisted compared with  $\beta$ 1 and  $\beta$ 2, and there is an unusually large loop between  $\beta$ 3 and  $\beta$ 4 that contains a third  $\alpha$ -helix and is folded over onto the surface of the  $\beta$ -sheet (Figure 2.2c). The two cysteines at residues 141 and 171 enclose a DSL that encompasses 29 residues (Figure 2.2c). The PilA<sub>0594</sub> DSL is mostly unstructured with a fourth short  $\alpha$ -helix and retains a highly conserved aromatic residue at the base of the loop (Phe166) that forms hydrophobic interactions with  $\alpha$ 1, similar to other *P. aeruginosa* pilins (50, 70).

The DSL is a characteristic structural feature of most type IV pilins. In *P. aeruginosa*, this subdomain has been the subject of intense research

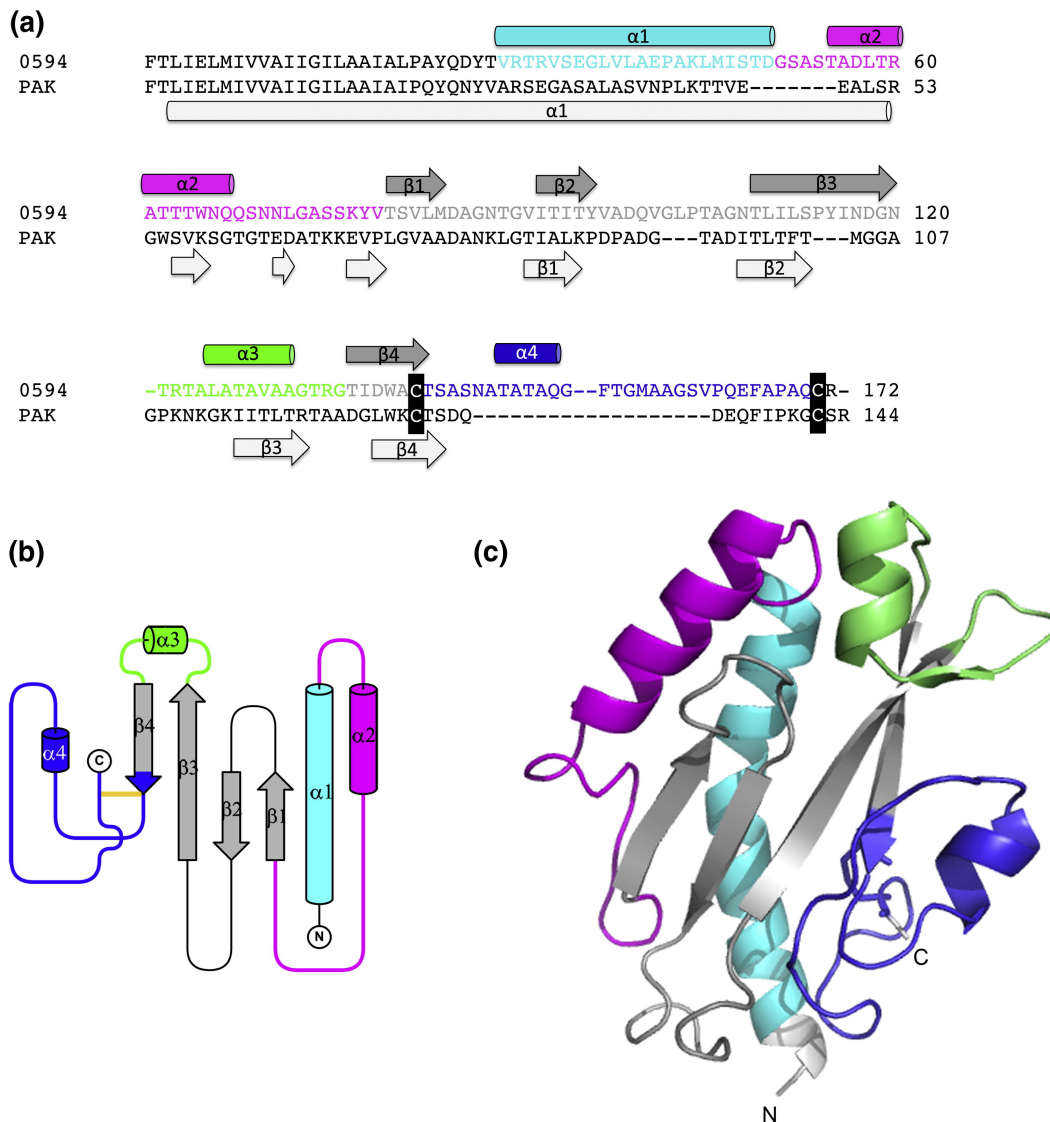


**Figure 2.2. Structure of *P. aeruginosa* PilA<sub>0594</sub>.** (a) shows a protein sequence alignment between mature *P. aeruginosa* pilins from strains PAK and Pa11054 (0594) from ClustalW2, suggesting PilA<sub>0594</sub> maintains the same secondary structure elements as PilA<sub>PAK</sub> despite the difference in sequence. Secondary structure is indicated above for PilA<sub>0594</sub>, according to the α1-N-truncated structure of PilA<sub>0594</sub> shown in (c), and below for PilA<sub>PAK</sub>. Cysteines involved in disulfide bond formation are shown in white font on black. α-helices are depicted as barrels and β-strands are shown as arrows. Residues and secondary structure from α1-

C are shown in cyan,  $\alpha\beta$ -loop in magenta,  $\beta$ -sheet in gray, in exception to the  $\beta$ 3/4 loop that is in green and the DSL in blue. (b) shows a topology diagram from TopDraw corresponding to the structure of PilA<sub>0594</sub>. The same colors depict the same features as in A, except the disulfide bond is shown with a yellow line. (c) shows the cartoon representation of the crystal structure of PilA<sub>0594</sub> solved showing a long N-terminal kinked  $\alpha$ -helix, an  $\alpha\beta$ -loop with an extra  $\alpha$ -helix, a four-stranded antiparallel  $\beta$ -sheet with a large loop between the long and twisted  $\beta$ 3 and  $\beta$ 4, which connects to the disulfide bond loop with the cysteines shown as sticks.

focus due to data implicating it in the adhesive function of T4P (68, 105).

Recent evidence from our group showed that mutation of either Cys residue involved in disulfide bond formation to Ala prevents pilus assembly altogether (70), suggesting that the configuration of the disulfide loop is essential for recognition by the pilus assembly system or for the inter-subunit interactions needed for stable pilus formation. In the process of preparing SeMet-labeled protein, we found that expression of PilA<sub>0594</sub> in a methionine-auxotrophic strain of *E. coli* (B384) with a typical reducing cytoplasm resulted in low yields of soluble protein that subsequently precipitated, suggesting that the protein was not correctly folded. In contrast, expression of PilA<sub>0594</sub> in Origami (DE3) cells (which have mutations in the thioredoxin and glutathione reductase genes and therefore support cytoplasmic disulfide bond formation) grown in SeMet-supplemented minimal medium gave high yields of stable protein that was

fully labeled at all three Met positions based on mass spectrometry analysis (data not shown). Therefore, it is possible to use non-auxotrophic “specialty” expression strains for SeMet labeling without sacrificing the efficient incorporation of label into the protein of interest.

PilA<sub>0594</sub> crystals had either a diamond-like or a needle-like morphology. Superimposition of the structures from each of the two crystal forms revealed that they were identical (Figure 2.3a), indicating that crystal packing does not alter the structure. Although the crystal structures were identical, the packing of the molecule in each of the two crystal forms was different. However, examination of crystal packing within the two forms revealed no interactions that were considered to be biologically relevant to pilus assembly; that is, the molecules were not oriented with respect to one another in a way thought to be conducive to fiber formation. This finding suggests that even when the subunits are placed in the conditions of high protein concentration required for crystal formation, spontaneous helical pilus-like fiber formation cannot arise solely due to interactions between the C-terminal domains of truncated pilins. This observation is supported by a recent study (110) that showed T4b pilins in assembled fibers had levels of hydrogen-deuterium exchange similar to truncated pilin monomers; therefore, inter-subunit packing interactions mediated by the C-termini were limited. Audette *et al.* showed previously that while truncated T4a pilins could spontaneously self-associate into hollow

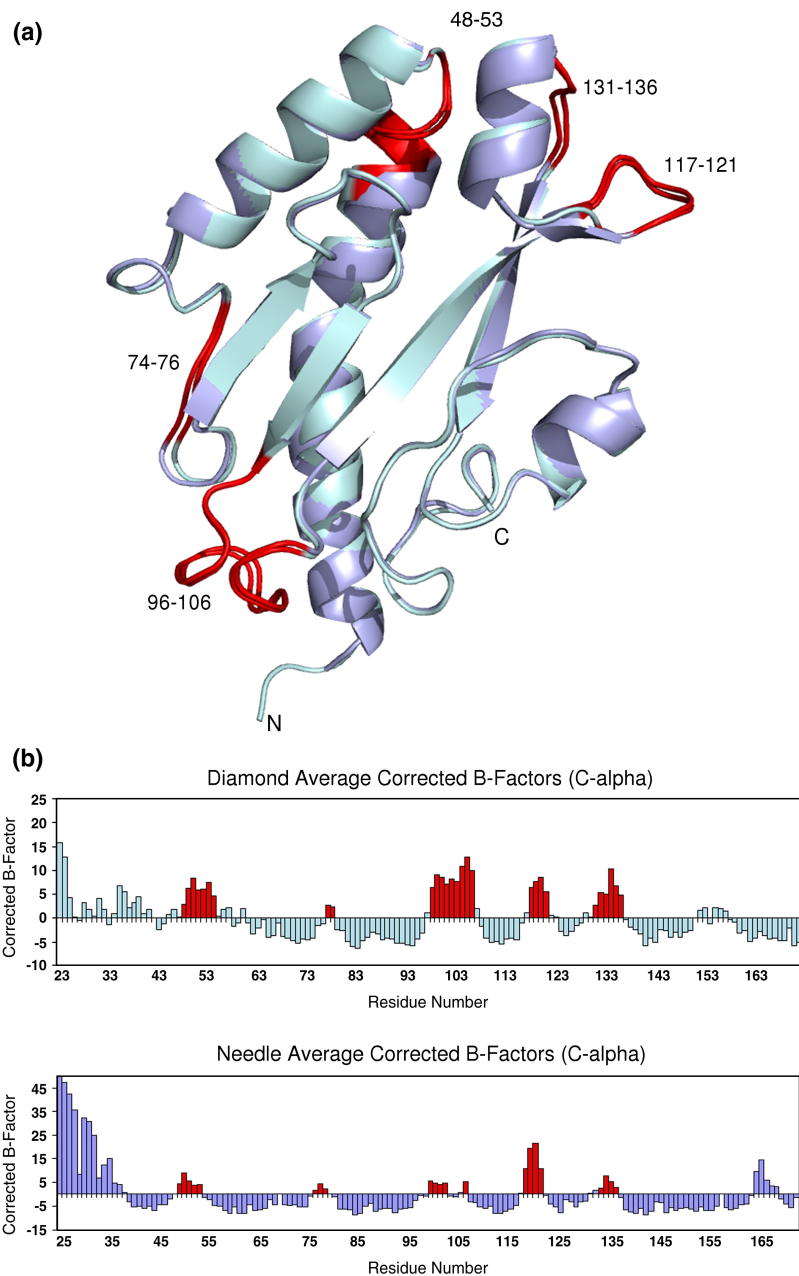


**Figure 2.3. B-factor analysis of PilA<sub>0594</sub> structures.** PilA<sub>0594</sub> crystallized as different morphologies, diamond and needle, for the SeMet and native PilA<sub>0594</sub> proteins, respectively. (a) shows the structural alignment of the SeMet PilA<sub>0594</sub> structure, in pale cyan, and native PilA<sub>0594</sub> structure, in light blue, with areas with higher-than-average *B*-factors in red, corresponding to the data in the graphs in (b).

nanotube-like structures, this self-association required the addition of a hydrophobic agent (13). Their data suggest that when the truncated subunits assemble into a fibrous structure, they may create a partly hydrophobic surface within the nanotube lumen (normally occupied by the hydrophobic  $\alpha$ 1-N helices) that leads to unstable fiber formation in the absence of an alternate hydrophobic compound. It is also possible that the initiation of fiber formation normally requires additional factors, such as the minor pilins, to nucleate or facilitate pilin assembly.

Although crystal packing in the case of PilA<sub>0594</sub> was not considered physiologically relevant, *B*-factor analysis provided some information regarding flexibility in the structure. Figure 2.3b delineates those regions of PilA<sub>0594</sub> that have higher-than-average *B*-factors in the structures from each of the two crystal forms. These regions include the beginning of the  $\alpha\beta$ -loop, the  $\beta$ 2/ $\beta$ 3 loop and the  $\beta$ 3/ $\beta$ 4 loop. The rest of the structure, including  $\alpha$ 1-C,  $\alpha$ 2, the  $\beta$ -sheet, and the DSL, has lower-than-average *B*-factors, suggesting that these regions are more rigid; all of these regions contain some secondary structure that may increase stiffness. More flexible regions with higher *B*-factors may therefore be important for mediating protein-protein interactions, such as packing of pilin subunits into the fiber, or for interactions with other proteins, such as the TfpZ accessory protein. However, regions with low *B*-factors can still be involved in protein-protein interactions.

### **Comparison of PilA<sub>0594</sub> with T4a and T4b pilins**

Although the structures of two *P. aeruginosa* pilins belonging to group II have been solved (12, 50, 71, 90), neither they nor pilin structures from other species were found to be suitable models for phasing of the PilA<sub>0594</sub> data using molecular replacement methods. This finding suggested that the structure of PilA<sub>0594</sub> and related pilins deviated significantly from existing structures. Inspection of the final PilA<sub>0594</sub> structure confirmed that although it clearly belongs to the T4a pilin family, it has some unusual features not typical of the previously solved T4a pilins from *P. aeruginosa* (12, 50, 71, 90) and *Neisseria gonorrhoeae* (51, 138) (Figure 2.4).

A structure homology search of all available structures in the Protein Data Bank (PDB) using Dali-Lite (78) revealed that PilA<sub>0594</sub> is more similar overall to the *N. gonorrhoeae* pilin (Figure 2.4, top right) than to the *P. aeruginosa* pilin structures from strains PAK and K122-4 (Figure 2.4, top left and middle).  $\beta$ 3 and  $\beta$ 4 of PilA<sub>0594</sub> are long and twisted like those of the *Neisseria* pilin, unlike the short  $\beta$ 3 and  $\beta$ 4 strands of the *Pseudomonas* pilins (Figure 2.4). At 29 residues, the DSL in PilA<sub>0594</sub> is the same size as that of the *N. gonorrhoeae* pilin and larger than the group II *P. aeruginosa* pilin DSLs, which contain 12 residues. However, the *N. gonorrhoeae* pilin DSL contains a  $\beta$ -hairpin turn, whereas the PilA<sub>0594</sub> DSL is less structured, with some helical character resembling that

of the DSL in T4b pilins from *Vibrio*, *Salmonella* and *E. coli* (50, 149, 187) (Figure 2.4, bottom). In addition to the more helical DSL, PilA<sub>0594</sub> has an  $\alpha$ -helix ( $\alpha_2$ ) in the  $\alpha\beta$ -loop, which is a feature more typical of T4b pilins, although in the latter proteins, the helix does not lie in the same plane as the  $\beta$ -sheet (Figure 2.4). Dali-Lite analysis suggests that after the *N. gonorrhoeae* PilE, K122-4, and PAK pilins from *P. aeruginosa*, the closest relatives of PilA<sub>0594</sub> are the pseudopilins Gspl (96) and PulG (93), from the type II secretion systems of *E. coli* and *Klebsiella*, respectively, and the minor pilin PilX (75) from *N. meningitidis*. No T4b pilins were identified. Interestingly, PilX (which has no equivalent in *P. aeruginosa*) has two  $\alpha$ -helices in the  $\alpha\beta$ -loop as well as a helix in the DSL (75), similar to PilA<sub>0594</sub>. However, the large bent loop between  $\beta_3$  and  $\beta_4$  (shown in green in Figure 2.4) appears to be a novel feature of PilA<sub>0594</sub>. Therefore, although PilA<sub>0594</sub> is identifiable as a T4a pilin, it also has characteristics of the T4b class of pilins.

The finding that PilA<sub>0594</sub> is structurally unique supports our hypothesis regarding its unusual architecture, based on our observations of its limited primary-sequence similarity with other *Pseudomonas* pilins, its poor complementation of assembly and twitching motility in recombinant *P. aeruginosa* strains of other pilin groups, and the lack of immunological cross-recognition between pilins of different groups using anti-pilus antibodies (11). Identification of unusual features in this new

pilin shows the importance of obtaining a broader picture of the extent of structural diversity in pilins and pilin-like proteins, as it is relevant to the design of pilus-based vaccines.

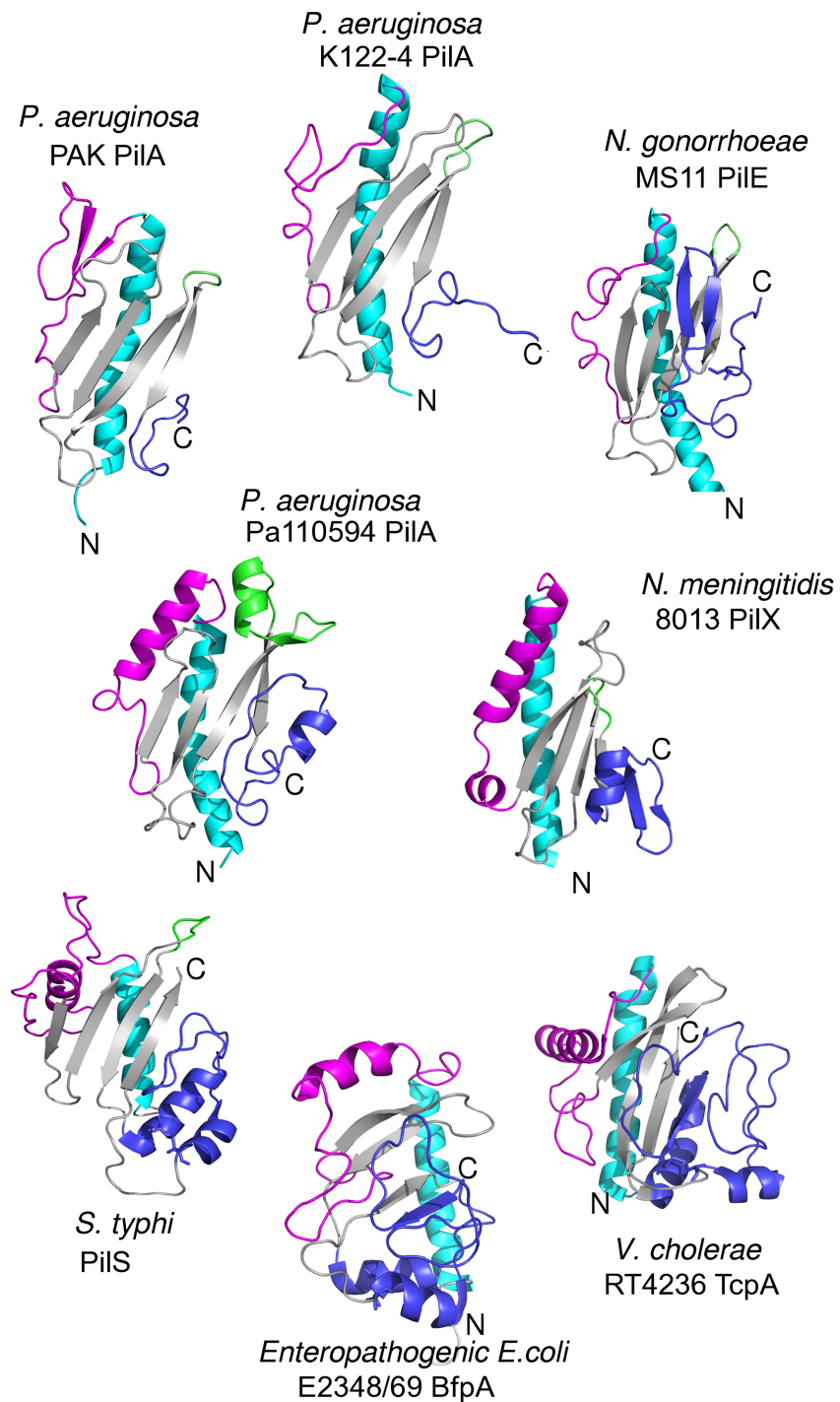


**Figure 2.4. Comparison of PilA<sub>0594</sub> with T4a and T4b pilins.** The three structures at the top of the figure are those of previously solved T4a pilins from *P. aeruginosa* PAK PilA (PDB code: 1dzo) and K122-4 PilA (PDB code: 1qve) and *N. gonorrhoeae* MS11 PilE (PDB code: 1ay2), while the three structures at the bottom are previously solved T4b pilins from *S. typhi* PilS (PDB code: 1q5f), EPEC BfpA (PDB code: 1zwt) and *V. cholerae* TcpA (PDB code: 1oqv). The structure of minor pilin, PilX, from *N. meningitidis* (PDB code: 2opd) is at center right for comparison with the structure of *P. aeruginosa* PilA<sub>0594</sub> solved here (center left). Similar features compared to PilA<sub>0594</sub> are similarly colored with  $\alpha$ 1-C in cyan, the  $\alpha$  $\beta$ -loop in magenta,  $\beta$ -sheet in gray, the equivalent loop between  $\beta$ 3 and  $\beta$ 4 in green, and the DSL in blue.

### Implications for pilus structure

To further classify the structural relationships of PilA<sub>0594</sub> with other pilins and to model how PilA<sub>0594</sub> subunits may assemble into a pilus fiber (Figure 2.5a), we conducted tertiary and quaternary structural comparisons with members of both T4P subclasses (T4aP and T4bP). Since PilA<sub>0594</sub> is a T4a pilin most similar to *N. gonorrhoeae* PilE but with some characteristics of T4b pilins, and models of the pilus fiber are available for the *N. gonorrhoeae* GC (T4aP) (51) and *V. cholerae* Tcp (T4bP) pili (110), those pilus models were chosen for comparative analysis.

As shown in Figure 2.5b, the tertiary structures of PilA<sub>0594</sub> and PilE<sub>MS11</sub> align very well over the central  $\beta$ -sheet and N-terminal helical

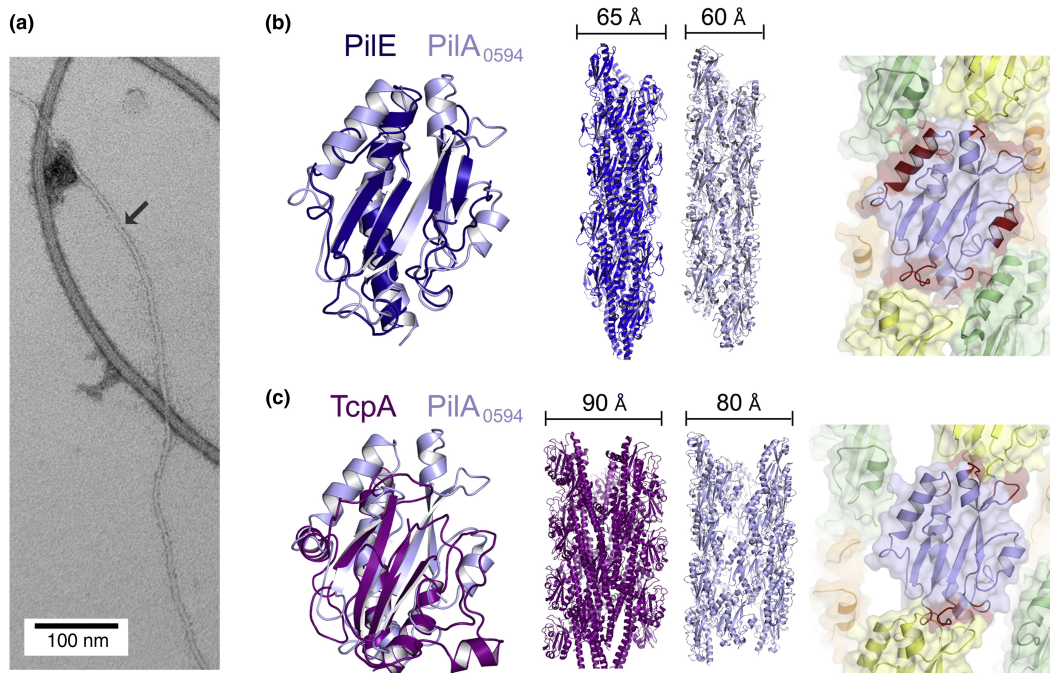


**Figure 2.5. Comparison of T4aP and T4bP-based 0594 pilus homology models.** (a) shows a transmission electron micrograph of *P. aeruginosa* Pa110594 T4P (arrow) and flagella. Pilus homology models were constructed using the T4a *N. gonorrhoeae* MS11 GC pilus model (2hil) (b) and T4b *V. cholerae* TCP model (provided by Lisa Craig) (c) after structural alignments with PilE and TcpA, respectively (b and c, left). PilA<sub>0594</sub> is in light blue while PilE is in blue and TcpA is in purple. The central panels of (b) and (c) compare the GC pilus model (blue) and the Tcp pilus model (purple) with our homology model (light blue). Diameters of each pilus are designated in angstroms. The last panel gives a close-up view of the potential protein-protein interactions (red) observed for a single PilA<sub>0594</sub> subunit (light blue) when present in a pilus assembled based on a T4a and T4b pilus structure. Other repeating subunits immediately adjacent to the central subunit (light blue) are colored green, yellow, and orange.

regions. Despite the notable additions of the helix in the  $\alpha\beta$ -loop, the insertion in the  $\beta 3/\beta 4$  loop, and an altered DSL region, the overall shape (surface contour) relative to the central curved N-terminal helix remains similar between these two proteins. In contrast (Figure 2.5C), TcpA does not maintain the same degree of shape complementarity with PilA<sub>0594</sub> although it has a helix in the  $\alpha\beta$ -loop. It is therefore not surprising that a pilus homology model of PilA<sub>0594</sub> generated using the *N. gonorrhoeae* GC pilus data is more feasible than one based on a *V. cholerae* Tcp model. Comparison of the PilA<sub>0594</sub> subunit contacts (shown in red in Figure 2.5B and C) adopted within these two homology models clearly indicates a greater contact surface and superior shape complementarity when the *P. aeruginosa* 0594 pilus is modeled using the GC pilus (Figure 2.5B). The Tcp-based 0594 pilus model not only lacks subunit contact along an entire face (see space between the blue- and green- colored subunits in Figure 5C), but also, perhaps more importantly, exhibits severe steric clashes between subunits along its opposite face (see secondary-structure overlaps between blue and yellow subunits, Figure 2.5C).

Furthermore, the internal diameter available to accommodate  $\alpha 1$ -N varies greatly between the two models. The model based on the GC pilus has an internal diameter of 20 Å, which is similar to that suggested by the pilus model of *P. aeruginosa* PAK (49), whereas the central core based on the Tcp model is 40 Å, likely too large for  $\alpha 1$ -N interactions required to

stabilize the pilus. Based on this analysis, it would appear that *P. aeruginosa* group V pilins are more likely to assemble into a pilus that resembles that of the T4a subclass.

### **Sequence and structural homology with group III PA14 PilA**

In our survey of pilin allele distribution in the *P. aeruginosa* species, the group III pilins were found to be the third most frequent, after groups I and II (101). Among the well-characterized strains expressing group III pilins is strain PA14, which was recently shown in a global survey of the *P. aeruginosa* species to be the most widely distributed clone (181). Because of the high level of sequence similarity between the group III and group V pilins (75% over 175 residues), we used the PilA<sub>0594</sub> structure to generate a high-confidence model of the PA14 pilin, PilA<sub>PA14</sub> (Figure 2.6). An alignment of the PilA<sub>0594</sub> and PilA<sub>PA14</sub> proteins with one additional sequence each of a group III (strain C3719) and group V (strain 5325) pilin demonstrates the sequence differences between groups (Figure 2.6a). The few substitutions within groups (shown in white on gray text) are mostly conservative. However, there are a total of 44 nonconservative changes between the two groups (highlighted in grey and green).

The central panel of Figure 2.6b shows a superimposition of the PilA<sub>0594</sub> structure (in blue) with the PilA<sub>PA14</sub> model (in tan). The proteins are very similar, with the exception of the one- and two-residue insertions in PilA<sub>PA14</sub> that are visible in the  $\beta$ 3/ $\beta$ 4 and DSL loops of the model. To

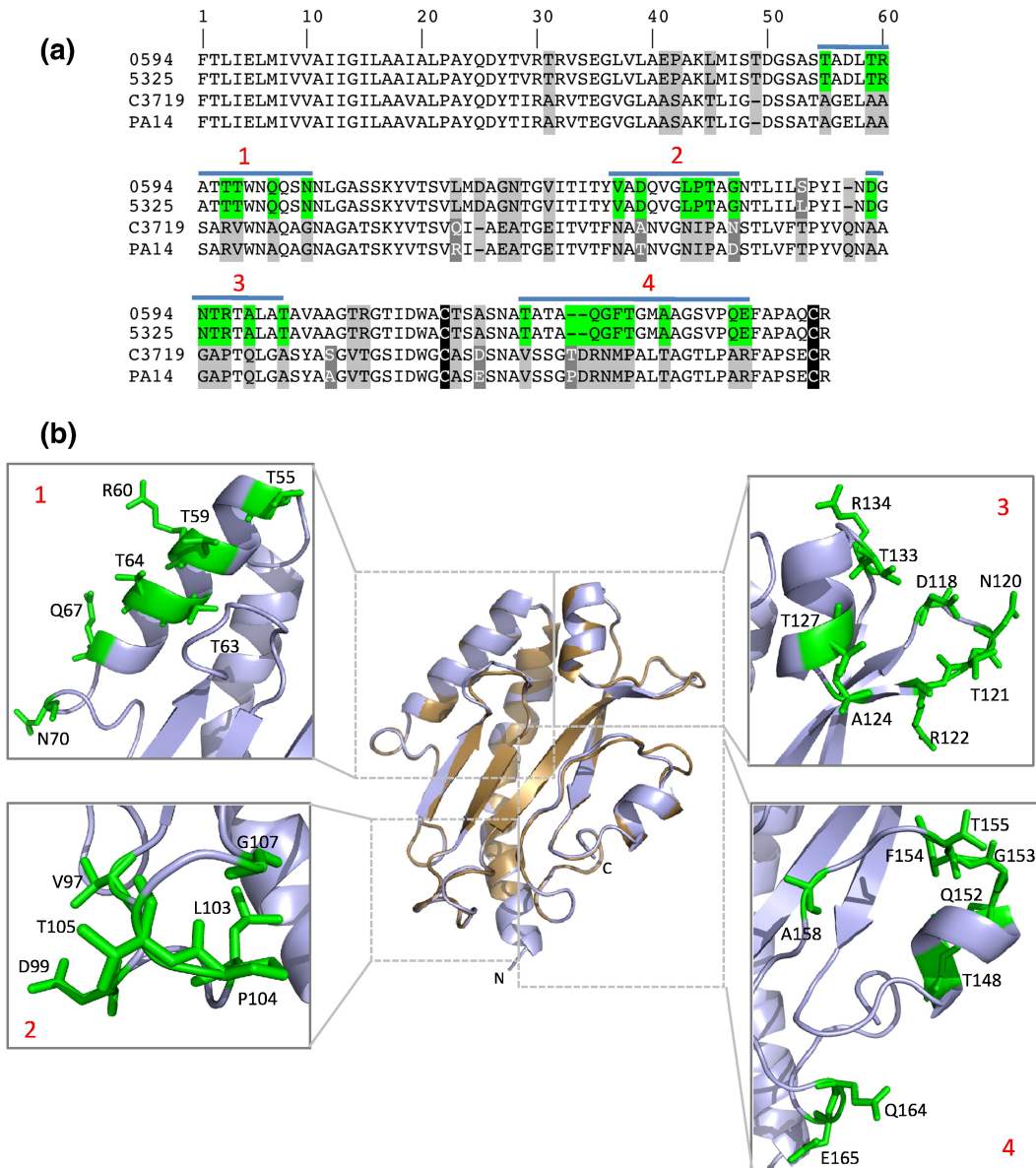


**Figure 2.6. Comparison of group III and group V pilins.** (a) shows an alignment of representative group III (from strains C3719 and PA14) and group V (from strains Pa110594, abbreviated 0594, and 5325) pilins (101). The conserved Cys residues that form the disulfide bond essential for function are shown in white text on black; residues highlighted in white on gray text differ within the groups, while those in light gray and green differ between groups III and V; the locations of four select clusters of residues

in green are shown in the correspondingly numbered insets of (b). The centre of (b) shows the PilA<sub>0594</sub> structure in light blue, superimposed with a model of the PA14 pilin in tan (generated using MODELLER). Four regions of PilA<sub>0594</sub> are expanded to show residues (in green) that vary from those at the corresponding positions in the PA14 pilin.

locate the nonconservative substitutions between the group III and group V pilins (as shown in Figure 2.6a) on the PilA<sub>0594</sub> structure, we examined four stretches of residues (highlighted in green and labeled 1 through 4) more closely. The numbered insets in Figure 2.6b correspond to the labeled residues in Figure 2.6a. It is interesting to note that a large proportion of the nonconservative changes between group III and V pilins occur in surface-exposed loop regions, while the conserved secondary-structure elements such as the  $\beta$ -sheet have few changes.

Inset 1 shows that differences in  $\alpha 2$  of the  $\alpha\beta$ -loop occur mainly on the exterior face of the helix. These non-conserved residues, as well as those shown in the remaining three insets, occur in regions of the protein that could be involved in intermolecular contacts in the pilus fiber (compare with those regions highlighted in red in Figure 2.5b), either with other pilin subunits or potentially with the minor pilins involved in assembly. The fact that the non-conserved residues tend to cluster at surface-exposed regions may also help to explain why our previous attempts to complement a group V TfpZ accessory protein mutant with the

group III TfpY accessory protein were not successful (11). These patches of non-conserved residues would significantly affect the surface topology of the pilins and likely their interactions with their cognate accessory protein.

It is worth noting that a few of the non-conserved substitutions (i.e., E41-P42 in PilA<sub>0594</sub> and A41-S42 in PilA<sub>PA14</sub>) lie in the  $\alpha$ 1-C region, where they would be expected to face the lumen of an assembled fiber. It has been shown that T4P are unlikely to be hollow, as the interior diameter is estimated to be narrow and occluded with side chains. Therefore, these differences are not likely to reflect changes in accessibility to the fiber lumen, although the extra proline in PilA<sub>0594</sub> may introduce additional flexibility to the assembled fiber. The combination of the small proline residue with the bulky glutamate may reflect a compensatory combination of residues.

## Conclusions

The structure of PilA<sub>0594</sub> reported here provides a new perspective on the diversity of *P. aeruginosa* pilins, as it is the first example from a group other than group II that has been solved. Although features such as the  $\alpha$ -helix in the  $\alpha\beta$ -loop give PilA<sub>0594</sub> some T4b-like characteristics, our analysis suggests that it most likely forms a pilus similar to other T4a pilins. Our model of the related group III pilin, PilA<sub>PA14</sub>, shows that it is

likely to be structurally similar to the group V pilins, despite their differences in primary sequence. Although the specific role of the accessory protein, TfpZ, in relation to pilin assembly still remains to be elucidated, the data presented here provide important information necessary to develop a broad pilus-based vaccine.

## **Materials and methods**

### **Expression and purification of recombinant PilA<sub>0594</sub>**

A truncated form of the Pa110594 *pilA* gene lacking the first 102 nucleotides (corresponding to the first 34 amino acids of the prepilin) was PCR-amplified with forward primer 5'CACCGTTCGTACCCGTGTCAGTGAAG and reverse primer 5'TTAGCGGCACTGAGCAGGAGCAA from *P. aeruginosa* strain Pa110594 (101) chromosomal DNA prepared using the Instagene reagent (BioRad) using the manufacturer's instructions. Oligonucleotides were synthesized by ACGT Corp or Mobix. Ligation of the PCR product into the pET151/D-TOPO vector (Invitrogen) generated a fusion construct expressing an N-terminal 6xHis purification tag and V5 epitope tag followed by a tobacco etch virus protease cleavage site for subsequent removal of the tags. Expression and purification of PilA<sub>0594</sub> was performed as in (70). In brief, *E. coli* Origami cells expressing the pET151- PilA<sub>0594</sub> vector were grown overnight at 16°C following induction of protein

expression with IPTG (final concentration 1.0 mM). Cells were lysed by French press, and PilA<sub>0594</sub> was purified by nickel affinity chromatography, followed by tobacco etch virus cleavage and a second nickel affinity purification step. Fractions from the second Ni purification containing purified PilA<sub>0594</sub> were pooled, and the protein was buffer-exchanged using a HiPrep 26/10 desalting column (GE Healthcare Canada) into 20 mM Tris, pH 8, 75 mM KCl and concentrated to 15 mg/ml using Vivaspin 15R (Sartorius Stedim Biotech) concentrators.

Protein for SAD phasing was SeMet labeled at positions 18, 56 and 129 of the 144-residue truncated protein by expression in methionine-auxotrophic B834 (DE3) *E. coli* cells and grown in SeMet high-yield M9 minimal media (Shanghai Medicilon) according to the manufacturer's instructions. SeMet-labeled PilA<sub>0594</sub> was also expressed in Origami (DE3) cells grown under the same conditions. SeMet PilA<sub>0594</sub> was purified from both strains using Ni affinity chromatography as above and protein isolated from Origami cells concentrated to 15 mg/ml. Electrospray ionization mass spectrometry confirmed complete incorporation of SeMet at all three positions for protein purified from both expression strains; however, protein expressed in Origami (DE3) cells generated diffraction quality crystals for SAD phasing.

### **Crystallization and X-ray diffraction data collection**

All crystals were grown at 20 °C using the hanging drop/vapor diffusion method. Hanging drops containing 1 µl of native protein solution (15 mg/ml) and 1 µl of mother liquor [0.1 M Hepes, pH 7.5, and 20% (w/v) PEG 10000; 8% (v/v) ethylene glycol] were dehydrated over a reservoir containing 500 µl of 1.5 M (NH<sub>4</sub>)<sub>2</sub>SO<sub>4</sub>. Needle-shaped crystals (400 µm x 100 µm x 50 µm), suitable for data collection, grew after approximately 1-2 days of incubation. SeMet-labeled crystals were grown using a different mother liquor (0.1 M Tris-HCl, pH 8.5, and 2.0 M ammonium sulfate) and drops equilibrated over 2 M (NH<sub>4</sub>)<sub>2</sub>SO<sub>4</sub>. Diamond-shaped crystals (~ 200 µm x 200 µm x 200 µm) grew in 1-2 days. All crystals were flash frozen directly in a nitrogen cold stream (100 K) with no further cryo-protection. Diffraction data sets for native and SeMet crystals were collected at wavelengths of 1.1 and 0.979 Å, respectively. All data were collected at the X12C beamline of National Synchrotron Light Source (NSLS) (Brookhaven, NY).

### **PilA<sub>0594</sub> X-ray crystal structure determination and refinement**

Native and SAD data sets were processed using the HKL2000 program suite (137) to 1.6 and 1.55 Å, respectively. Using HYSS (4), all three of the expected SeMet sites were located. Phasing, density modification, auto model building and refinement were carried out using the PHENIX suite of programs (4, 120). With the use of Coot (58),

iterative rounds of manual model building and refinement were performed until  $R$  and  $R_{free}$  values converged and could no longer be improved. The structure of native PilA<sub>0594</sub> was determined by molecular replacement using the PilA<sub>0594</sub>-SeMet structure as an initial search model. Molecular replacement and model refinement were performed using the PHENIX suite of programs (4, 120). Stereochemical quality of the models were verified using PROCHECK, and the statistics are shown in Table 1 (103). Data collection and model refinement statistics for both native and SeMet-labeled PilA<sub>0594</sub> are listed in greater detail in Table 1.

Structure similarity searches were performed using the program Dali-Lite v3 (78). Structural illustrations presented in figures were generated with PyMOL (53).

### **Electron microscopy of *P. aeruginosa* Pa110594**

For visualization by electron microscopy, strain Pa110594 was grown on LB and a small amount of bacteria from the outer edge was resuspended in 200  $\mu$ l of ddH<sub>2</sub>O. A Formvar-coated carbon grid (supplied by the McMaster Electron Microscopy Facility) was floated on a 50  $\mu$ l drop of bacterial suspension for 5 min followed by wicking of excess liquid with Whatman paper. The grid was stained on a 25  $\mu$ l drop of 2% uranyl acetate for 45 s and the excess was removed with Whatman paper as before. Bacteria were examined with a JEOL JEM 1200 TEMSCAN (Peabody, MA, USA) microscope operating at an accelerating voltage of

80 kV and photos were taken with a 4-megapixel digital camera (AMT (Advanced Microscopy Techniques Corp., Danvers, MA) coupled to a digital imaging system.

### **PilA<sub>0594</sub> pilus models**

PilA<sub>0594</sub> homology models were generated by first structurally aligning individual pilin subunits using the program Coot (58). The structure of PilA<sub>0594</sub> was aligned separately with *N. gonorrhoeae* PilE (T4aP) and *V. cholerae* TcpA (T4bP) structures. Using Coot, we generated complete pilus homology models by aligning PilA<sub>0594</sub> subunits onto individual pilin subunits (PilE or TcpA) within the GC (PDB code: 2HIL) or Tcp pilus models (structure data kindly provided by Lisa Craig).

### **PilA<sub>PA14</sub> model**

The PilA<sub>PA14</sub> model was generated by MODELLER (156) using a sequence alignment between PilA<sub>PA14</sub> and PilA<sub>0594</sub> from ClustalW2 (102).

### **PDB accession codes**

The coordinates of the final SeMet-labeled PilA<sub>0594</sub> model were deposited in the PDB under accession code 3JYZ. Coordinates of the native PilA<sub>0594</sub> model were deposited in the PDB under accession code 3JZZ.

## **Acknowledgements**

We thank Carmen Giltner for assistance with electron microscopy and Lisa Craig for providing the Tcp model data. This work was funded by grants from the Canadian Institutes of Health Research (CIHR) to L.L.B. (MOP86639) and M.S.J. (MOP89903). L.L.B. is the recipient of a CIHR New Investigator Award. S.G.J. is a recipient of a CIHR CGS Award.

# **CHAPTER THREE**

***Pseudomonas aeruginosa* minor pilins  
prime type IVa pilus assembly and  
promote surface display of the PilY1  
adhesin**

## **Preface**

Chapter Three consists of the following publication:

**Nguyen Y, Sugiman-Marangos S, Harvey H, Bell SD, Charlton, CL, Junop MS, Burrows LL.** 2015. *Pseudomonas aeruginosa* minor pilins prime type IVa pilus assembly and promote surface display of the PilY1 adhesin. *J Biol Chem.* 290: 601-611.

Attributions:

Y.N. performed sheared surface protein experiments and interaction experiments. Y.N. and S.D.B. purified the proteins and S.D.B. set up crystal trays. S.S.M. and M.S.J. collected diffraction data. S.S.M solved the structure. H.H. made the minor pilin and minor pseudopilin operon mutants and complementation constructs. Y.N., C.L.C., M.S.J. and L.L.B designed the experiments. Y.N. and L.L.B. wrote the manuscript with input from C.L.C., S.S.M. and M.S.J.

This research was originally published in *The Journal of Biological Chemistry*. Nguyen Y, Sugiman-Marangos S, Harvey H, Bell SD, Charlton, CL, Junop MS, Burrows LL. *Pseudomonas aeruginosa* minor pilins prime type IVa pilus assembly and promote surface display of the PilY1 adhesin. *J Biol Chem.* 2015; 290: 601-611. © the American Society for Biochemistry and Molecular Biology.

**Pseudomonas aeruginosa minor pilins prime type IVa pilus assembly  
and promote surface display of the PilY1 adhesin\***

Ylan Nguyen<sup>1</sup>, Seiji Sugiman-Marangos<sup>1</sup>, Hanjeong Harvey<sup>1</sup>, Stephanie D.  
Bell<sup>1</sup>, Carmen L. Charlton<sup>2,3</sup>, Murray S. Junop<sup>4</sup> & Lori L. Burrows<sup>1</sup>

<sup>1</sup> Department of Biochemistry and Biomedical Sciences and the Michael  
G. DeGroote Institute for Infectious Disease Research, McMaster  
University, Hamilton, ON, CANADA

<sup>2</sup> Department of Laboratory Medicine and Pathology, University of Alberta,  
Edmonton, AB, CANADA

<sup>3</sup> Provincial Laboratory for Public Health (ProvLab), Edmonton, AB,  
CANADA

<sup>4</sup> Department of Biochemistry, Western University, London, ON, CANADA

\*Running Title: Minor pilins and PilY1 prime type IV pilus assembly

To whom correspondence should be addressed:

Dr. Lori L. Burrows, 4H18 Health Sciences Centre, 1200 Main St. West,  
Hamilton, ON, L8N 3Z5, CANADA, Tel: (905)-525-9140 ext: 22029, Fax:  
(905) 522-9033, E-mail: burrowl@mcmaster.ca

**Background:** Type IV pili (T4P) are virulence factors composed of major and minor pilins.

**Results:** Minor pilins prime pilus assembly and traffic anti-retraction protein PilY1 to the surface; FimU and GspH are structurally similar.

**Conclusions:** Minor pilins are essential for pilus assembly and function.

**Significance:** This work expands the structural and functional similarities between the T4P and T2S systems.

## ABSTRACT

Type IV pili (T4P) contain hundreds of major subunits, but minor subunits are also required for assembly and function. Here we show that *Pseudomonas aeruginosa* minor pilins prime pilus assembly and traffic the pilus-associated adhesin and anti-retraction protein, PilY1, to the cell surface. PilV, PilW and PilX require PilY1 for inclusion in surface pili and vice versa, suggestive of complex formation. PilE requires PilVWXY1 for inclusion, suggesting that it binds a novel interface created by two or more components. FimU is incorporated independently of the others and is proposed to couple the putative minor pilin-PilY1 complex to the major subunit. The production of small amounts of T4P by a mutant lacking the minor pilin operon was traced to expression of minor pseudopilins from the *P. aeruginosa* type II secretion (T2S) system, showing that under retraction-deficient conditions, T2S minor subunits can prime T4P

assembly. Deletion of all minor subunits abrogated pilus assembly. In a strain lacking the minor pseudopilins, PilVWXY1 and either FimU or PilE comprised the minimal set of components required for pilus assembly. Supporting functional conservation of T2S and T4P minor components, our 1.4 Å crystal structure of FimU revealed striking architectural similarity to its T2S ortholog GspH, despite minimal sequence identity. We propose that PilVWXY1 form a priming complex for assembly and that PilE and FimU together stably couple the complex to the major subunit. Trafficking of the anti-retraction factor PilY1 to the cell surface allows for production of pili of sufficient length to support adherence and motility.

## **INTRODUCTION**

Type IV pili (T4P) are long, thin hair-like protein polymers that mediate functions ranging from attachment to host cells and surfaces, flagella-independent twitching motility, biofilm formation, and DNA uptake to electron transfer in bacteria and archaea (30, 49, 141). There are two major classes of T4P, T4aP and T4bP. Twitching motility, which involves repeated rounds of pilus assembly, adherence and disassembly that pull the cells towards the point of pilus attachment, is associated mainly with the T4aP class (30, 118, 141).

The T4P assembly system is evolutionarily related to the type II secretion (T2S) system, and both are proposed to function by the dynamic

assembly and disassembly of pilin subunits. In the T2S system, the resulting short pseudopilus is thought to span only the width of the periplasm of a Gram-negative bacterium. The pilins (called pseudopilins in the T2S system) have a long hydrophobic N-terminal  $\alpha$ -helix preceded by a characteristic type III leader sequence and a globular C-terminal domain (157, 171). The subunits are inserted into the membrane by the Sec system as pre-pilins, with the C-termini outside the cytoplasmic membrane (10, 62). The pilins are processed by a dedicated pre-pilin peptidase (PilD in *Pseudomonas aeruginosa*) that cleaves the leader peptide at the cytoplasmic face of the membrane and methylates the mature pilin (133, 167, 170). Mature pilins are retained in the membrane prior to assembly and, in the case of T4aP, are thought to return to this compartment upon disassembly for reuse in subsequent assembly cycles (48, 118, 162).

In *P. aeruginosa*, T4aP are composed mainly of the highly abundant major pilin subunit, PilA, but minor pilins FimU and PilVWXE are also present at low abundance (65, 119). Similar to the major pilin, minor pilins are processed by the pre-prepilin peptidase, PilD (65, 184). The proposed functions of the minor pilins include priming of assembly, counteracting retraction, contributing to adhesion, and/or modulating the balance between pilus extension and retraction (6-8, 65, 154). The *P. aeruginosa* minor pilins FimU and PilVWXE are encoded in a polycistronic operon with PilY1, a large (~125 kDa) non-pilin protein implicated in anti-

retraction, attachment, and other T4P-related functions (6, 23, 73, 97, 135) (Figure 3.1). In *Neisseria meningitidis* and *P. aeruginosa*, minor pilins are required for surface piliation (36, 65, 73). In *Neisseria gonorrhoeae*, the minor pilins are dispensable, although mutants have a 10-fold or greater reduction in surface piliation (184). In both *P. aeruginosa* and *N. meningitidis*, a few pili are assembled in retraction-deficient double mutants, suggesting that the role of the minor pilins is to optimize assembly (36, 65, 73, 184). Minor pilins are also involved in surface expression of PilY1 and its PilC1/PilC2 counterparts in *Neisseria*, although the specific mechanisms and components required have not been defined (73, 184).

Minor pilins FimU-PilVWX are homologs of the T2S minor pseudopilins GspHIJK (called XcpUVWX in *P. aeruginosa*, EpsHIJK in *Vibrio* spp. and PulHIJK in *Klebsiella* spp.), suggesting that these four proteins are core components of the assembly machinery (66). There are no equivalents of PilE and PilY1 in the T2SS (21, 132) (Figure 3.1). In *N. meningitidis*, the PilE homolog PilX<sub>Nm</sub> was proposed to antagonize pilus retraction, promoting bacterial cell-cell aggregation (74, 75), and to allow conformational changes in the pilus fiber that are important for T4P-mediated signaling (26).

The minor pseudopilins interact via their globular and transmembrane domains (43, 188). The soluble C-terminal domains of

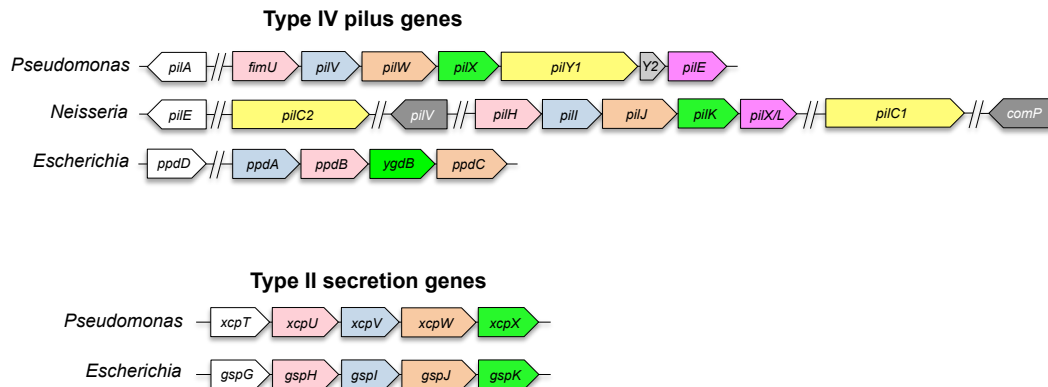


**Figure 3.1. Gene organization of T4P and T2S minor components.**

The organization of pilin, minor pilin, pseudopilin, and minor pseudopilin genes in type IV pili and type II secretion systems of model organisms *P. aeruginosa*, *E. coli* and, *Neisseria* spp. Equivalent genes are similarly colored. Major subunit genes are shown in white. *P. aeruginosa* adhesin and anti-retraction factor PilY1 (yellow) is encoded in the minor pilin operon, whereas its *Neisseria* equivalents, PilC1 and PilC2, are not. *Neisseria*-specific minor pilin genes *pilV* and *comP* (gray) are not clustered with other minor pilin genes. *P. aeruginosa* gene *pilY2*, encoded between *pilY1* and *pilE*, may be a pseudogene. Line breaks (//) denote noncontiguous genomic organization.

*Escherichia coli* GspIJK were crystallized as a heterotrimer (96) whose large size and architecture suggested that it forms the tip of the pseudopilus, with GspK at the distal position to avoid steric clashes.

Studies of *P. aeruginosa* minor pseudopilins revealed similar interactions between the C-terminal domains of XcpVWX and XcpUW (54). However, no interactions between truncated versions of the major pseudopilin XcpT and any of the minor pseudopilins were detected (54), although cross-

linking studies showed interactions between full-length major pseudopilins and minor pseudopilin XcpU in *P. aeruginosa* or its *Xanthomonas campestris* equivalent, XpsH (99, 113). These data imply that the hydrophobic domains normally truncated for biochemical and structural studies are important for interactions between major and minor pilins.

In a recombinant *E. coli* strain overexpressing the *Klebsiella oxytoca* major pseudopilin PulG, the PulHIJK minor pseudopilin complex initiated pseudopilus assembly (44, 55, 158, 177). In the absence of the minor pseudopilins, only rare pseudopili were observed (44). The PulHIJK complex was proposed to initiate assembly by priming the addition of major subunits or by stimulating the assembly motor through formation of a membrane-distorting pseudohelix (43). The first scenario, which implies that the priming complex becomes part of the resulting filament, was not supported experimentally in that study. Interestingly, Cisneros *et al.* (44) later showed that the T4P minor pilins of *E. coli* were interchangeable with the *Klebsiella* T2S minor pseudopilins for priming of either pilus or pseudopilus assembly. However, the T4aP system of *E. coli* is atypical, with only four minor pilins instead of five (no PilE equivalent), and no PilY1 homolog, making it more similar to the T2S system. These features may have provided unusually permissive conditions for cross-complementation.

Here, we used genetic, biochemical, and structural studies to investigate the specific roles of the T4aP minor pilins in *P. aeruginosa*.

PilV, PilW, PilX, and the adhesin PilY1 were mutually dependent on each other for inclusion in pili, and all four were required to recruit PilE. In contrast, FimU was incorporated independently and interacted directly *in vivo* with the major pilin PilA, as well as with minor pilins PilV and PilE. A 1.4 Å high-resolution x-ray crystal structure of FimU revealed its strong resemblance to minor pseudopilin GspH, despite minimal sequence identity. *P. aeruginosa* minor pilins or minor pseudopilins expressed from their native loci primed T4aP assembly and were incorporated into surface-exposed pili, although the full set of T4aP components including PilY1 was required to produce pili in retraction-proficient backgrounds. Together, the data suggest that the T4aP minor pilins form a complex that primes pilus assembly and traffics the T4aP-specific anti-retraction component PilY1 to the cell surface.

## **EXPERIMENTAL PROCEDURES**

*Strains and Growth Conditions* - Bacterial strains were stored at -80 °C in Luria-Bertani broth with 15% glycerol. *P. aeruginosa* strains were grown at 37°C on LB agar plates supplemented with gentamicin (30 µg/ml) or carbenicillin (200 µg/ml). *E. coli* strains were grown at 37°C on LB agar plates supplemented with gentamicin (15 µg/ml), ampicillin (100 µg/ml) or kanamycin (50 µg/ml), as appropriate.

*Generation of Mutants and Complementation Constructs* - Minor pilin and minor pseudopilin operon deletion mutants of *P. aeruginosa* were generated by biparental mating with *E. coli* SM10. 1 kb upstream and downstream of the minor pilin or minor pseudopilin operon were amplified from mPAO1 and cloned into pEX18Gm or pEX18Ap with a GmFRT cassette inserted between the fragments for selection. The pEX18Gm- $\Delta$ MP and pEX18Ap- $\Delta$ MPP::GmFRT were transformed into *E. coli* SM10 for biparental mating with mPAO1 wild-type and *pilT*::Tn strains. The gentamicin resistance cassette was excised using Flp recombinase. Mutants were verified through PCR.

Minor pilin complementation constructs were made previously (64, 65). The *pilY1* complementation construct and minor pseudopilin *xcpUVWX* complementation constructs were created by PCR-amplifying genes from mPAO1 using *Taq* polymerase. *pilY1* was ligated into pCR 2.1 (Invitrogen) and subcloned into pBADGr using the *EcoRI* restriction sites. The *xcpUVWX* PCR product was digested with *EcoRI* and *HindIII* (Thermo Scientific) and ligated with T4 DNA Ligase (Invitrogen) into pUCp20 linearized with the same enzymes. Ligated constructs were transformed into *E. coli* DH5 $\alpha$  and verified by DNA sequencing.

*Isolation of Sheared Surface Proteins, SDS-PAGE Analysis* - Surface proteins were isolated as previously described (67) with the following modifications. Bacterial strains were streaked in a cross-hatched

fashion on a large (150 x 15 mm) 1.5% LB-agar plate containing gentamicin (30 mg/L) or no antibiotic and grown overnight at 37 °C. Centrifugation was performed at 16,100 x g. The pellets for each sample were pooled and resuspended in 120 µl of 1x SDS loading buffer.

*Western Blot Analysis of Sheared Surface Fractions* - Sheared surface protein samples were separated on 15% SDS-PAGE gels for α-FimU, PilV, PilX and PilE blots; 12.5% gels for α-PilW and α-XcpW blots; and 7.5% gels for α-PilY1 blots. Proteins were transferred to nitrocellulose membrane and blocked with 5% (w/v) skim milk at room temperature for 3 h. Blots were incubated with rabbit polyclonal α-FimU (65), PilV, PilW (65), PilY1 (gift from Matthew Wolfgang) (135), PilE (65), XcpW (gift from Romé Voulhoux) at a 1:1000 dilution or α-PilX antibody at a 1:500 dilution overnight at 4°C. Blots were washed with 1x PBS three times for 10 min each and incubated with secondary goat anti-rabbit IgG- alkaline phosphatase conjugated antibody (BioRad) for 1 h at room temperature. Blots were washed as above and developed using NBT/BCIP.

*Interaction of FimU with PilA and Minor Pilins* - Direct protein-protein interactions were tested using the bacterial adenylate cyclase two-hybrid assay as described in Ref. (88) with modifications. Briefly, full-length mature FimU was N-terminally tagged with T18 by cloning it in frame into pUT18C whereas full-length mature PilA and PilV/W/X and PilE were N-terminally tagged with T25 using pKT25. pUT18C-*fimU* was co-

transformed with pKT25-*pilA/V/W/X/E* into the *cya* mutant strain BTH101 (F<sup>-</sup>, *cya*-99, *araD*139, *galE*15, *galK*16, *rpsL*1 (Str<sup>r</sup>), *hsdR*2, *mcrA*1, *mcrB*1). Three colonies of similar size were selected and grown overnight at 30 °C followed by subculturing with 1mM isopropyl β-D-thiogalactopyranoside for induction. Cells were grown to  $A_{600} = 0.6$ . These were spot plated on LB Agar + X-gal and McConkey + maltose and incubated at 30 °C for 24 h. 1 ml of cells were harvested to test β-galactosidase activity using a modified β-galactosidase enzyme assay system with reporter lysis buffer (Promega) where cells were resuspended in 1x PBS and lysed with FastPrep for 20 s prior to following manufacturer's protocol.

*Expression and Purification of FimU, PilV and PilX* - Truncated form of PAO1 *fimU* encoding 1-28 amino acid N-terminally truncated mature protein was PCR-amplified and ligated into the pET151/D-TOPO vector (Invitrogen) to generate an N-terminally His<sub>6</sub> and V5 epitope-tagged protein with TEV protease cleavage site for subsequent removal of the tags. Expression and purification of FimU was performed previously (65) with a few changes. Briefly, *E. coli* Origami B (DE3) cells expressing HisV5- FimU<sub>Δ1-28</sub> were grown overnight at 16 °C following induction of protein expression with isopropyl β-D-thiogalactopyranoside (final concentration 1.0 mM). Cells were lysed by French Press, and proteins were purified by nickel affinity chromatography, followed by TEV cleavage

and a second nickel affinity purification step. Fractions from the second nickel purification containing purified protein were pooled, buffer-exchanged using a HiPrep 26/10 desalting column (GE Healthcare Canada) into 20 mM Tris, pH 8, 50 mM NaCl and concentrated to 25 mg/ml using Vivaspin 15R (Sartorius Stedim Biotech) concentrators. For SAD phasing, selenomethionine (SeMet)-labeled proteins were expressed in Origami B (DE3) using SeMet high-yield M9 minimal media (Shanghai Medicilon) according to the manufacturer's instructions and purified as above.

For polyclonal antibody production, truncated forms of *pilV* and *pilX*, encoding, respectively, 1-28 amino acid and 1-25 amino acid N-terminally truncated proteins were PCR amplified and ligated into pET151/D-TOPO as above. PilV was expressed and purified as above and concentrated to 1 mg/ml. PilX was expressed and lysed as above. To purify the protein from inclusion bodies under denaturing conditions, the pellet was resuspended in 100 mM NaH<sub>2</sub>PO<sub>4</sub>, 10 mM Tris, pH 8, 6 M guanidine HCl, and centrifuged for 20 min at 11,952 x g. The supernatant was loaded onto a nickel affinity chromatography column and purified protein eluted with 250 mM imidazole following a wash with 25 mM imidazole. Both purified PilV and PilX were dialyzed into 1x PBS and sent to Cedarlane Laboratories (Burlington, ON) for immunization of rabbits.

*Structure Determination* - FimU crystals were grown using the hanging drop/vapor diffusion method. Native protein crystals grew in a 1:1 ratio of protein (25 mg/ml FimU in 20mM Tris, pH 8, 50mM NaCl) and precipitant solution (0.2 M sodium chloride, 0.1 M Tris-HCl, pH 8.5, and 25% (w/v) PEG 3350) at 4 °C. FimU SeMet crystals were grown at 20 °C using a 2:1 ratio of protein: precipitant (0.2M ammonium formate, pH 6.6, and 20% (w/v) PEG 3350). All crystals were flash frozen directly in a nitrogen cold stream (100 K) with no further cryo-protection. Diffraction data sets for native and SeMet crystals were collected at wavelengths of 1.1 and 0.979 Å, respectively at the Beamlines X29 and X25 of the National Synchrotron Light Source (Brookhaven, NY).

Data sets were processed using the HKL2000 program suite (137). Using HYSS (4), the expected SeMet sites were located. Phasing, density modification, auto model building, and refinement were carried out using the PHENIX suite of programs (4, 120). Using Coot (58), iterative rounds of manual model building and refinement were performed until R and  $R_{\text{free}}$  values converged and could no longer be improved. The structure of native FimU<sub>Δ1-28</sub> was determined by molecular replacement using the FimU<sub>Δ1-28</sub>-SeMet structure as an initial search model. Molecular replacement and model refinement were performed using the PHENIX suite of programs (4, 120). Stereochemical quality of the models were verified using PROCHECK (103). Data collection and model refinement

statistics for both are listed in greater detail in Table 3.1. Structural illustrations were generated with PyMOL (53).

**Table 3.1. Data collection and refinement statistics**

	SeMet-FimU	Native-FimU
<b>Data Collection</b>		
Beamline	NSLS X25	NSLS X29
Wavelength	0.979	1.100
Space group	P2 <sub>1</sub>	P6 <sub>5</sub>
Unit-cell parameters		
a,b,c (Å)	61.98, 37.25, 103.1	40.69, 40.69, 272.92
$\alpha$ , $\beta$ , $\gamma$ (°)	90.0, 105.3, 90.0	90.0, 90.0, 120.0
No. of mol in ASU	4	2
Resolution range (Å) <sup>a</sup>	50.0-1.35 (1.37-1.35)	50.0-1.40 (1.42-1.40)
Unique reflections	99, 928	49, 829
Data redundancy <sup>a</sup>	6.3 (4.7)	15.4 (8.7)
Completeness (%) <sup>a</sup>	99.8 (96.9)	99.4 (93.9)
I/ $\sigma$ (I) <sup>a</sup>	20.5 (3.2)	53.8 (5.9)
R <sub>merge</sub> (%) <sup>a</sup>	6.5 (42.4)	4.4 (35.4)
Wilson B	14.1	12.94
<b>Model and Refinement</b>		
Resolution range (Å)	49.76-1.35	35.25-1.40
R <sub>work</sub> (%)	17.63	16.42
R <sub>free</sub> (%)	20.27	19.59
No. of reflections	99, 216	48, 996
No. of amino acid residues/atoms	4,733	2,315
No. of waters	821	528
r.m.s.d. bond lengths (Å)	0.006	0.005
r.m.s.d. bond angles (°)	1.052	1.022
Average B (Å <sup>2</sup> )	26.19	24.35
Ramachandran statistics (%)		
Favored	99.45	100.0
Allowed	0.37	0.0
PDB code	4IPU	4IPV

<sup>a</sup> Values in parentheses represent the highest-resolution shell.

## RESULTS

*PilVWX and PilY1 are Dependent on One Another for Incorporation into Pili* - We and others showed previously that minor pilins and PilY1 are present in sheared pilus fractions and that association of PilY1 with T4P depends on one or more of the minor pilins (65, 73, 135). Those data suggested that the minor pilins might form a complex with PilY1 that is subsequently incorporated into T4P. To test this idea, sheared surface proteins that were recovered from retraction-deficient mutants lacking individual minor pilins or PilY1 were probed with specific antibodies to determine how the absence of each component affected incorporation of the others into pili.

All the minor pilins (less FimU) and PilY1 were present in sheared pili from a *fimU pilT* mutant, and FimU was incorporated into pili when any of the other minor pilins or PilY1 was absent (Figure 3.2). We showed previously that pilus assembly was severely impaired in retraction-deficient *pilV*, *pilW* and *pilX* mutants (65), and saw the same trend in the absence of *pilY1* (Figure 3.2). PilV, PilW, and PilX were each dependent on the others for incorporation into pili, and when PilY1 was missing, none of PilV, PilW, or PilX was present. Similarly, PilY1 was detected in sheared surface fractions only when PilV, PilW, and PilX were present. Although full-length PilY1 has a predicted mass of ~125 kDa, we and others (23) routinely detected a smaller fragment (~80 kDa) associated with sheared

T4P. This fragment is recognized by an antibody raised against a C-terminal 60-kDa fragment of PilY1 (135), suggesting it contains this region of the protein. It is not clear if the truncated form of PilY1 is functionally relevant or simply an artifact of the pilus purification procedure. Finally, although PilE was not required for inclusion of PilVWX or PilY1, the absence of any of PilVWX or PilY1 prevented incorporation of PilE into pili (Figure 3.2). In summary, the data suggest that PilVWX and PilY1 form a subcomplex that recruits PilE, and that FimU is not essential for formation of the putative PilVWXY1E complex or its incorporation into pili.

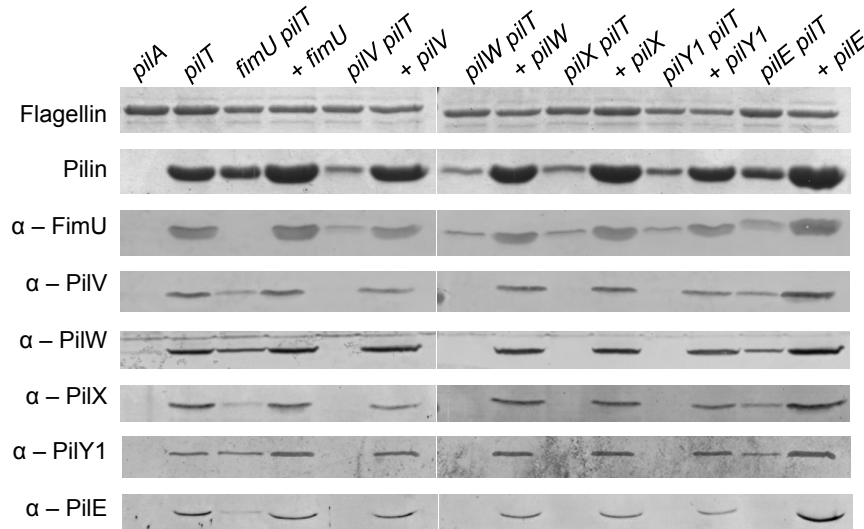


**Figure 3.2. Incorporation of minor pilins into pili.** Pili were sheared from the surface of minor pilin-*pilT* mutants and fractions probed by Western blot for incorporation of the minor pilins using anti-FimU (1/1000), anti-PilV (1/1000), anti-PilW (1/1000), anti-PilX (1/500), anti-PilY1 (1/1000), and anti-PilE (1/1000) antibodies. Proteins were detected at their expected masses except for PilY1, which had an apparent mass of ~80 kDa.

*FimU Interacts with the Major Pilin and Specific Minor Pilins -*

Because FimU was incorporated into pili in the absence of other minor components, we reasoned that it must interact directly with PilA, the major pilin subunit. The interaction of full-length FimU with PilA and the other minor pilins was tested using a bacterial adenylate cyclase two-hybrid assay (88), in which the T18 and T25 fragments were fused to the N termini of mature pilins. FimU interacted with PilA, but also with the minor pilins, particularly PilV and PilE (Figure 3.3). According to the indicator plate assay, FimU interacts with PilX, but the interaction resulted in  $\beta$ -galactosidase activity values only slightly higher than the negative control (Figure 3.3). These data, plus the pilus incorporation data, suggest FimU might couple the putative minor pilin-PilY1 complex to the major pilin through direct interactions with PilE, PilV and PilA.

*High Resolution Crystal Structure of FimU -* To gain further insight into FimU function, we solved the x-ray crystal structures of native and SeMet-substituted versions of its soluble C-terminal domain lacking the N-terminal 28 hydrophobic residues (numbering based on the mature protein; FimU $_{\Delta 1-28}$ ). The protein crystallized in space group P2<sub>1</sub> for the SeMet form and P6<sub>5</sub> for the native form, containing four or two monomers, respectively, in the asymmetric unit. In both crystal forms, FimU was arranged as a tilted antiparallel dimer, with each monomer rotated ~135° relative to the other. The final structures were refined to 1.35 Å (SeMet)

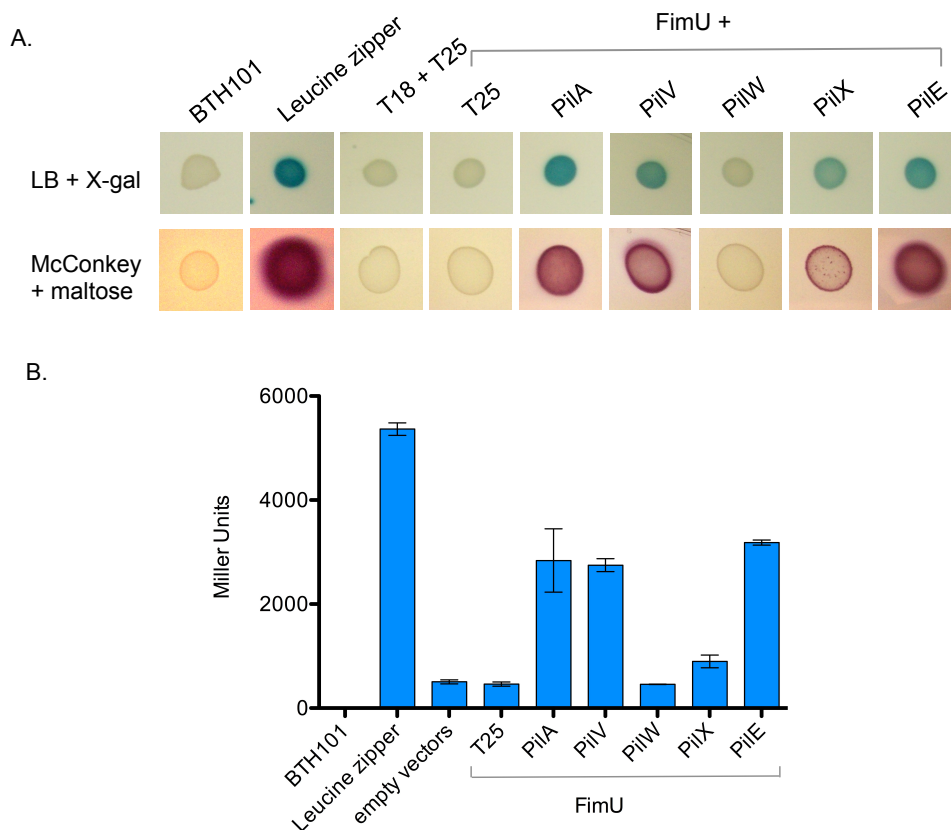


**Figure 3.3. Interaction of FimU with major pilin and minor pilins.**

Direct protein-protein interactions of FimU with the major pilin and other minor pilins were probed using a bacterial adenylate cyclase two-hybrid assay. FimU was N-terminally tagged with the T18 fragment and the major pilin and other minor pilins were N-terminally tagged with the T25 fragment. A, *E. coli* BTH101 recombinants were grown on LB agar + X-gal and McConkey + maltose, producing blue or red colonies, respectively, if there is an interaction. B,  $\beta$ -galactosidase activity of the same strains was measured as described under “Experimental Procedures”. The leucine zipper constructs T18-zip and T25-zip were used as positive controls.

and 1.4 Å (native) resolution. In the SeMet model, all residues of FimU<sub>Δ1-28</sub> could be built into the electron density except for the first two in monomer A, and the first four in monomer B. Details of data collection and model refinement are summarized in Table 3.1.

FimU has a modified type IV pilin fold (Figure 3.4), with an N-terminal α-helix leading into a total of eight β-strands, forming two four-stranded antiparallel β-sheets with noncontinuous strand connectivity. Strands β1, β2, β3 and β5 comprise the first β-sheet, and strands β4, β6, β7 and β8, the second β-sheet. The strands are joined by short loops lacking regular secondary structure. Residues Cys<sup>127</sup> and Cys<sup>158</sup> are connected via a disulfide bond, generating a loop encompassing β7 and β8 that connects the C-terminus to β6.

*FimU is Structurally Similar to T2S Minor Pseudopilin GspH* - The equivalent of FimU in the *P. aeruginosa* T2S system is XcpU (GspH; Figure 3.1), which was previously proposed to connect the minor pseudopilin complex to the major pseudopilin (54). Three structures of GspH homologs have been solved: EpsH from *Vibrio cholerae*, by x-ray crystallography (PDB codes 2QV8 and 4DQ9) (148, 189), and GspH from *E. coli* (PDB code 2KNQ) by NMR spectroscopy. Although there is less than 20% sequence identity between FimU and its GspH homologs, the proteins have similar architectures, characterized by two four- or five-stranded β-sheets with a central β-strand swap (Figure 3.5).

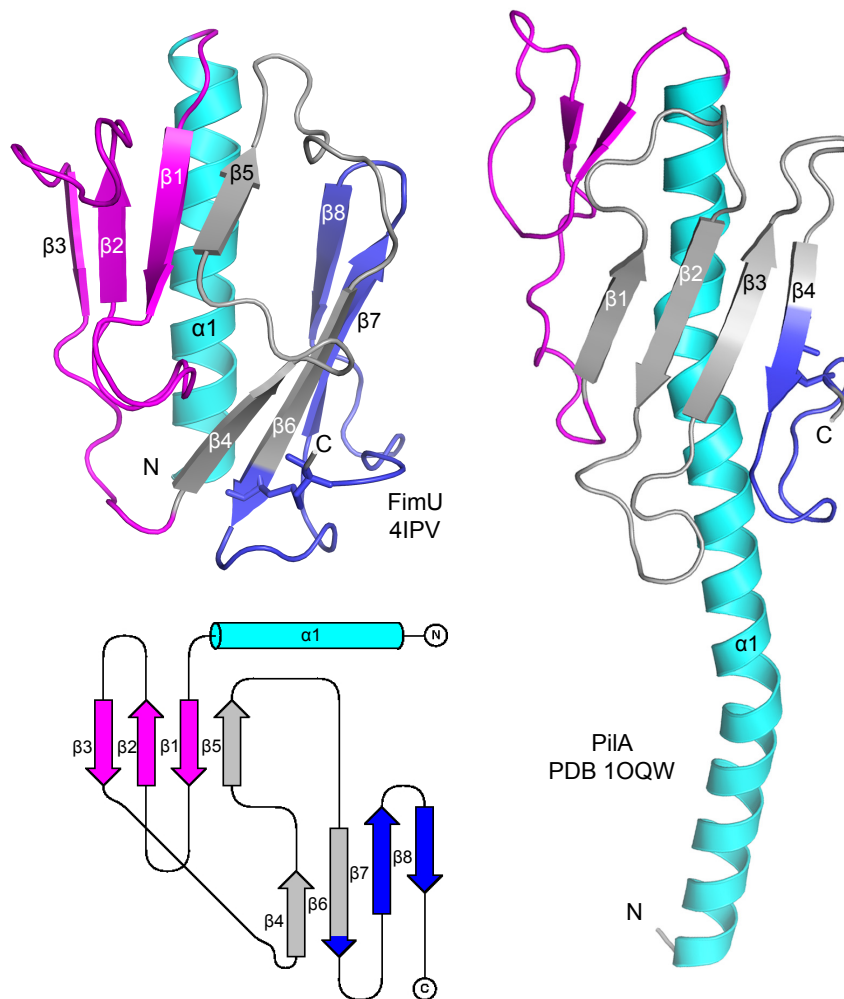


**Figure 3.4. Crystal structure of FimU $_{\Delta 1-28}$ .** The x-ray crystal structure of native FimU $_{\Delta 1-28}$  was solved to 1.4 Å (top left panel). For comparison, the full-length structure of *P. aeruginosa* Pila (PDB code 1OQW) is shown in the right panel. The N-terminal  $\alpha$ -helix is colored cyan;  $\alpha\beta$ -loop is magenta, and the disulfide-bonded loop is blue. The intervening  $\beta$ -strands are colored gray. A topology diagram of FimU (produced using the TopDraw algorithm) depicting the organization of the structural elements is shown in the bottom left panel.

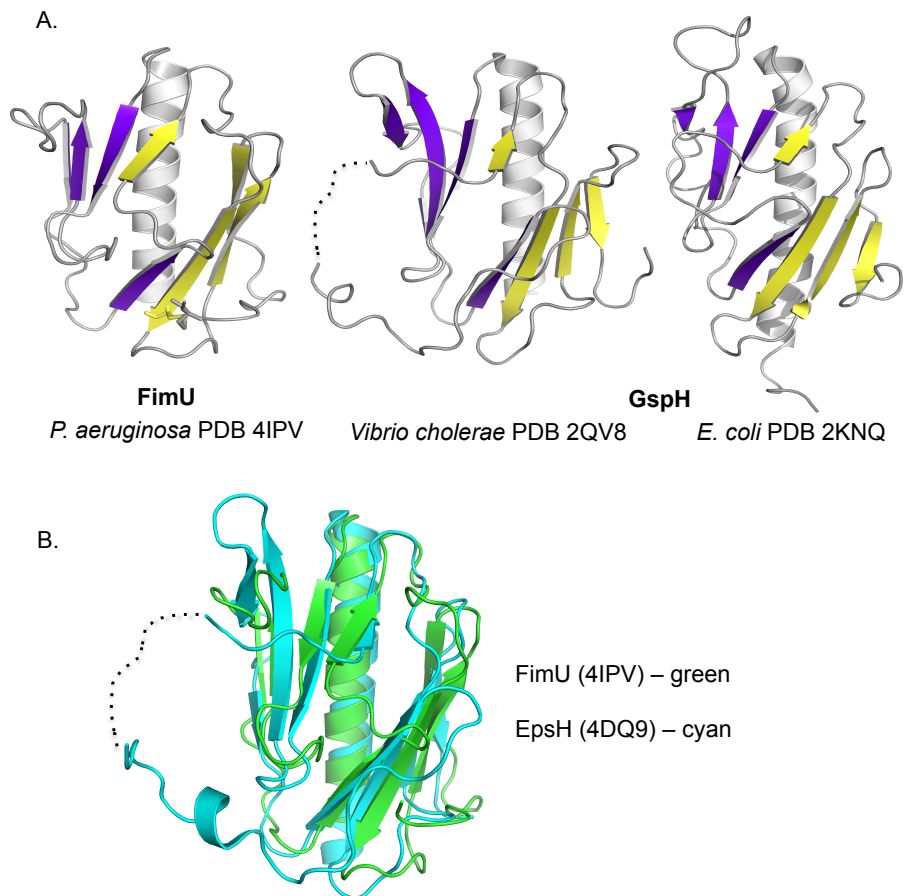


**Figure 3.5. Structural comparison of FimU and T2S pseudopilin GspH.** A, comparison of FimU $_{\Delta 1-28}$  (left panel) with the x-ray crystal structure (middle panel) and NMR solution structure (right panel) of T2S pseudopilin GspH (EpsH) reveals similar architecture. The first four  $\beta$ -strands (five for *V. cholerae* EpsH) are colored in purple. The remaining four are colored in yellow. B, chain A of FimU (green) and EpsH (cyan) align with a root mean square deviation of 2.2 Å.

FimU (PDB code 4IPV, chain A) aligns with EpsH (PDB code 4DQ9, chain A) with a root mean square deviation of 2.2 Å over 106 residues, although EpsH has five  $\beta$ -strands in the first  $\beta$ -sheet, whereas FimU has four (Figure 3.5B). In addition, EpsH has a long, partly disordered loop between swapped  $\beta$ -strands 5 and 6, which extends from the core of the protein. Those residues that could be resolved in this disordered region have different conformations in the two structures, as well as in separate monomers in the asymmetric unit (148). Based on its charged and apparently dynamic properties, this region of EpsH was suggested to be involved in recognition of T2SS secretion substrates (148). In FimU, the corresponding segment (connecting  $\beta$ -strands 4 and 5) is much shorter (five amino acids) and lacks charged residues, resulting in a more compact protein. Despite this difference, the overall striking similarity of the FimU and EpsH/GspH structures and the ability of FimU to interact directly with major and minor pilin subunits support the proposed role for FimU in connecting the major pilin to a putative minor pilin-PilY1 complex.

*Type IVa Pilus Assembly Can Be Primed by Minor Pseudopilins -*

We showed previously that a retraction-deficient mutant lacking the positive regulator of minor pilin operon expression, AlgR, had a small amount of T4aP on the surface, implying that some assembly proceeds in the absence of minor subunits (17, 67). Similarly, Heiniger *et al.* (73)

recovered a small amount of pili in a retraction-deficient strain when all the minor pilin genes were deleted. However, a recent study (44) showed that heterologous expression of T2S minor pseudopilins from *K. oxytoca* supported assembly of the *E. coli* major pilin PpdD in the absence of its cognate minor pilins. *P. aeruginosa* PAO1 encodes a T4aP, a T4bP (Tad) and two T2S systems, Xcp and Hxc (homologous to Xcp) although the Tad and Hxc systems are not expressed under laboratory growth conditions (16, 52). To learn whether the few pili recovered from retraction-deficient mutants lacking the minor pilins could be the result of cross-priming by T2S components, we made mutants lacking the minor pilins and/or the Xcp minor pseudopilins.

Consistent with previous studies (67, 73, 184), when the entire minor pilin operon was deleted (denoted  $\Delta MP$ ) in a retraction-deficient strain, the  $\Delta MP$  *pilT* double mutant retained a small amount of surface pili (Figure 3.6A). There was no effect on piliation when the minor pseudopilin genes were deleted (denoted  $\Delta MPP$ ) in the *pilT* background. However, when both sets of minor subunit genes were deleted, no surface pili were recovered (Figure 3.6A). Therefore, pili assembled in the absence of the minor pilin operon were primed by the minor pseudopilins, and at least one set of minor components is necessary for pilus assembly. Levels of surface pili commensurate with the *pilT* control were restored upon complementation with either the minor pilin or the minor pseudopilin genes

in *trans*. In contrast, piliation of the  $\Delta MP$  *pilT* double mutant – in which the minor pseudopilins are expressed at native (low) levels from their chromosomal locus – was reduced compared to the *pilT* control (Figure 3.6A). Expression of the minor pseudopilins from a multicopy vector increases their levels in the cell and thus the amount of pili assembled (Figure 3.6A and B, compare the third and last lanes).

In a previous study (44), *E. coli* T4aP assembly could be primed by *Klebsiella* minor pseudopilins, but it was unclear whether the minor subunits were incorporated into the pili or simply activated the assembly machinery (29, 44). To resolve this uncertainty, we probed sheared pilus fractions from retraction-deficient mutants with an antibody to the minor pseudopilin, XcpW. In the absence of the T4aP minor pilins, XcpW was found in sheared surface protein fractions, suggesting it was incorporated into pili (Figure 3.6A). However, when both sets of minor components were expressed at native levels from their chromosomal loci, in the *pilT* single mutant, XcpW was not detectable in sheared pili. Taken together, the data suggest that the T2S minor pseudopilins can prime T4aP assembly and as a result become part of the filament. However, the T4aP minor pilins are used preferentially for assembly when both sets of minor subunits are expressed at physiological levels.

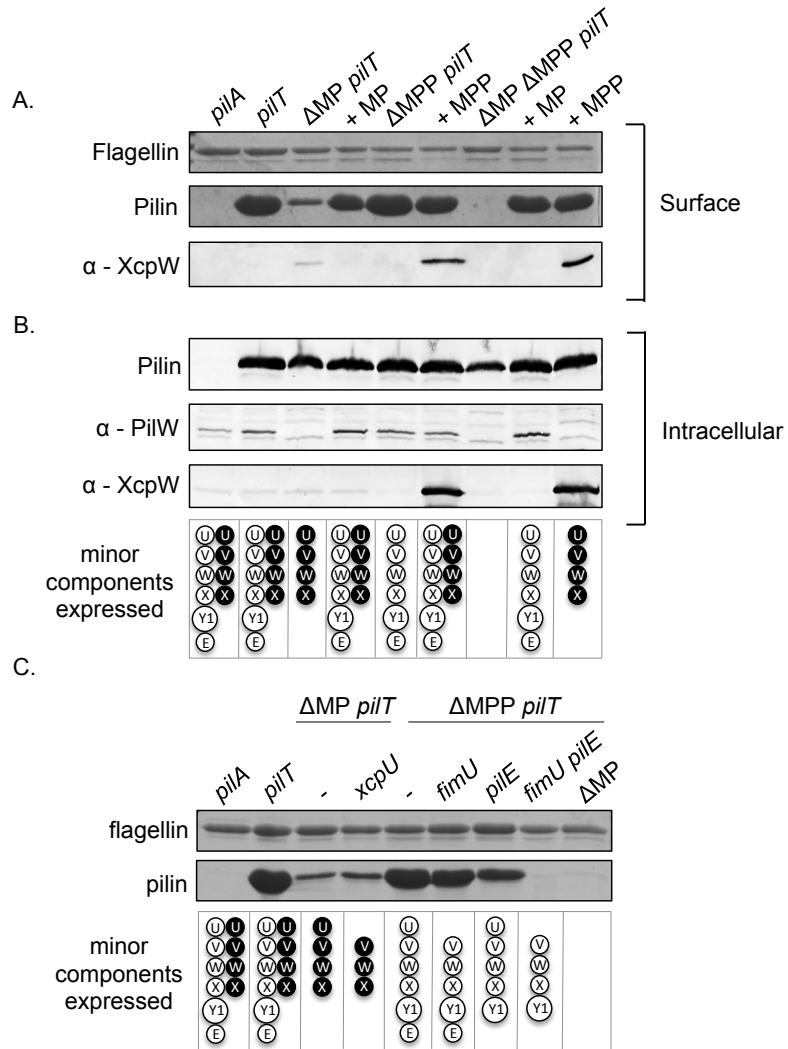


**Figure 3.6. Pilus assembly in the absence of minor components.** A, pilus assembly in the absence of minor components was probed by shearing surface proteins from a *pilT* mutant lacking the minor pilin *fimUpilVpilWpilXpilY1pilE* and minor pseudopilin *xcpUVWX* operons compared with single operon mutants and complementation with either operon and analyzing by SDS-PAGE. The flagellin band was used as a loading control. The sheared surface protein samples were probed for the incorporation of minor pseudopilin XcpW into the pilus by Western blot analysis with an XcpW specific antibody (1/1000). B, cells recovered following shearing of surface proteins were lysed, separated by SDS-

PAGE, and probed for levels of PilA, PilW, and XcpW using PilA (1/5000), PilW (1/1000), and XcpW (1/1000) specific antibodies. C, mutants made in minor pilin or minor pseudopilin retraction-deficient backgrounds were used to identify the minimum number of minor components required for pilus assembly by shearing the surface proteins from the cell and analyzing the surface pilus fractions by SDS-PAGE. The flagellin band was used as a loading control.

*A Subset of Minor Components Can Prime Assembly - To*

determine how many and which minor components are required for pilus assembly, additional mutations were introduced into  $\Delta MP$  *pilT* or  $\Delta MP$  *pilT* mutant backgrounds. In the absence of both the putative connectors FimU and XcpU, assembly of surface pili could still be initiated by the minor pilins PilVWXE plus PilY1, or by the minor pseudopilins, XcpVWX (Figure 3.6C). In the absence of both FimU and PilE, where only PilVWXY1 are expressed, surface piliation was abolished (Figure 3.6C). These data suggest that despite being the nominal equivalent of the XcpVWX subcomplex, PilVWXY1 alone are insufficient for priming of surface piliation and that FimU and PilE may cooperate to stably couple the priming complex to the major subunit (Figure 3.7).

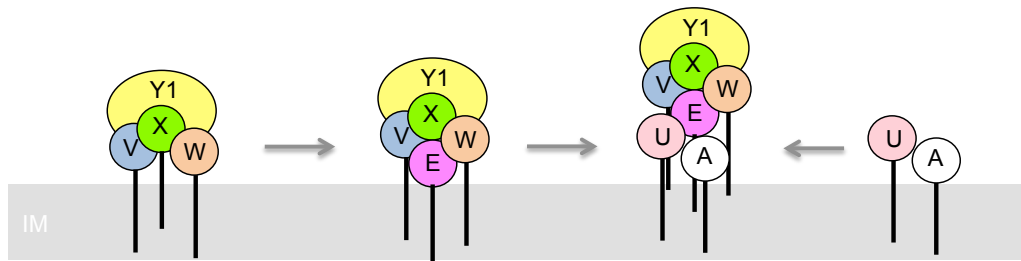


**Figure 3.7. Model of pilus assembly.** PilVWX and PilY1 interact, creating an interface that is bound by PilE. FimU interacts directly with PilA and connects it with the PilVWXY1E subcomplex through interactions with PilV and PilE.

## DISCUSSION

*Identification of a Putative Minor Pilin-PilY1 Complex* - It has been challenging to assign specific functions to minor pilins because individual mutants have a similar “no pili” phenotype (6-8, 36, 65, 154). We found that PilVWX and the large ~125-kDa non-pilin protein PilY1 depend on one another for pilus incorporation, implying that they form a putative complex that becomes incorporated into pili. The late recruit PilE is encoded by the last gene in the minor pilin operon (Figure 3.1), positioning it as a potential quality control checkpoint; it appears to recognize an interface formed by the putative PilVWXY1 subcomplex and does not appear in sheared pili if any of those components is missing. PilE interacts with the other minor pilins in the BTH assay, supporting this idea (Nguyen, Bell, Sugiman-Marangos, Junop, and Burrows, in preparation). Finally, under retraction-deficient conditions, FimU is not essential for formation or

incorporation of PilVWXY1E into pili, and vice versa, consistent with its proposed role as a stabilizing ‘connector’ subunit (below).

PilY1 is implicated in a number of pilus-related functions including adhesion, calcium-dependent antagonism of pilus retraction, and integrin binding (73, 82, 135). Our results suggest that PilVWX and PilY1 form a subcomplex that associates with PilE, although the exact nature of their interactions is not yet clear. *P. aeruginosa* PAO1 PilY1 was previously suggested to have a type IV pilin-like N terminus with a potential PilD cleavage site (108), but the N-terminal sequence is not conserved among *P. aeruginosa* strains (182). Instead, its hydrophobic N-terminal signal is more likely cleaved by signal peptidase 1, as predicted by SignalP (142).

Based on its size and adhesin function, we propose that PilY1 could be located at the distal position of a putative PilVWXY1E complex, placing it ultimately at the tip of a pilus. This hypothesis is based in part on the structure of the *E. coli* minor pseudopilin complex, where GspK, a subunit with a large  $\alpha$ -domain insertion between  $\beta$ 2 and  $\beta$ 3 that would prohibit the addition of subunits above it because of potential steric clashes, occupies the distal position (60, 96). The equivalent of GspK in the T4aP system, PilX, is significantly smaller (185 residues versus 316), which may allow for an additional component at the distal position. The exact nature and duration of PilY1 association with the minor pilins remains under investigation, but positioning PilY1 at the tip of the pilus could facilitate its

anti-retraction function, which requires a conserved calcium-binding motif in the C-terminal portion of the protein (135). We propose that calcium binding by PilY1 causes a conformational change, similar to opening of a drywall anchor, that enhances adhesiveness and/or prevents re-entry into the cell upon retraction. As a result, a minor pilin-PilY1 complex may be retracted only as far as the outside of the secretin but not re-enter the cell, explaining why PilY1 has been reported to be both T4aP- and cell surface-associated (23, 73). This scenario could allow for efficient pilus re-extension, since major subunits need only be added at the base of an existing pilus stub.

A link between minor pilins and PilY1-like proteins has also been reported in *Neisseria*. In *N. gonorrhoeae*, the PilY1 homologs PilC1 and PilC2 were undetectable in purified pili fractions in the absence of minor subunits PilHIKL (equivalent to FimU-PilVXE) and when *pilC1* or *pilC2* was deleted, the minor pilins PilHIKL were missing from purified pili (184). In addition, PilHIJKL are required for adherence (184), which we suggest is potentially due to association with PilC1/2. In *N. meningitidis*, *pilIJK* (equivalent to *pilVWX*) retraction-deficient mutants are also defective for adherence, although whether PilC1/2 was present in those mutant pili was not determined (36).

Unfortunately, we currently lack biochemical evidence for a minor pilin-PilY1 complex. Extensive efforts to purify individual components for

protein interaction studies, as was done for the T2S minor subunits (54), have not been successful in all cases. PilX in particular has been insoluble in all forms tested so far, and purification of full-length PilY1 by our lab and others has also proven difficult (135). We are now working towards co-purifying all six components expressed from a single construct to preserve their native stoichiometry and interactions.

*The Putative Connector Subunit, FimU* - Our FimU structure (Figure 3.4) is the first for a T4P minor pilin from *P. aeruginosa*, and for the FimU/PilH family. The structures of *N. meningitidis* minor pilins PilX<sub>Nm</sub> (equivalent to PilE) and ComP (no equivalent in *P. aeruginosa*) have been solved (42, 75); however, deletion of these proteins does not affect piliation, suggesting that they modulate pilus properties, rather than controlling pilus assembly (27, 74, 80). FimU strongly resembles minor pseudopilin GspH (Figure 3.5), proposed to link the GspIJK tip subcomplex to the major pseudopilin (54).

One notable difference between FimU and GspH is the length of the loop between the swapped  $\beta$ -strands (Figure 3.8). In the pseudopilin, this region was proposed to participate in selection of secretion substrates (148). There is no evidence that T4aP system of *P. aeruginosa* is involved in secretion, and the short uncharged loop in the corresponding position of FimU may reflect this divergence in function. A Phyre2 (91) model of the FimU equivalent from *N. meningitidis*, PilH<sub>Nm</sub>, suggests that it too has a

short loop between the central swapped  $\beta$  strands, but a predicted loop insertion between  $\beta$ -strands 1 and 2 that accounts for its larger size (213 residues for mature PilH<sub>Nm</sub> compared to 159 for FimU; Figure 3.8).

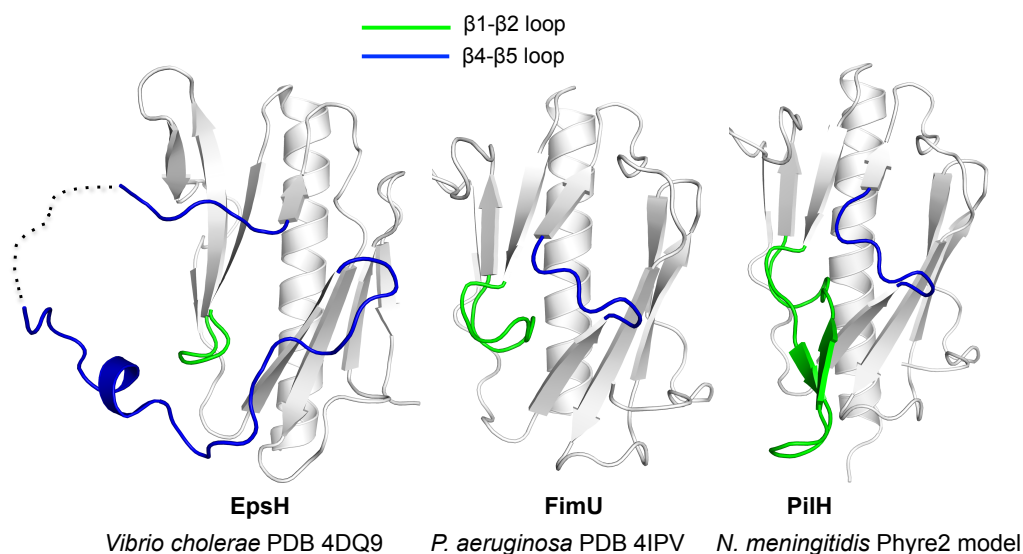


**Figure 3.8. Comparison of loops in FimU, PilH<sub>Nm</sub>, and EpsH.**

Comparison of truncated *V. cholerae* T2S pseudopilin EpsH (left panel) with *P. aeruginosa* FimU (center panel) and a Phyre2-generated model of *N. meningitidis* PilH (right panel) showing differences in the  $\beta$ 1-  $\beta$ 2 (colored green) and  $\beta$ 4-  $\beta$ 5 loops (colored blue).

Although incorporation of FimU into surface-exposed pili was independent of the other minor pilins and PilY1 (Figure 3.2), this pattern is not conserved among species. In *N. gonorrhoeae*, the PilJ<sub>Ng</sub> protein (equivalent to *P. aeruginosa* PilW) was the only component found in surface pili in the absence of the others. Incorporation of PilH<sub>Ng</sub> (equivalent

to FimU) into surface pili depends on PilJJK (PilVWX) (184). The reasons for these differences are unclear, but may reflect the need for the *Neisseria* minor pilin complex to accommodate more than one PilC variant and/or the minor pilins PilV and ComP (2, 152, 183), not present in *P. aeruginosa*. The predicted insertion between  $\beta$ 1- $\beta$ 2 in PilH<sub>Nm</sub> may also be related to these differences between species.

Although our data support a role for FimU in connecting a minor pilin-PilY1 complex to the major pilin, it was dispensable for pilus assembly in a retraction-deficient background. In *fimU pilT* mutants, PilA likely interacts with the minor pilin-PilY1 subcomplex via PilE and PilV, its closest homologs among the minor pilins, to allow for assembly. When both of FimU and PilE were absent, no pili were assembled (Figure 3.6C). Interestingly, FimU and PilE are the only minor pilins with a Pro<sup>22</sup> residue, similar to the major pilin. Pro<sup>22</sup> creates a kink in the N-terminal helix, controlling inter-subunit packing. The conformation conferred by this residue may facilitate interactions of FimU and PilE with one another and with major pilin subunits. These similarities may also lead to the occasional incorporation of individual minor subunits into the pilus that we reported previously (15).

*Minor Subunits Prime Pilus Assembly* - Because a few pili were still produced in minor pilin-deficient strains when retraction was blocked, the roles of minor pilins have been unclear (67, 73, 184). Here we found that

pilus assembly is abolished when both the minor pilins (plus PilY1) and minor pseudopilins are missing (Figure 3.6A), and that the minor pilins plus PilY1 or the minor pseudopilins can restore piliation (Figure 3.6A), suggesting a conserved role in initiation of pilus assembly. Cisneros *et al.* (44) showed that *K. oxytoca* minor pseudopilins primed assembly of *E. coli* PpdD pili and *E. coli* minor pilins primed assembly of *K. oxytoca* pseudopili. As a caveat, *E. coli* has only four minor pilins (equivalent to FimU-PilVWX) and lacks PilY1 and PilE homologs (Figure 3.1), making its T4aP system more similar to the T2S system and potentially facilitating the reported cross-complementation. Our data show that the Xcp minor pseudopilins, expressed at native levels from their chromosomal locus in the  $\Delta$ MP *pilT* mutant, can prime pilus assembly (Figure 3.6A), confirming the findings in *E. coli* and showing that a subcomplex containing the T4aP-specific components PilY1 and PilE is not essential for initiation of *P. aeruginosa* T4aP assembly.

*Minor Subunits Are Part of the Pilus Filament* - Cisneros *et al.* (43, 44) suggested that priming of pilus assembly by minor subunits could occur by creation of a priming complex to which major subunits were subsequently added or by stimulation of motor activity, without minor subunits becoming part of the resulting filament (29, 43, 44). Our data and that of Winther-Larsen *et al.* (184) support a model (Figure 3.7) in which the minor subunits and PilY1 form a complex that becomes part of the

pilus, because all components are found in sheared fractions (Figure 3.2). In the case of priming by the minor pseudopilins, we had antisera for only XcpW (Figure 3.6). However, XcpUVWX have been shown to form a complex (54); thus XcpUVX are likely also present. Despite this evidence for incorporation of minor subunits into pili, we note recent reports suggesting that minor pilins can exert specific functions from within the periplasm. When fused to a bulky fluorescent protein that prevented them from being displayed on the cell surface, *N. meningitidis* minor pilins PilX<sub>Nm</sub> (equivalent of PilE) and PilV<sub>Nm</sub> (no *P. aeruginosa* equivalent) modulated pilus assembly independent of pilus incorporation (80). Although these proteins were not detected in surface pilus fractions, processing by the prepilin peptidase PilD was required for their function, suggesting that at least partial extraction from the inner membrane was necessary. In *P. aeruginosa*, PilW, PilX, and PilY1 repressed swarming motility independent of PilD processing and pilus assembly, by modulating levels of secondary messenger c-di-GMP (97, 98). The signaling pathways involved in these novel phenotypes require further investigation.

*Minor Pseudopilins Cannot Replace Minor Pilins when Retraction is Active* - When retraction is active, *P. aeruginosa* cells become non-piliated if they are missing even a single minor pilin or PilY1 (6-8, 65, 154), even though the Xcp minor pseudopilins are concurrently expressed (based on detection of XcpW in whole cell lysates; data not shown). Increased

expression of XcpUVWX from a plasmid in trans does not restore surface piliation or twitching motility in retraction-proficient minor pilin mutants (data not shown). There are at least two reasons why the minor pseudopilins may be unable to substitute for minor pilin function under conditions where retraction is active.

First, the minor pilins are used preferentially for assembly when both sets of minor components are expressed at physiological levels (Figure 3.6A), suggesting a higher affinity for the major pilin. Lower affinity of the minor pseudopilins for the major pilin may lead to inefficient pilus extension that is unable to compete with retraction. We showed previously (67) that compatibility between major and minor subunits was important for efficient piliation. Each *P. aeruginosa* strain encodes one of two different sets of minor pilins, each associated with specific major pilin alleles. When the major subunit from one strain is expressed in another that has heterologous minor pilins, both assembly and twitching motility are impaired (67). Thus, optimal interactions among the major and minor subunits have an important role in regulating extension-retraction dynamics.

Alternatively, incorporation of a stable subcomplex containing the anti-retraction factor PilY1 may be mandatory for pili to remain on the cell surface in retraction-proficient strains. Although the minor pseudopilins can prime assembly in retraction-deficient backgrounds, the resulting pili

lack PilY1 and PilE (data not shown), suggesting that those components are unable to interact with the Xcp subunits. Thus, pili primed by the T2S minor subunits lack factors that oppose retraction. In *P. aeruginosa* *fimU* or *pilE* single mutants that express pili containing PilVWX-PilY1 complexes (Figure 3.2), we speculate that stable interaction of the PilVWX-PilY1 subcomplex with the major subunit, as well as the resulting capacity to oppose retraction, is compromised. The evolution of a pilus-associated subcomplex containing the T4aP-specific components PilY1 and PilE, coupled with the high expression level of major subunits compared to the T2S system, likely represent adaptations of the ancestral secretion system to promote formation of long surface-exposed filaments that perform the myriad of functions associated with T4aP.

## **ACKNOWLEDGMENTS**

We thank Rami El-Sebai and Colin Rous for generating pilY1 mutants and complementation constructs, and Drs. Romé Voulhoux and Matthew Wolfgang for providing antisera. This work was funded by grants from the Canadian Institutes of Health Research (CIHR) MOP 93585 to LLB and MOP 89903 to MSJ. YN held a Graduate Studentship from Cystic Fibrosis Canada and holds a Banting Scholarship from CIHR.

# **CHAPTER FOUR**

**Structural and functional studies of the**

***Pseudomonas aeruginosa* minor pilin,**

**PiE**

## **Preface**

Chapter Four consists of the following manuscript for submission:

**Nguyen Y, Harvey H, Sugiman-Marangos S, Bell SD, Buensuceso RNC, Junop MS, Burrows LL. 2015.** Structural and functional studies of the *Pseudomonas aeruginosa* minor pilin, PilE.

Attributions:

Y.N. performed the interaction experiments and twitching motility assays.

Y.N. isolated sheared surface fractions and intracellular fractions, H.H.

performed SDS-PAGE and western blot analysis. Y.N. cloned and

expressed the protein, S.D.B. purified the protein and set up crystal trays.

R.N.C.B. performed fluorescence microscopy. S.S.M. and M.S.J. collected

diffraction data. Y.N. solved the structure with help from S.S.M. Y.N.,

M.S.J. and L.L.B designed the experiments. Y.N. and L.L.B. wrote the

manuscript.

**Structural and functional studies of the *Pseudomonas aeruginosa***

**minor pilin, PiE**

Ylan Nguyen<sup>1</sup>, Hanjeong Harvey<sup>1</sup>, Seiji Sugiman-Marangos<sup>1</sup>, Stephanie D. Bell<sup>1</sup>, Ryan N.C. Buensuceso<sup>1</sup>, Murray S. Junop<sup>2</sup> & Lori L. Burrows<sup>1</sup>

<sup>1</sup> Department of Biochemistry and Biomedical Sciences and the Michael G. DeGroote Institute for Infectious Disease Research, McMaster University, Hamilton, ON, CANADA

<sup>2</sup> Department of Biochemistry, Western University, London, ON, CANADA

**\*Running Title:** *Pseudomonas aeruginosa* minor pilin, PiE

**To whom correspondence should be addressed:**

Dr. Lori L. Burrows, 4H18 Health Sciences Centre, 1280 Main St. West,  
Hamilton, ON, L8S 4K1, CANADA

Tel: (905)-525-9140 ext: 22029,

Fax: (905) 522-9033,

E-mail: burrowl@mcmaster.ca

## ABSTRACT

Many bacterial pathogens including *Pseudomonas aeruginosa* use type IV pili (T4P) for attachment, motility and biofilm formation. T4P are primarily composed of monomers of the major pilin subunit, which can be repeatedly assembled and disassembled to mediate function. A group of pilin-like proteins called the minor pilins (FimU, PilV/W/X/E) prime pilus assembly, resulting in their incorporation into the pilus. Our previous work showed that minor pilin PilE is dependent on the putative priming subcomplex of PilVWX plus PilY1 for incorporation into pili, and that with FimU, PilE functions as a connector protein to couple the priming subcomplex to the major pilin PilA, allowing for efficient pilus assembly. Here we provide support for this model, showing direct interaction of PilE with other minor pilins and the major pilin. The 1.25 Å crystal structure of PilE<sub>Δ1-28</sub> shows a typical type IV pilin fold, showing how it may be incorporated into the pilus. Despite very low sequence identity, PilE has a high level of structural similarity to *Neisseria meningitidis* minor pilins PilX<sub>Nm</sub> and PilV<sub>Nm</sub>, recently suggested via characterization of mCherry fusions to modulate pilus assembly from within the periplasm. In *P. aeruginosa*, a PilE-mCherry fusion failed to complement twitching motility or piliation of a *pilE* mutant. However, in a retraction-deficient background, engineered so that surface piliation depends solely on PilE, the fusion construct restored low levels of surface piliation. The PilE-mCherry fusion

was present in sheared surface fractions from that strain, suggesting that both it was incorporated into pili. Together, these data provide evidence that PilE, the sole equivalent of PilX<sub>Nm</sub> and PilV<sub>Nm</sub> in *P. aeruginosa*, likely connects a priming subcomplex to the major pilin to promote efficient assembly of T4aP.

## INTRODUCTION

Type IV pili (T4P) are long, thin, fibrous surface appendages found in gram-negative and gram-positive bacteria, as well as archaea (5, 141). They function in attachment, twitching motility, DNA uptake, electron transfer, and biofilm formation (49, 141). There are two main classes of T4P, type IVa and type IVb, distinguished by characteristic differences in their subunits and assembly machineries (14, 49, 141). The pili are typically composed mainly of thousands of major subunits, but minor (low abundance) subunits are also present, potentially at the tip of the pilus due to their role in priming of pilus assembly (48, 65, 74, 118, 130, 184).

Major pilin subunits are expressed as pre-pilins, which are processed to assembly-competent mature subunits by removal of their type III signal sequence and methylation of the new N-terminus by a bi-functional pre-pilin peptidase/N-methylase (157, 167, 170, 171). While diverse in sequence, T4a major pilins share a conserved fold, consisting of an extended N-terminal  $\alpha$ -helix connected to a four-stranded antiparallel  $\beta$ -

sheet (48). The N-terminal  $\alpha$ -helices, which form the hydrophobic inner core of an assembled pilus fiber, can be divided into two segments,  $\alpha$ 1-N and  $\alpha$ 1-C, with the highly conserved, hydrophobic  $\alpha$ 1-N segment retaining the monomers in the inner membrane prior to assembly. The globular C-terminal head domains decorate the exterior of the pilus and commonly contain a disulfide bond connecting the C-terminus to the conserved  $\beta$ -sheet, forming a disulfide-bonded loop (DSL) also known as the D-region (49). Consistent with their incorporation into pili, the minor pilins are also processed by the pre-pilin peptidase and, based on the limited number of structures available, have an architecture similar to major pilins (42, 65, 75, 130, 184).

The T4P system is evolutionarily related to the type II secretion (T2S) system, which forms a short pilus-like fibre in the periplasm that acts as a piston during the secretion of select exoproteins (55, 76). The T2S system has a set of four minor subunits, called the minor pseudopilins, which prime pseudopilus assembly (43). The four minor (pseudo)pilins are conserved between T2S and T4aP systems, suggesting that they are core components of (pseudo)pilus assembly (66). In support of this idea, the *Escherichia coli* K-12 T4aP core minor pilins can prime heterologous assembly of *K. oxytoca* pseudopili and vice versa (44).

Unlike *E. coli*, the T4aP systems of *Pseudomonas aeruginosa* and *Neisseria* spp. have additional, non-core T4P-specific minor pilins (66). In

*P. aeruginosa*, the core minor pilins are called FimU, PilV, PilW, PilX, and are encoded in an operon with anti-retraction protein PilY1 and the non-core minor pilin, PilE (17). We recently showed (130) that PilVWX and PilY1 are dependent on each other for incorporation into the pilus, suggesting they form a subcomplex, and that the presence of this putative subcomplex was required for PilE to be recovered in the pilus fraction. We proposed that (among other functions) the minor pilins prime pilus assembly, similar to the minor pseudopilins, and are thus assembled into the pilus fiber (130).

While *P. aeruginosa* has only 1 non-core minor pilin called PilE, *N. meningitidis* has three non-core minor pilins, PilX<sub>Nm</sub>, PilV<sub>Nm</sub>, and ComP. The PilX<sub>Nm</sub> protein (called PilL<sub>Ng</sub> in *N. gonorrhoeae*) is potentially orthologous to *P. aeruginosa* PilE, based on the syntenic location of both genes at the 3' ends of their respective minor pilin operons and their limited sequence identity. However, PilV<sub>Nm</sub>, another non-core subunit encoded elsewhere in the *Neisseria* genome, is also a potential PilE orthologue. It is more similar to *P. aeruginosa* PilE than PilX<sub>Nm</sub> (35% identity, versus 27% for PilX<sub>Nm</sub>), and in length (122 residues for mature PilV<sub>Nm</sub>, 134 for PilE, and 152 for PilX<sub>Nm</sub>), raising the possibility that *N. meningitidis* encodes two PilE equivalents. PilX<sub>Nm</sub> and PilV<sub>Nm</sub> share 25% identity (Figure S4.1), can be incorporated into pili, and modulate a number of pilus-associated phenotypes, though neither is essential for

assembly (74, 75). Previous studies reported only subtle differences in piliation status of single mutants, but *pilV<sub>Nm</sub> pilX<sub>Nm</sub>* double mutants have no surface pili (27, 80, 172, 184). The X-ray crystal structure of the C-terminal domain of PilX<sub>Nm</sub> revealed a canonical type IV pilin fold, with  $\alpha$ 1-C connected to a four-stranded antiparallel  $\beta$ -sheet ending in a disulfide bonded loop (75). Its D-region contained an additional short helix and a hook-like loop implicated in opposing pilus retraction, via inter-subunit interactions between antiparallel pilus fibres (75).

A recent study suggested that PilX<sub>Nm</sub> and PilV<sub>Nm</sub> do not have to be incorporated into pili to function (80). Imhaus and colleagues fused the fluorescent mCherry protein to the minor pilins' C-termini, with the assumption that the fusion proteins became too bulky to traverse the outer membrane secretin, trapping them in the periplasm. However, both fusions complemented their cognate mutants (80). They further showed that pilus-related functions are dependent on the number of pili expressed on the surface, and suggested that PilX<sub>Nm</sub> and PilV<sub>Nm</sub> optimize the initiation of pilus assembly, thus influencing the number of surface pili produced and the resulting biological outputs (80).

Here, we investigated the role of the *P. aeruginosa* minor pilin PilE in pilus assembly. We show that PilE interacts with the major pilin subunit and other minor pilins, supporting its proposed role as a connector of a minor pilin subcomplex to the major pilin-containing fiber during initiation of

pilus assembly. Our 1.25 Å high-resolution structure of PilE<sub>Δ1-28</sub> revealed a high level of structural similarity to PilX<sub>Nm</sub> despite their limited sequence identity, and structural modeling suggested that PilV<sub>Nm</sub> is more similar to PilE than to PilX<sub>Nm</sub>. A PilE-mCherry fusion failed to complement a *pilE* single mutant for piliation and motility, but expression of PilE-mCherry in a retraction-deficient background where pilus assembly depends solely on PilE revealed that the fusion was functional, and incorporated into surface pili. We suggest that *Neisseria* may have two PilE orthologues that can partly compensate for one another's function, while *P. aeruginosa* has only a single – and thus essential – non-core subunit. These findings shed new light on the species-specific structural and functional differences between these related T4aP minor subunit proteins.

## **EXPERIMENTAL PROCEDURES**

### **Bacterial strains and plasmids**

Bacterial strains and plasmids used in this study are listed in Table 4.1. Bacterial strains were stored at -80 °C in LB supplemented with 15 % glycerol. *E. coli* strains were grown at 37°C, unless otherwise stated, on LB agar containing ampicillin (100 µg/ml), kanamycin (50 µg/ml), gentamicin (15 µg/ml) or chloramphenicol (30 µg/ml), as appropriate. *P. aeruginosa* strains were grown at 37°C on LB agar containing gentamicin (30 µg/ml).

### **Bacterial adenylate cyclase two-hybrid assay**

A bacterial adenylate cyclase two-hybrid assay (88) was used to test for protein-protein interactions between PilE and other pilins. The DNA sequence encoding full-length, mature *P. aeruginosa* PAO1 PilE was PCR-amplified using the forward and reverse primers: 5' GCATCTAGACTTCACGTTGCTGGAAATGGTGGTGGT 3' and 5' CATGGTACCTCAGCGCCAGCAGTCGTTGAC 3', respectively, followed by restriction digest with XbaI and KpnI for directional cloning into pUT18C for a T18 N-terminally tagged protein. Similarly, full-length mature FimU was N-terminally tagged with T25 by PCR amplifying *fimU* with the forward and reverse primers: 5' GCATCTAGACTTCACCCTGATCGAGTTGCTGAT 3' and 5' CATGAATTCTCAATAGCATGACTGGGGCGCCT 3', respectively, followed by digestion with XbaI and EcoRI for cloning into pKT25. Plasmids were confirmed by sequencing. pUT18C-*pilE* was co-transformed with pKT25-*fimU* or pKT25-*pilA/V/W/X* (130) into *E. coli* BTH101 for interaction experiments. Briefly, a single colony from each transformation was grown in LB supplemented with kanamycin (50 µg/ml) and ampicillin (100 µg/ml) overnight at 30°C, followed by subculturing into fresh media with antibiotics and 1 mM IPTG for induction. Cells were grown to OD<sub>600</sub> = 0.6 and spot plated in triplicate on LB agar + X-gal and McConkey agar + maltose and incubated at 30 °C for 24 h. A T18 and T25

tagged leucine zipper expressed from pT18-zip and pT25-zip (88) was used as a positive control. The experiment was performed in triplicate and representative images were taken.

### **Protein expression and purification**

PAO1 *pilE* encoding N-terminally truncated mature PilE<sub>Δ1-28</sub> was PCR amplified using forward primer 5' CACCATCCGCTCCAACCGC 3' and reverse primer 5' TCAGCGCCAGCAGTCGTT 3'. This fragment was ligated into pET151/D-TOPO (Invitrogen) and transformed into TOP10 cells for propagation. The correct construction of pET151 *pilE*<sub>Δ1-28</sub> encoding N-terminal 6xHis V5 epitope tagged PilE<sub>Δ1-28</sub> with a TEV protease cleavage site to remove the tags was verified by DNA sequencing. The construct was transformed into *E. coli* Origami B (DE3) cells, and protein expressed and purified as described previously (130). Briefly, SeMet labeled PilE<sub>Δ1-28</sub> was expressed from *E. coli* Origami cells in selenomethionine (SeMet) high-yield M9 minimal media (Shanghai Medicilon) following the manufacturer's instructions. Cells were harvested by centrifugation at 3,200 x g and the pellet resuspended in lysis buffer (20 mM Tris pH 8, 500 mM NaCl and 0.1% LDAO) with 1x benzamidine. Cells were lysed by three passages through a French Press and after centrifugation to remove cell debris, the clarified lysate was applied on an AKTAFPLC system to a 5-ml Ni HiTrap Chelating HP column (GE

Healthcare, Canada) pre-charged with 100mM NiCl<sub>2</sub>. The column was washed in a step-wise manner with 15 mM, 30 mM and 45 mM imidazole followed by elution of bound proteins with 300 mM imidazole. The elution fraction was dialyzed into 20 mM Tris pH 8, 100 mM NaCl, treated with TEV protease at a final concentration of 0.04 mg/ml for 3 h at room temperature and applied to a second nickel affinity chromatography column as above. Untagged PilE<sub>Δ1-28</sub> was collected in the flow-through fraction, buffer exchanged into 20 mM Tris pH 8, 50 mM NaCl and concentrated to 4 mg/ml.

### **Crystallization and structure determination**

SeMet PilE<sub>Δ1-28</sub> crystals were grown using the hanging drop/vapour diffusion method in a 1:1 ratio of protein (4 mg/ml SeMet PilE<sub>Δ1-28</sub> in 20 mM Tris pH 8, 50 mM NaCl) and precipitant (0.2 M ammonium tartrate dibasic, 20% (w/v) PEG 3350) over 1.5 M ammonium sulfate at 20 °C. Crystals were flash frozen in a nitrogen cold stream with no further cryo-protection. Diffraction data were collected at the X25 beamline of NSLS in Brookhaven, NY with a wavelength of 0.979 Å.

Single anomalous diffraction data were processed using the HKL2000 program suite (137). The HySS submodule was used to locate the single SeMet site followed by phasing, density modification, automated model building and refinement in the Phenix suite of programs (4, 120).

Iterative rounds of manual model building and refinement were performed in Coot (58) until  $R_{\text{work}}$  and  $R_{\text{free}}$  values converged and could no longer be improved. Greater detail on data collection and model refinement statistics are listed in Table 4.2. The coordinates of the final SeMet Pile $_{\Delta 1-28}$  model were deposited in the PDB under accession code 4NOA.

### **Construction of fluorescently tagged Pile**

PAO1 *pilE* with the gene encoding mCherry fused on the 3' end was synthesized by GenScript (Piscataway, New Jersey) with flanking EcoRI and HindIII restriction sites. The insert was subcloned into the EcoRI and HindIII sites of the *P. aeruginosa* compatible and arabinose-inducible vector pBADGr (70) to generate pBADGr-*pilE*- *mCherry*.

### **Twitching motility assay**

Twitching motility stab assays were performed as previously described (65). Briefly, strains of interest were stab inoculated in duplicate to the plastic-agar interface of an LB 1% agar plate which was incubated at 37°C for 24 h. The agar was carefully removed and adherent bacteria stained with 1% crystal violet. The experiment was performed in triplicate. The area of the twitching zones were measured in ImageJ (3) and reported in comparison to wildtype levels.

### **Sheared surface protein preparation**

Proteins were sheared from the surface of *P. aeruginosa* cells as described previously (130). Briefly, bacterial strains were streaked in a cross-hatched manner on a 150 mm diameter LB-Agar (1.5%) plate containing gentamicin (30 µg/ml) and grown overnight at 37°C. Cells were scraped using a glass coverslip, resuspended in 1 x PBS and vortexed for 30 s to shear off surface proteins. Bacterial cells were pelleted by centrifugation at 16,100 x g for 5 min followed by a second spin of the supernatant for 20 min. Sheared surface proteins in the clarified supernatant were precipitated on ice for 1 h using 0.4 M NaCl and 2.4 % (w/v) PEG 8000 followed by centrifugation at 16,100 x g for 30 min. The pellets containing surface proteins (pilin and flagellin) were resuspended in 150 µl 1x SDS loading buffer and boiled for 10 min. Samples were separated on 15% SDS-PAGE gels and stained with Coomassie Brilliant Blue for visualization. Densitometry was performed using ImageJ (3), where pilin levels were standardized against the flagellin band.

For Western blot analysis of PilE in surface fractions, the sheared surface protein samples were separated by SDS-PAGE and transferred to nitrocellulose as described (130), followed by detection with 1:1000 dilution of rabbit polyclonal PilE antibody (65), and 1:3000 dilution of goat anti-rabbit IgG-alkaline phosphatase conjugated secondary antibody,

developed using nitro-blue tetrazolium/5-bromo-4-chloro-3-indolylphosphate (NBT/BCIP).

### **Intracellular PilE protein levels**

Bacterial cell pellets, recovered after removal of surface proteins by mechanical shearing as described above, were resuspended in 1x PBS to an OD<sub>600</sub> of 0.6. Two ml of bacterial suspension were centrifuged at 16,100 x g for 2 min, and the pellets resuspended in 200 µl 1x SDS loading buffer and boiled for 10 min. The lysates were separated by SDS-PAGE and transferred to nitrocellulose for immunoblot analysis with anti-PilE polyclonal antibody as described above.

### **Fluorescence microscopy**

Overnight cultures of the strains of interest were stab-inoculated into individual chambers of 1.0 borosilicate chambered cover glass slides (Lab-Tek) containing 1% LB agar. Slides were incubated in the dark for 1 h at 37°C. Cells were then visualized using an EVOS FL Auto microscope (Life Technologies) with a Plan Apochromat 60X oil immersion objective, using either transmitted (white) light or a Texas Red LED light cube (emission 585/29, excitation 624/40). Images were acquired using the EVOS FL Auto Cell Imaging System software (Life Technologies) and exported as TIFF files. TIFF images were processed in ImageJ

(<http://rsb.info.nih.gov/ij/>) by cropping representative regions of interest, and adjusting their brightness to improve visualization of mCherry.

## RESULTS

### PilE interacts with major and minor pilins

We showed previously (130) that incorporation of the *P. aeruginosa* minor pilin PilE into T4aP depended on the presence of the putative PilVWXY1 priming subcomplex, and that pilus assembly required, at a minimum, PilVWXY1 plus either FimU or PilE as putative connectors of the priming subcomplex to the major subunit, PilA. To support the idea that PilE contacts both major and minor pilins during pilus assembly, we tested the interactions of full-length mature PilE with PilA and the other minor pilins with a bacterial adenylate cyclase two-hybrid assay (88). PilE was N-terminally tagged with the T18 fragment of the *Bordetella pertussis* adenylate cyclase, while PilA, FimU, PilV, PilW and PilX were N-terminally tagged with the T25 fragment, and the proteins tested for interactions using two different indicator media (Figure 4.1). On both LB + X-gal and McConkey + maltose plates, PilE interacted with FimU, consistent with previous results (130). Similar to the other putative connector, FimU, PilE interacted with the major pilin PilA and the minor pilins PilV and PilX, but not with PilW. These data support the proposed role for PilE in stably

linking the minor pilin PilVWXYZ1 priming subcomplex to the major subunit PilA.

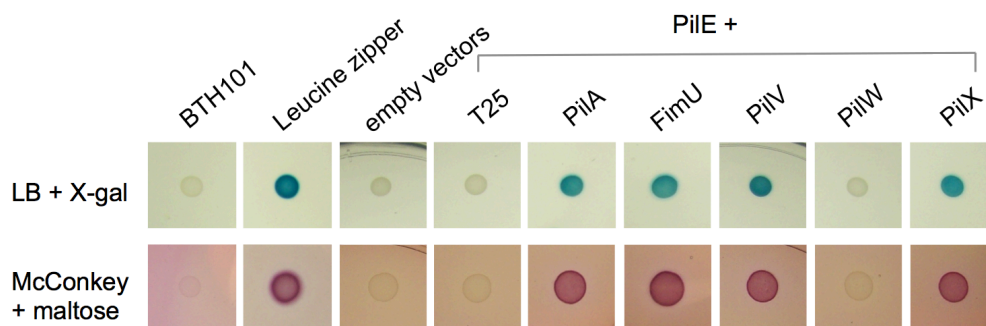


**Figure 4.1. Interactions of PilE with minor pilins and PilA.** Direct protein-protein interactions were tested using a bacterial adenylate cyclase two hybrid system (BACTH). Mature PilE was N-terminally tagged with T18 while PilA, FimU, PilV, PilW and PilX were N-terminally tagged with T25. Interactions were tested in *E. coli cya* mutant strain BTH101 on LB agar + X-gal and MacConkey + maltose indicator plates, which result in blue or red colonies if there is an interaction. A leucine zipper was used as a positive control.

### **The high-resolution crystal structure of PilE reveals characteristic pilin architecture**

To gain further insight into the function of PilE, we solved a 1.25 Å high resolution X-ray crystal structure of SeMet-labeled PilE<sub>Δ1-28</sub>. The protein lacks only the first 28 N-terminal hydrophobic residues of the mature minor pilin, removed to improve its solubility. We also obtained native PilE<sub>Δ1-28</sub> crystals and collected data; the protein crystallized in the

same space group, C2, as the SeMet form, but the data were of lower resolution. Crystallographic data collection and refinement statistics are detailed in Table 4.2.

PilE<sub>Δ1-28</sub> has a typical type IV pilin fold, characterized by an N-terminal  $\alpha$ -helix connected to a four-stranded antiparallel  $\beta$ -sheet, terminating with a disulfide bonded loop (Figure 4.2A). The N-terminal residues from Asn32 to Ser52 form the  $\alpha$ 1-C helix, which likely extends in the full-length protein from the N-terminal hydrophobic  $\alpha$ 1N-helix of a full-length pilin. The  $\alpha$ 1-C helix is packed against a four-stranded anti-parallel  $\beta$ -sheet, to which it is connected by a 26-residue loop containing a  $3_{10}$  helix. Between the  $\beta$ 2 and  $\beta$ 3 strands of the  $\beta$ -sheet, residues Ile97 to Lys108 form a long loop with a  $3_{10}$  helix. Cys106 and Cys132 form a disulfide bond encompassing 25 residues that make up the D-region of PilE. In type IV pilins, the D-region is hypervariable in sequence, and in major pilins, Cys residues typically staple the C-terminus to the last  $\beta$ -strand (66). In contrast, the C terminus of PilE is linked by a disulfide bond to the  $\beta$ 2- $\beta$ 3 loop, and the D-region encompasses  $\beta$ 3,  $\beta$ 4, and a short 2-turn helix. Mutation of Cys132 to Ala resulted in protein instability and loss of pilus assembly and twitching motility (data not shown) suggesting the disulfide bond is a critical stabilizing feature of PilE. Similar results have been reported for Cys point mutants of the major pilin, PilA (70).

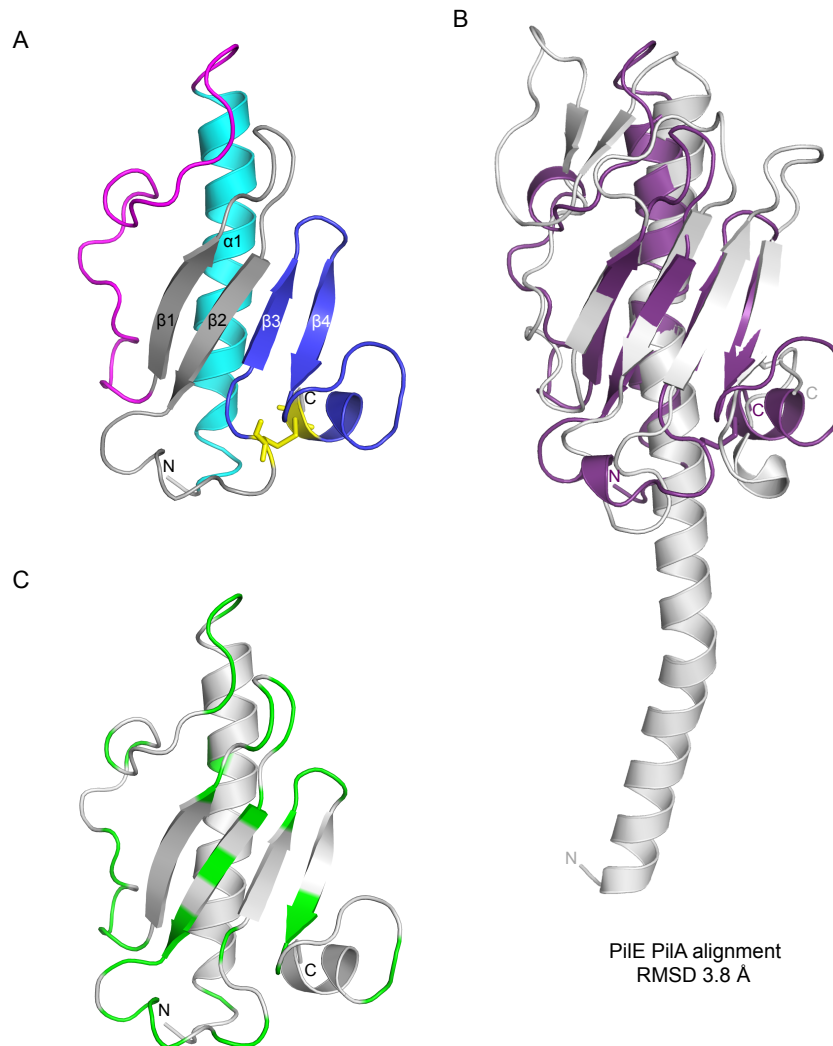


**Figure 4.2. X-ray crystal structure of PilE $\Delta$ 1-28.** A. The X-ray crystal structure of selenomethionine labeled PilE $\Delta$ 1-28 was solved to 1.25 Å (PDB code: 4NOA). The N-terminal  $\alpha$ -helix is colored cyan,  $\alpha\beta$ -loop in magenta,  $\beta$ -sheet in gray and D-region in blue. Cys residues are represented as sticks and colored yellow. B. Structural alignment between PilE $\Delta$ 1-28 (purple) and PilA<sub>PAK</sub> (gray, PDB code: 1OQW). 96 residues aligned with an RMSD of 3.8 Å. C. Mapping of residues differing between PilE<sub>PA01</sub> and PilE<sub>PA14</sub>. Non-conservative residues are colored green. Structural illustrations and alignments generated with PyMOL (version 1.3, Schrodinger, LLC.).

Of the *P. aeruginosa* minor pilins, PilE is the most similar to PilA, with 38% sequence similarity between full-length proteins. Despite the sequence differences and the differences in the connectivity of the disulfide bond in the D-region, 96 of 108 residues of PilE $_{\Delta 1-28}$  could be aligned with the structure of PilA $_{PAK}$  (PDB 1OQW), with a root mean square deviation (RMSD) of 3.8 Å (Figure 4.2B). The  $\alpha 1$ -helix of major pilins has a characteristic shallow S-shaped curve created by residues Pro22 and Pro or Gly42 (50, 69, 138). Mature PilE has an Asp residue at position 42, and its truncated  $\alpha 1$ -C helix was not curved in our structure (Figure 4.2A and 4.2B). However, there is a Pro22 residue in the PilE sequence that likely creates a kink in the  $\alpha 1$ -N helix region of PilE. The  $\alpha\beta$ -loop of major pilins are involved in inter-subunit interactions between pilin subunits in the pilus (51). In *P. aeruginosa* PilA $_{PAK}$ , this region forms a minor  $\beta$ -sheet, while in PilE $_{\Delta 1-28}$  this region is less extended and has a  $3_{10}$  helix, possibly to accommodate interactions with the other minor pilins. Although  $\beta 3$  and  $\beta 4$  of PilE $_{\Delta 1-28}$  are part of the D-region, the length and orientation of the four  $\beta$ -strands of central  $\beta$ -sheet are generally conserved between PilA $_{PAK}$  and PilE $_{\Delta 1-28}$ , as is the packing of the  $\beta$ -sheet against  $\alpha 1$ -C.

Each *P. aeruginosa* strain carries one of two different sets of T4aP minor pilin genes (exemplified by those of common laboratory strains PAO1 and PA14), which are encoded with specific major pilin genes in a

'pilin island' that bears signatures of acquisition via horizontal gene transfer (67). The sequence similarities between the orthologues in the two sets of minor pilins range from ~60-75%, with higher similarity in the N-termini and lower in the C-termini of each pair (11). With the exception of *pilX<sub>PA14</sub>*, cross-complementation of PAO1 minor pilin mutants with PA14 minor pilin genes restored surface piliation and twitching motility to various degrees, suggesting that most subunits can make functional interactions with heterologous partners (67). PilE<sub>PAO1</sub> and PilE<sub>PA14</sub> share 61% amino acid sequence similarity (67), and we found that most of the divergent residues map to loops or solvent-exposed surfaces (Figure 4.2C). These results suggest that overall conservation of PilE architecture is important for its function.

### **Comparison of PilE and PilX<sub>Nm</sub> structures**

The top hit from a structural comparison of PilE <sub>$\Delta$ 1-28</sub> with others in the Protein Data Bank (PDB) using DaliLite (77) was the PilX<sub>Nm</sub> minor pilin from *N. meningitidis* (75). PilX<sub>Nm</sub> is encoded with the *Neisseria* PilHIJK equivalents of the core minor pilins FimU-PilVWX, and has been implicated in controlling efficient pilus biogenesis, as well as in attachment and aggregation of surface-exposed pili (74, 75, 80). PilE and PilX<sub>Nm</sub> share 25% overall sequence identity, concentrated in the  $\alpha$ 1-N region (18 of 28 residues, 64%) that was deleted for structural studies (Figure S4.1).

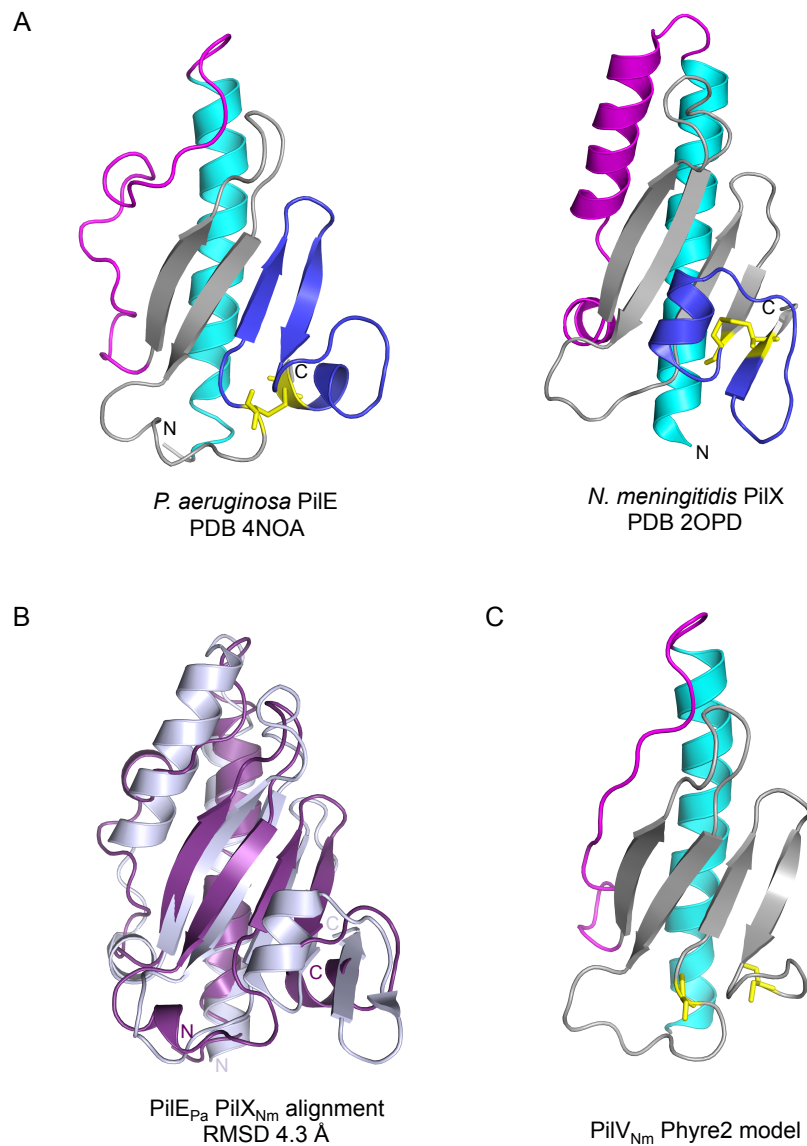


**Figure 4.3. Comparison of PilE $\Delta_{1-28}$  with *N. meningitidis* PilX<sub>Nm</sub>.** A. Side-by-side comparison of PilE $\Delta_{1-28}$  and PilX<sub>Nm,  $\Delta_{1-28}$</sub>  with the N-terminal  $\alpha$ -helices coloured in cyan,  $\alpha\beta$ -loops in magenta,  $\beta$ -sheets in gray and D-regions in blue with the cysteines represented as sticks in yellow. B. Structural alignment of PilE $\Delta_{1-28}$  (purple) and PilX<sub>Nm,  $\Delta_{1-28}$</sub>  (light blue). 104 residues are aligned with an RMSD of 4.3 Å. C. Phyre<sup>2</sup> generated model of PilV<sub>Nm</sub> based on PilE. Structural illustrations and alignments generated with PyMOL (version 1.3, Schrodinger, LLC.).

The structure of N-terminally truncated PilX<sub>Nm</sub> is comprised of the typical N-terminal  $\alpha$ 1-C helix connected to a four-stranded antiparallel  $\beta$ -sheet (75) (Figure 4.3A). Although there is only 14% sequence identity between the C-terminal domains of PilE and PilX<sub>Nm</sub>, the critical pilin structural elements are maintained, and the C $\alpha$  align over 104 residues with a RMSD of 4.3 Å (Figure 4.3B).

Like PilE, the N-terminal  $\alpha$ 1-C helix in the PilX<sub>Nm</sub> structure lacks a kink at position 42, although it has a flexible Gly at this position (75), which in other pilin structures allows for a second bend in the S-shaped  $\alpha$ 1 helix (51, 69, 138). Of note, the D-regions of both PilE and PilX<sub>Nm</sub> have hook-like protrusions (Figure 4.3B). This feature was previously suggested to be important for protein-protein interactions between PilX<sub>Nm</sub> subunits on neighbouring but antiparallel pilus fibres, opposing pilus retraction and thereby promoting aggregation (75). Complementation of a *pilE* mutant with a plasmid containing an in-frame deletion of the corresponding region (residues 120-127) of mature PilE had no effect on pilus assembly or twitching motility (data not shown), suggesting that this region of PilE is not crucial for function in *P. aeruginosa*.

### **PilV<sub>Nm</sub> is predicted to be structurally similar to PilE**

Although there is no structure yet available for PilV<sub>Nm</sub>, it more similar in amino acid sequence to PilE than to PilX<sub>Nm</sub> (Figure S4.1), and

this level of similarity is greater than that between the obvious structural homologues, PilE and PilX<sub>Nm</sub> (Figure 4.3A). We used the Phyre<sup>2</sup> structural prediction algorithm (91) to search for the best homology model for PilV<sub>Nm</sub>, using only its C-terminal region (residues 29 to 122, mature PilV<sub>Nm</sub> numbering). Interestingly, the top hit for PilV<sub>Nm</sub> was our PilE structure, with a confidence level of 99.9% over an alignment of 90 residues. The structural model for PilV<sub>Nm</sub> is shown in Figure 4.3C. The next 3 hits were *N. meningitidis* minor pilin ComP (PDB 2MK3), *P. aeruginosa* PilA (PDB 1OQW) and *N. gonorrhoeae* PilE (PDB 2PIL), with decreasing levels of confidence. Of note, the PilX<sub>Nm</sub> structure was not among the hits for the PilV<sub>Nm</sub> C-terminal region, suggesting that the level of sequence identity between them was too low to generate even a low-confidence model. Repeating the search with the full-length mature PilV<sub>Nm</sub> sequence returned similar results.

Although PilV<sub>Nm</sub> has Cys residues in the same position as PilX<sub>Nm</sub> according to the alignment, no disulphide bond was present in the Phyre<sup>2</sup> generated models of PilV<sub>Nm</sub>. These structures do not model the last four residues of PilV<sub>Nm</sub> after the last Cys, suggesting there are sufficient differences within this region to preclude high confidence predictions. Nevertheless, PilV<sub>Nm</sub> likely has a fold similar to PilE, consistent with reports that it is incorporated into pili (172, 183).

### **PilE incorporation into pili is necessary for function**

Imhaus and Dumenil (80) recently reported that PilX<sub>Nm</sub> and PilV<sub>Nm</sub> are required for efficient pilus biogenesis in *N. meningitidis*. They suggested that the functional pool of PilX<sub>Nm</sub> and PilV<sub>Nm</sub> was located in the periplasm rather than on the cell surface (as might be expected for integral components of assembled pili), since mCherry fusions considered too bulky to pass through the secretin were capable of complementing their cognate mutants. However, the proteins were unable to complement unless processed by the pre-pilin peptidase (80), an essential prerequisite for pilus incorporation (167). This finding was consistent with other studies showing that minor pilins are present in sheared surface fractions, suggesting incorporation into pili (65, 184).

To reproduce this experiment in *P. aeruginosa*, mCherry was fused to the C-terminus of PilE and its ability to complement a *pilE* mutant was tested. Analysis of cells complemented with the fusion protein by fluorescence microscopy revealed peripheral staining, confirming its expected periplasmic localization (Figure 4.4A). However, complementation of a *pilE* mutant with PilE mCherry resulted in no recoverable surface pili or twitching motility, similar to the negative control (Figure 4.4B and C). The levels of PilE mCherry expressed from the pBADGr vector were intermediate between those of wild type PilE expressed from the same plasmid, and those expressed from the native

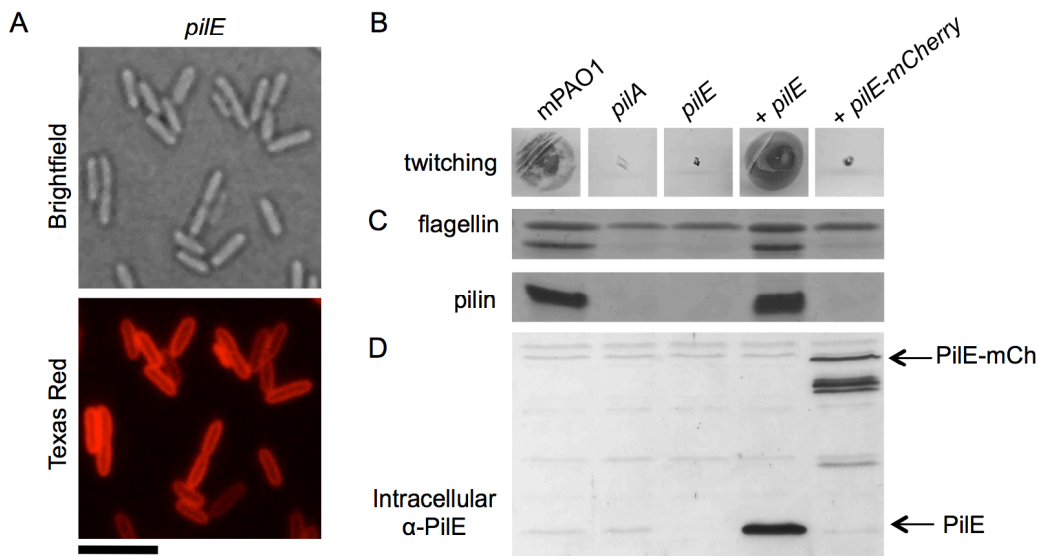


**Figure 4.4. Complementation of *pilE* with PilE mCherry.** mCherry was fused to the C-terminal end of PilE and the level of complementation of a *pilE* mutant was assessed. A. Fluorescence microscopy analysis of PilE mCherry localization. Scale bar represents 5 $\mu$ m. B. Twitching motility was tested by stab-inoculating to the bottom of an LB 1% agar plate and staining with 1% crystal violet after 24h incubation at 37°C. C. Pili were sheared from the surface of cells of interest and separated on a 15% SDS-PAGE gel. The flagellin band is used as a loading control. D. Intracellular levels of PilE were probed by western blot analysis with an  $\alpha$ -PilE peptide antibody (1:1000 dilution). Arrows indicate the bands of interest.

locus (Figure 4.4D), both of which restore similar levels of twitching motility. Therefore, the amount of fusion protein expression is unlikely to underlie the absence of twitching motility or pili in the strain expressing the PilE mCherry fusion. Consistent with our model – in which PilE stabilizes interactions between the major and minor pilins for efficient pilus

biogenesis – these data suggest that *P. aeruginosa* PilE cannot restore pilus biogenesis from a periplasmic location. Alternatively, attachment of a bulky fluorescent protein could impair PilE's ability to function efficiently in the initiation of pilus assembly, leading to a lack of surface pili under circumstances where retraction is active due to unbalanced extension/retraction dynamics.

To examine the latter possibility, we tested whether pBADGr-*pilE*-*mCherry* could complement piliation in a previously characterized  $\Delta$ *fimU pilE*  $\Delta$ *MPP pilT* mutant (130). This strain is retraction-deficient due to inactivation of the *pilT* gene encoding the retraction ATPase, and non-piliated because it lacks the putative connector proteins FimU and PilE as well as the T2S minor pseudopilins, which can prime pilus assembly in the absence of the T4aP minor pilins in *P. aeruginosa* (130). In this strain, either *pilE* or *fimU* can restore surface piliation (130). When expressed in this mutant, PilE-mCherry restored ~20% of surface piliation compared to wild type PilE, where levels were commensurate with the *pilT* control (Figure 4.5A). The decrease in surface piliation is likely not due to differences in the levels of PilE (Figure 4.5C). These data suggest that PilE-mCherry is partially functional in terms of initiation of pilus assembly, but they do not reveal whether it is incorporated into pili. To address that question, we probed sheared surface protein fractions using a PilE-specific antibody, and readily detected a band with a mass corresponding

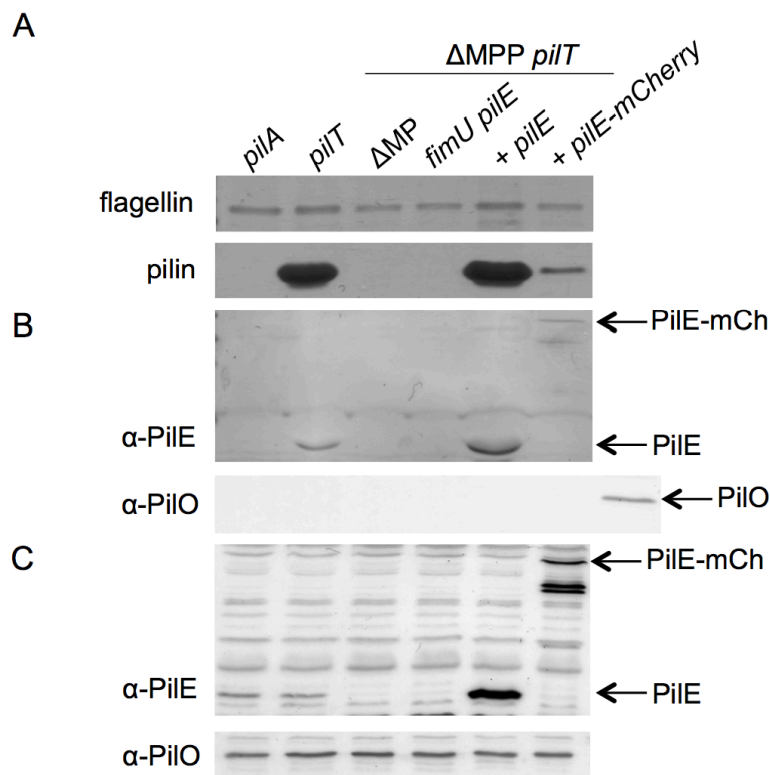


**Figure 4.5. Pilus assembly by PilE mCherry in a retraction-deficient background.** The ability of PilE mCherry to support pilus assembly in a retraction deficient strain was tested in the *pilE pilT  $\Delta MPP \Delta fimU$*  mutant that lacks surface piliation in the absence of *fimU* and *pilE*. A. Pilus assembly was probed by shearing proteins from the surface of the cell and analyzing the surface fractions by SDS-PAGE. The flagellin band is used as a loading control. B. Incorporation of PilE mCherry was examined by western blot analysis of surface fractions above and probing for PilE using an  $\alpha$ -PilE peptide antibody (1:1000). Arrows indicate the bands of interest. The samples were probed with  $\alpha$ -PilO (1:5000) antibody as a control of cell lysis, the last lane is a mPAO1 intracellular sample as a positive control for PilO. C. Intracellular levels of PilE and PilO were probed by western blot analysis with an  $\alpha$ -PilE peptide antibody (1:1000 dilution) and an  $\alpha$ -PilO antibody, respectively.

to PilE-mCherry (Figure 4.5B). The presence of PilE-mCherry in sheared surface fractions was not the result of cell lysis, as another inner membrane protein, PilO, was undetectable in surface fractions (Figure 4.5B and C). Taken together, these results suggest that PilE-mCherry is incorporated into pili during pilus biogenesis, and that the presence of the fusion tag may inhibit its incorporation, reducing the efficiency of assembly initiation to the point where surface piliation and motility are lost when retraction is active.

## DISCUSSION

Our previous results (130) suggested that the minor pilins prime T4aP assembly by forming a priming complex, analogous to that formed by minor pseudopilins (43), to initiate fibre polymerization. In our model, PilVWXY1 form a subcomplex, which is then bound by PilE and coupled to the major subunit PilA through interactions with both PilE and FimU, which interact with one another (130). Here we show that PilE interacts with the major pilin PilA and minor pilins PilV and PilX (Figure 4.1), further supporting its role as a connector. PilE has a typical type IV pilin structure (Figure 4.2), likely facilitating its interactions with the major pilin and incorporation into the pilus.

PilE is structurally similar to *N. meningitidis* PilX<sub>Nm</sub> (Figure 4.3). Both are proposed to be involved in efficient initiation of pilus assembly

(80, 130). In the absence of PilX<sub>Nm</sub> or its homologue in *N. gonorrhoeae*, PilL<sub>Ng</sub>, piliation is reduced (27, 184), whereas without PilE, *P. aeruginosa* cells are non-piliated (65, 154). In trying to understand this difference between model species, we noticed that PilE and the *N. meningitidis* non-core minor pilin PilV<sub>Nm</sub> were potentially orthologous, with higher sequence identity than the structural homologues, PilE and PilX<sub>Nm</sub>. A Phyre<sup>2</sup> analysis of the sequence of the C-terminal domain of PilV<sub>Nm</sub> yielded a high-confidence structural model on the PilE template, but returned no match with PilX<sub>Nm</sub>, even though Dali-lite analysis suggested that PilX<sub>Nm</sub> is the top structural match for PilE (Figure 4.3A). Based on these data, we propose that both PilV<sub>Nm</sub> and PilX<sub>Nm</sub> are PilE orthologues. This hypothesis may explain why single *P. aeruginosa pilE* mutants lack surface pili, but both *pilV<sub>Nm</sub>* and *pilX<sub>Nm</sub>* must be inactivated in *Neisseria* before piliation is lost (80).

Imhaus and Dumenil (80) created mCherry fusions to prevent the incorporation of PilX<sub>Nm</sub> or PilV<sub>Nm</sub> into surface-exposed pili, with the assumption that the fusions would be too large to fit through the secretin pore. However, it is difficult to differentiate that phenotype from one in which pilus assembly is impaired due to changes in interactions among major and minor pilin subunits due to the fusion. In *P. aeruginosa*, complementation of a *pilE* mutant with *pilE*-mCherry blocked surface piliation (Figure 4.4C); however, in a retraction-deficient background, we

recovered a small amount of pili in which PilE-mCherry could be detected (Figure 4.5A and B). This result is consistent with our model of pilus assembly initiation (130), in which only one PilE subunit per pilus is required. Pilus assembly is likely less efficient with PilE-mCherry versus wild type PilE, potentially due to suboptimal interactions with the fusion protein, resulting in inefficient priming and thus no recoverable surface pili if retraction is active.

PilE, PilX<sub>Nm</sub>, and PilV<sub>Nm</sub> plus the third non-core *Neisseria* subunit ComP, have been shown to co-purify with pili, suggesting that they are part of the fibre (42, 65, 74, 75, 172, 183, 184). PilX<sub>Nm</sub> and PilV<sub>Nm</sub> G-1N variants, which cannot be processed by the pre-pilin peptidase, were defective for complementation and processing, and for assembly of major pilins (80). In a previous study, we found that all of PilVWXY1 were required for PilE to be incorporated into surface-exposed pili (130). In *N. gonorrhoeae*, the PilX<sub>Nm</sub> orthologue PilL<sub>Ng</sub> was similarly dependent on the core minor pilins, PilHIJK, as well as the T4P adhesin and anti-retraction protein, PilC, for pilus incorporation (184). Similarly, PilV<sub>Ng</sub> is dependent on PilC (mutant of both) for pilus incorporation although the dependence on other minor pilins was not tested (183). Like PilY1, which is not dependent on PilE for incorporation, PilC is still observed in the surface pilus fraction in the absence of either PilX<sub>Nm</sub>, PilL<sub>Ng</sub>, PilV<sub>Nm,Ng</sub> (74, 172, 183, 184). Interestingly, *Neisseria* spp. have two PilY1-like proteins, PilC1

and PilC2 (83, 125) which are not encoded with the minor pilins PilHIJK(X/L) (184), although their expression and regulation is poorly understood. We suggest that like PilE, PilX<sub>Nm</sub> and PilV<sub>Nm</sub> interacts with one or more of the core minor pilins, plus the large non-pilin PilC, either PilC1 or PilC2, to modulate initiation of pilus assembly.

PilE is 38% similar to the major pilin subunit PilA and they share structural similarity (Figure 4.2). However, PilE does not form pilus fibres, even when overexpressed (data not shown). PilE tolerates a wide range of expression levels while still supporting similar amounts of twitching motility (Figure 4.4). This may be related to the dependence of PilE on PilVWXY1 for incorporation into pili (130). Simply increasing intracellular levels of PilE would not necessarily affect the amount of PilE in the pilus if a stoichiometric interaction with PilVWXY1 is necessary for its inclusion in pili. In addition, the architecture of the minor pilins may preclude their polymerization into a fibre. Major pilins have a Gly or Pro residue at position 42, creating a kink in their  $\alpha$ 1C-helices allowing for inter-subunit interactions and maintaining flexibility of the fibre (28, 50, 110, 138). Both PilE $_{\Delta 1-28}$  and PilX<sub>Nm</sub> lack curvature in their  $\alpha$ 1-C helices (Figure 4.3). In addition, structures of other minor pilins, including FimU from *P. aeruginosa* (130) and PilJ, a minor pilin from *C. difficile* (143), reveal a similar lack of curvature in the truncated N-terminal  $\alpha$ -helix. The absence of curvature may have implications in the packing of these minor pilins in

the pilus, or possibly their recognition by the assembly machinery, differentiating them from the major pilin proteins.

The T2S system lacks both PilE and PilY1 equivalents. We showed previously that PilY1 is required for PilVWX incorporation into pili, and that all four members of this putative subcomplex must be present for noncore minor pilin PilE to be incorporated into pili, suggesting that PilE recognizes a novel subcomplex interface (130). The connector function of PilE may act as a quality control for the incorporation of non-pilin protein PilY1. Like *P. aeruginosa*, other species such as *Xyella fastidiosa*, *Ralstonia solanacearum* and *Chromobacterium violaceum* carry T4aP minor pilin operons that encode both PilY1-like proteins and PilE (184), suggesting a functional link between these proteins. Although *Neisseria* minor pilins PilV and PilX/PilL are not encoded with the PilY1-like proteins PilC1 and PilC2, our data support a common role in pilus assembly, suggesting the function of non-core PilE-like minor pilins may be universally-conserved across T4aP species.

## **ACKNOWLEDGEMENTS**

This work was funded by operating grants from the Canadian Institutes of Health Research (CIHR) MOP 86639 to LLB and MOP 89903 to MSJ. YN held a Graduate Studentship from Cystic Fibrosis Canada and holds a Banting Scholarship from CIHR.

```

          1                    28
Pa Pile  ---MRTRQKGFTLLEMVVVAVIGILLGIAIPSYQNYVIRSNRTEGQALLSDAAARQERY  50
Nm PilX  MMSNKMEQKGFTLIEMMIVVAILGIIISVIAIPSYQSYIEKGYQSPLYTEMVGINNISKQF  50
Nm PilV  ---MKNVQKGFTLLELMIAVAILGILTLITYPSYKTYIRRVRLSEVVRTLLHNAQTMARY  50
          .  *****:*:::.**:*:::  *:  ***:.*:  .  ::  :  :  :  :  :  :  :  :

Pa Pile  YSQNPVGGYTKDVAKL-----GMSSANSFNPNLYNLT---IATPTSTTYTLTATP-----  96
Nm PilX  ILKNPLDDNQTIKSKLERFVSGYKMNPKIAEKYNVSVHFVNKEKPRAYSLVGVPKTGTGY  110
Nm PilV  YRQK-GTFKTYDKNKL-----KQNKYFNVT---LSKVSPDHFTLQADP-----  89
          ::          **          .  :  *::  :  .  .  .  :  *  .  *

Pa Pile  -----INSQTRDKTCGKLTNLQLGERGAAGKTGNNSTVNDWCWR  134
Nm PilX  TLSVWMNSVGDGYKC-RDAASARAHLETLSDDVGCEAFSNRKK  152
Nm PilV  -----NPPTNDGETC-VVTLNDGGTIAASGTNQSCPFGD-----  122
          :  .  .*  :  .  .  :  .  .  .  .  .
    
```

**Figure S4.1. Sequence alignment of Pile with PilX<sub>Nm</sub> and PilV<sub>Nm</sub>.**

Sequence alignment between *P. aeruginosa* Pile from strain PAO1 and *N. meningitidis* PilX and PilV from strain 8013 using MUSCLE (57).

Numbering is according to the mature pilin with the leader sequence in gray. The first 28 residues that were removed for structural studies are colored red.

**Table 4.1. Strains and plasmids used in this study**

<b>Strains and plasmids</b>	<b>Description</b>	<b>Reference</b>
<b><i>E. coli</i> strains</b>		
DH5 $\alpha$	F' Phi80dlacZ $\Delta$ M15 $\Delta$ (lacZYA-argF)U169 deoR recA1 endA1 hsdR17(rK-mK+)phoA supE44 lambda- thi-1	Invitrogen
TOP10	F- <i>mcrA</i> $\Delta$ ( <i>mrr-hsdRMS-mcrBC</i> ) $\phi$ 80 <i>lacZ</i> $\Delta$ M15 $\Delta$ <i>lacX74</i> <i>recA1</i> <i>araD139</i> $\Delta$ ( <i>ara-leu</i> )7697 <i>galU</i> <i>galK</i> <i>rpsL</i> <i>endA1</i> <i>nupG</i>	Invitrogen
Origami B (DE3)	F' <i>ompT</i> <i>hsdS<sub>B</sub></i> (r <sub>B</sub> <sup>-</sup> m <sub>B</sub> <sup>-</sup> ) <i>gal</i> <i>dcm</i> <i>lacY1</i> <i>ahpC</i> (DE3) <i>gor522::</i> Tn10 <i>trxB</i> (Kan <sup>R</sup> , Tet <sup>R</sup> )	Novagen
BTH101	F', <i>cya-99</i> , <i>araD139</i> , <i>galE15</i> , <i>galK16</i> , <i>rpsL1</i> ( <i>Str<sup>R</sup></i> ), <i>hsdR2</i> , <i>mcrA1</i> , <i>mcrB1</i>	Euromedex
<b><i>P. aeruginosa</i> strains</b>		
mPAO1	Wild-type laboratory strain	(81)
mPAO1 <i>pilA::</i> Tn	IS <i>phoA</i> /hah transposon insertion at position 163 of <i>pilA</i>	(81)
mPAO1 <i>pilT::</i> Tn	IS <i>phoA</i> /hah transposon insertion at position 885 of <i>pilT</i>	(81)
mPAO1 <i>pilE::</i> Tn	IS <i>phoA</i> /hah transposon insertion at position 183 of <i>pilE</i>	(81)
mPAO1 <i>pilT::</i> Tn $\Delta$ MP $\Delta$ MPP :: FRT	IS <i>phoA</i> /hah transposon insertion at position 885 of <i>pilT</i> and deletion of <i>fimTU</i> <i>pilVWXYZ1Y2E</i> and deletion of <i>xcpUVWX</i> replaced with an FRT scar	(130)
mPAO1 <i>pilE::</i> Tn <i>pilT::</i> FRT $\Delta$ <i>fimU</i> $\Delta$ MPP :: FRT	IS <i>phoA</i> /hah transposon insertion at position 183 of <i>pilE</i> with FRT insertion in the Nrul site of <i>pilT</i> and deletion of <i>fimU</i> and deletion of <i>xcpUVWX</i> replaced with an FRT scar	(130)
<b>Plasmids</b>		

pBADGr	pMLBAD with <i>aacC1</i> gene (gentamicin resistance) disrupting <i>dhfrII</i> (trimethoprim resistance), arabinose inducible	(70)
pBADGr <i>pilE</i>	PAO1 <i>pilE</i> cloned in pBADGr, Gm <sup>R</sup>	(65)
pBADGr <i>pilE mCherry</i>	PAO1 <i>pilE</i> cloned in pBADGr encoding a C-terminal mCherry fluorescent tag	This study
pUT18C	pUC19-derived vector with T18 fragment (residues 225-399) of CyaA under control of lac promoter, MCS at 3' end of T18 ORF, Amp <sup>R</sup>	(89)
pUT18C <i>pilE</i>	mature PAO1 <i>pilE</i> cloned in pUT18C, Amp <sup>R</sup>	This study
pKT25	pSU40-derived vector with T25 fragment (residues 1-224) of CyaA under control of a lac promoter; MCS at 3' end of T25 ORF, Kan <sup>R</sup>	(89)
pKT25 <i>pilA</i>	mature PAO1 <i>pilA</i> cloned in pKT25, Kan <sup>R</sup>	(130)
pKT25 <i>fimU</i>	mature PAO1 <i>fimU</i> cloned in pKT25, Kan <sup>R</sup>	This study
pKT25 <i>pilV</i>	mature PAO1 <i>pilV</i> cloned in pKT25, Kan <sup>R</sup>	(130)
pKT25 <i>pilW</i>	mature PAO1 <i>pilW</i> cloned in pKT25, Kan <sup>R</sup>	(130)
pKT25 <i>pilX</i>	mature PAO1 <i>pilX</i> cloned in pKT25, Kan <sup>R</sup>	(130)
pT18zip	pT18 plasmid with 35-residue leucine zipper cloned into KpnI site, Amp <sup>R</sup>	(88)
pT25zip	pT25 plasmid with 35-residue leucine zipper cloned into KpnI site, Cm <sup>R</sup>	(88)
pET151 <i>pilE</i> Δ1-28	PilE (Δ1-28 of mature protein) expression vector with N-terminal 6xHis and V5 epitope tag	This study

**Table 4.2. PiIE data collection and refinement statistics**

<b>SeMet-PiIE</b>	
<b>Data Collection</b>	
Beamline	NLSL X25
Wavelength	0.979
Space group	C2
Unit-cell parameters	
a,b,c (Å)	76.16, 35.56, 43.54
$\alpha, \beta, \gamma$ (°)	90.0, 97.32, 90.0
No. of mol in ASU	1
Resolution range (Å) <sup>a</sup>	50.0-1.25 (1.27-1.25)
Unique reflections	30,749
Data redundancy <sup>a</sup>	6.4 (4.5)
Completeness (%) <sup>a</sup>	95.4 (89.6)
$I/\sigma(I)$ <sup>a</sup>	20.7 (7.6)
$R_{\text{merge}}$ (%) <sup>a</sup>	8.4 (21.0)
Wilson B	8.28
<b>Model and Refinement</b>	
Resolution range (Å)	43.21-1.25
$R_{\text{work}}$ (%)	15.90
$R_{\text{free}}$ (%)	17.53
No. of reflections	30,645
No. of amino acid residues/atoms	831
No. of waters	248
r.m.s.d. bond lengths (Å)	0.005
r.m.s.d. bond angles (°)	0.965
Average B (Å <sup>2</sup> )	11.51
Ramachandran statistics (%)	
Favored	99.12
Allowed	0.88
PDB code	4NOA

<sup>a</sup> values in parentheses represent higher resolution shell

# **CHAPTER FIVE**

## **Summary and Conclusions**

## Summary of findings

This thesis explored the structural diversity of major and minor pilins from the opportunistic pathogen *P. aeruginosa* and examined the functional implications of this diversity on pilus assembly and disassembly dynamics. The structure of PilA<sub>0594</sub> suggests a potential role of the largely uncharacterized accessory protein TfpZ and presents possible interaction interfaces for the minor pilins, which we show are involved in priming of pilus assembly and presentation of PilY1 on the bacterial surface. Together, these data provide a better understanding of pilin protein biology and mechanics of T4P assembly that can contribute to the development of therapeutics against *P. aeruginosa*.

### *Structure of PilA<sub>0594</sub>*

A comprehensive study of over 300 strains of *P. aeruginosa* revealed five phylogenetically-distinct groups of major pilins (101). These pilins vary in size, sequence and presence or absence of accessory protein(s), encoded immediately downstream of the pilin gene (101). Most studies of *P. aeruginosa* T4P biology, including structural characterizations, have used group II laboratory strains (e.g. PAO1, PAK, PA103), which are atypical in that they are the only group without a PilA-associated accessory protein (12, 50, 71, 90). Cross-complementation studies showed decreased twitching and piliation when heterologous pilins

were expressed in a group II background, suggesting that the differences in pilin sequence and the presence of accessory proteins translate into effects on function (11).

We solved the 1.6-Å X-ray crystal structure of the C-terminal domain of PilA from *P. aeruginosa* strain Pa110594 (group V), which was the first non-group II pilin structure solved (Chapter 2). The structure has the typical T4aP fold with an N-terminal  $\alpha$ 1-C helix connected to a four-stranded anti-parallel  $\beta$ -sheet, connected to the C-terminus through a disulphide bond. However, an additional  $\alpha$ -helix in the  $\alpha\beta$ -loop and a DSL with helical character give this novel pilin T4b-like characteristics, although our molecular modeling studies suggested that PilA<sub>V</sub> still assembles into a T4aP-like fibre.

Group III and V pilins are similar in size, and based on the structure of PilA<sub>V</sub> and the sequence similarity of the group V pilin to the group III pilin from strain PA14 – the most commonly isolated strain of *P. aeruginosa*, and widely used for virulence studies (181) – a high confidence model of PA14 PilA<sub>III</sub> was generated. The structure of the PilA<sub>PA14</sub> pilin was predicted to be similar to that of strain PilA<sub>0594</sub>, with the majority of sequence differences clustered in the surface-exposed regions of the pilin. These surface-exposed areas are predicted to be involved in subunit-subunit interactions between pilin subunits along the fibre, suggesting that sequence divergence can impact pilus assembly.

PilA<sub>0594</sub> and the model of PilA<sub>PA14</sub> have an unusually large loop insertion between  $\beta$ 3- $\beta$ 4 that is not present in any other pilin structures solved to date. It is also a region of sequence divergence between group III and V pilins. We hypothesize this region might interact with the accessory protein TfpZ (group V) or TfpY (group III), which are involved in modulating pilus disassembly dynamics in an unknown manner (11). These related accessory proteins, which are specific for their cognate pilins, were speculated to alter the conformation of the pilin around the  $\beta$ 3- $\beta$ 4 loop to allow proper assembly to occur. Interestingly, FimA from *D. nodosus* has a large loop region between  $\beta$ 1- $\beta$ 2 that occupies a similar location to the  $\beta$ 3- $\beta$ 4 loop of PilA<sub>0594</sub> (69). FimA is encoded with an accessory protein FimB that has 32% sequence identity to TfpZ, although FimB does not appear to have an effect on piliation or twitching motility (92). Together, these data show the structural diversity associated with type IV major pilins in *P. aeruginosa* and provide information about a potential binding site of the accessory proteins TfpY and TfpZ that modulate pilus assembly/disassembly dynamics.

However, the requirement for accessory proteins cannot fully explain the decrease in twitching motility seen in the cross-complementation studies (11). The structural diversity among pilins was hypothesized to modulate the presumed interactions between major and minor subunits during fibre assembly, since the genes encoding the major

pilin and minor pilins are part of a single, horizontally-transferred pilin island (67). This conjecture was supported by evidence showing that the minor pilins are important for priming pilus assembly (Chapter 3, below).

#### *Role of minor pilins in pilus assembly*

In *P. aeruginosa*, the minor pilins FimU-PilVWXE have pilin-like characteristics and are incorporated into the pilus fibre (65). However, whereas the major pilins play a structural role in T4P, the role of the minor pilins was unclear. We provided a concrete role for the minor pilins in priming pilus assembly and trafficking the adhesion and anti-retraction protein PilY1 to the cell surface (Chapter 3).

We showed that the small amount of pili observed in a retraction-deficient mutant lacking the minor pilin operon was due to expression of minor pseudopilins from the *P. aeruginosa* Xcp type II secretion (T2S) system, which also get incorporated into pili. These data suggest that T2S minor subunits can prime T4P assembly, similar to the heterologous assembly of *E. coli* pili primed by *K. oxytoca* minor pseudopilins that was reported previously (44). However, that study did not show whether cross-priming led to incorporation of minor pseudopilins into pili. Deletion of all minor subunits, minor pilins and minor pseudopilins, abrogated pilus assembly, suggesting that minor components are essential for priming.

Minor pilins PilVWX plus the adhesin and anti-retraction protein PilY1 are mutually dependent for inclusion in surface pili, suggesting that subcomplex formation is required for surface expression. PilE required all of PilVWXY1 for pilus incorporation, while FimU was incorporated independently of the others. In a strain lacking the minor pseudopilins, PilVWXY1 and either FimU or PilE were required for pilus assembly, suggesting that PilE and FimU together stably couple the priming subcomplex to the major subunit.

In support of this idea, FimU and PilE directly interact with the major pilin and minor pilins in a bacterial two-hybrid assay (Chapters 3 and 4). We solved the 1.4 Å crystal structure of FimU<sub>Δ1-28</sub>, which maintains the typical T4aP fold and has striking architectural similarity to its T2S ortholog GspH, proposed to connect the minor pseudopilin complex to the major pseudopilin (54, 99). The structure of FimU is the first core minor pilin structure to be solved and provides further evidence for likely mechanistic similarity between T4P and T2S systems.

We subsequently solved the 1.25 Å crystal structure of PilE<sub>Δ1-28</sub> and shows it too has a typical pilin fold, supporting its incorporation into the pilus (Chapter 4). Fusing PilE to mCherry impaired twitching motility and piliation, although in the absence of retraction, piliation was restored to 20% of wild-type PilE levels. PilE-mCherry could be detected in the pili sheared from the retraction deficient strain, suggesting that PilE is

incorporated into pili and supporting its putative connector function. Interestingly, *pilE* genes are frequently linked to the core minor pilin operon, which includes the gene for the adhesin and anti-retraction protein PilY1 (184) suggesting the non-core minor pilin may be associated with the proper incorporation of PilY1-like proteins into pili.

The structure of PilE strongly resembles that of *N. meningitidis* minor pilin PilX<sub>Nm</sub> (75), although another non-core *N. meningitidis* minor pilin, PilV<sub>Nm</sub>, has slightly higher sequence identity to PilE, and structural modeling suggests that they have similar architecture. Both PilX<sub>Nm</sub> and PilV<sub>Nm</sub> were recently suggested to modulate pilus assembly from within the periplasm, in an unknown manner (80). However, our data showing that both are PilE-like led us to propose that both PilX<sub>Nm</sub> and PilV<sub>Nm</sub> act as connectors in T4P assembly, potentially in association with the two *Neisseria* PilY1 homologues, PilC1 and PilC2. Together, these data support a role for the minor pilins in priming pilus assembly and the expression of PilY1 on the surface.

## **Future directions**

### *PilA-accessory protein interactions*

To test our hypothesis that TfpY and TfpZ accessory proteins modulate pilus retraction dynamics through interactions with their cognate pilins, resulting in conformational changes, evidence of a physical

interaction between these two proteins is required. The periplasmic domains of PilA<sub>V</sub> and TfpZ will be expressed in *E. coli*, either together from a Duet vector or separately. Using the N-terminal His-tag on PilA<sub>V</sub>, that was previously used for its purification for structural studies, and untagged TfpZ, nickel chromatography followed by gel filtration will be used to detect the potential interaction.

Since the  $\beta$ 3- $\beta$ 4 loop of group III and V PilA was implicated in the interaction between the pilin and the accessory protein, the importance of this region will be tested in *P. aeruginosa*. In existing constructs, pBADGR*pilA<sub>V</sub>* and pBADGR*pilA*tfpZ, the sequence of the  $\beta$ 3- $\beta$ 4 loop will be mutated to that of the group II pilin and complementation of twitching motility and piliation in the group II *pilA* mutant tested, as described previously (11). These data will identify if the  $\beta$ 3- $\beta$ 4 loop of groups III and V pilins is involved in interactions with the cognate accessory protein *in vivo* and supplement the *in vitro* interaction data to characterize the role of the TfpY and TfpZ in pilus retraction dynamics.

#### *Minor pilin-PilY1 interaction studies*

The data presented in Chapters 3 and 4 suggest that the minor pilins form a subcomplex with PilY1. To understand how these proteins come together, interaction studies will be performed on different sets of minor pilin C-terminal domains, using co-affinity purification combined with

gel filtration and western blot analysis of interacting proteins. Any complexes identified will be set up for crystallization, and the structures of any resulting crystals solved to identify interacting regions.

All the truncated minor pilins are soluble and can be purified except for PilX, which was proposed – based on its inability to cross-complement – to be a group specific factor (67). In addition, the expression and purification of full-length PilY1 has also been unsuccessful. As an alternative to purifying truncated minor pilins individually and to also include PilY1 in interaction studies, coexpression of all six full-length proteins will be attempted. An IPTG-inducible plasmid expressing the entire minor pilin operon (112) will be expressed in our *P. aeruginosa* minor pilin operon mutant or in *E. coli* and the products cross-linked with disuccinimidyl suberate (DSS). Proteins that are cross-linked will be identified by Western blot analysis with our specific antibodies and confirmed by mass spectrometry.

#### *Surface localization of PilY1*

Although our data suggest that the minor pilins are required for trafficking of PilY1 to the cell surface (Chapter 3), other groups recently suggested that piliation is dispensable for PilY1 expression on the surface and for PilY1-related regulation of swarming motility or virulence (97, 114, 161). In addition, a *pilX* deletion strain expressed an increased level of

PilY1 on the surface (114) suggesting the minor pilins are not required for its export. These discrepancies need to be resolved, as PilY1 is emerging as a key regulator of *P. aeruginosa* surface-associated virulence and thus a potential drug target.

PilY1 in strain PAO1 was previously been suggested to have a PilD cleavage site (108), which could support its association with pili and the minor pilins; however, this cleavage site is not conserved in other *P. aeruginosa* strains. Instead, the N-terminus of PilY1 appears to have a signal peptidase I site. These putative cleavage sites will be mutated to impair cleavage and strains tested for the presence of PilY1 and the minor pilins PilVWX in the surface fraction by western blot analysis using specific antisera. Processing of PilY1 by SP1 would imply that it is either periplasmic or secreted. A recent study (114) showed that when overexpressed, PilY1 was detected on the surface of mutants lacking the T4P and T2S secretins, suggesting that it is exported by an as-yet unidentified pathway, independent of pilus assembly.

To test if PilY1 can be detected on the cell surface in the absence of the minor pilins, we will overexpress PilY1 from an arabinose inducible plasmid in our minor pilin operon mutant and perform western blot analysis on surface fractions using a specific PilY1 antibody. Similarly, to determine if any pilin proteins are required for PilY1 export, we will make a *pilA*

deletion in a minor pilin operon deletion background, overexpress PilY1, and analyze the surface fraction as above.

### **Significance and Conclusions**

T4P are important virulence factors for *P. aeruginosa*. The combination of distinct alleles and groups of *P. aeruginosa* pilins with their associated accessory proteins plus two distinct sets of minor pilins increases the diversity of T4P in this pathogen. A complete understanding of this diversity and how these proteins function together is crucial for the understanding the T4P system, and may be broadly applicable to other organisms that express T4P, as we showed for example with our structural analysis of PilE and its relation to the *Neisseria* minor pilins PilX<sub>Nm</sub> and PilV<sub>Nm</sub>. Furthermore, since pilins and minor pilins are surface-exposed proteins and thus possible vaccine candidates, the structural and functional data presented in this work will add to the full understanding required for the development of a broadly-protective pilus-based vaccine against *P. aeruginosa*.

## REFERENCES

1. **Aas, F. E., H. C. Winther-Larsen, M. Wolfgang, S. Frye, C. Lovold, N. Roos, J. P. van Putten, and M. Koomey.** 2006. Substitutions in the N-terminal alpha helical spine of *Neisseria gonorrhoeae* pilin affect Type IV pilus assembly, dynamics and associated functions. *Mol. Microbiol.*
2. **Aas, F. E., M. Wolfgang, S. Frye, S. Dunham, C. Lovold, and M. Koomey.** 2002. Competence for natural transformation in *Neisseria gonorrhoeae*: components of DNA binding and uptake linked to type IV pilus expression. *Mol. Microbiol.* **46**:749-760.
3. **Abramoff, M. D., P. J. Magelhaes, and S. J. Ram.** 2004. Image Processing with ImageJ. *Biophotonics International* **11**:36-42.
4. **Adams, P. D., R. W. Grosse-Kunstleve, L. W. Hung, T. R. Ioerger, A. J. McCoy, N. W. Moriarty, R. J. Read, J. C. Sacchettini, N. K. Sauter, and T. C. Terwilliger.** 2002. PHENIX: building new software for automated crystallographic structure determination. *Acta crystallographica. Section D, Biological crystallography* **58**:1948-1954.
5. **Albers, S. V., and M. Pohlschroder.** 2009. Diversity of archaeal type IV pilin-like structures. *Extremophiles : life under extreme conditions* **13**:403-410.

6. **Alm, R. A., J. P. Hallinan, A. A. Watson, and J. S. Mattick.** 1996. Fimbrial biogenesis genes of *Pseudomonas aeruginosa*: *pilW* and *pilX* increase the similarity of type 4 fimbriae to the GSP protein-secretion systems and *pilY1* encodes a gonococcal PilC homologue. *Mol. Microbiol.* **22**:161-173.
7. **Alm, R. A., and J. S. Mattick.** 1995. Identification of a gene, *pilV*, required for type 4 fimbrial biogenesis in *Pseudomonas aeruginosa*, whose product possesses a pre-pilin-like leader sequence. *Mol. Microbiol.* **16**:485-496.
8. **Alm, R. A., and J. S. Mattick.** 1996. Identification of two genes with prepilin-like leader sequences involved in type 4 fimbrial biogenesis in *Pseudomonas aeruginosa*. *J. Bacteriol.* **178**:3809-3817.
9. **Alphonse, S., E. Durand, B. Douzi, B. Waegele, H. Darbon, A. Filloux, R. Voulhoux, and C. Bernard.** 2010. Structure of the *Pseudomonas aeruginosa* XcpT pseudopilin, a major component of the type II secretion system. *Journal of structural biology* **169**:75-80.
10. **Arts, J., R. van Boxtel, A. Filloux, J. Tommassen, and M. Koster.** 2007. Export of the pseudopilin XcpT of the *Pseudomonas aeruginosa* type II secretion system via the signal recognition particle-Sec pathway. *J. Bacteriol.* **189**:2069-2076.

11. **Asikyan, M. L., J. V. Kus, and L. L. Burrows.** 2008. Novel proteins that modulate type IV pilus retraction dynamics in *Pseudomonas aeruginosa*. *J. Bacteriol.* **190**:7022-7034.
12. **Audette, G. F., R. T. Irvin, and B. Hazes.** 2004. Crystallographic analysis of the *Pseudomonas aeruginosa* strain K122-4 monomeric pilin reveals a conserved receptor-binding architecture. *Biochemistry* **43**:11427-11435.
13. **Audette, G. F., E. J. van Schaik, B. Hazes, and R. T. Irvin.** 2004. DNA-Binding Protein Nanotubes: Learning from Nature's Nanotech Examples. *Nano Lett.* **4**:1897.
14. **Ayers, M., P. L. Howell, and L. L. Burrows.** 2010. Architecture of the type II secretion and type IV pilus machineries. *Future microbiology* **5**:1203-1218.
15. **Balakrishna, A. M., A. M. Saxena, H. Y. Mok, and K. Swaminathan.** 2009. Structural basis of typhoid: *Salmonella typhi* type IVb pilin (PilS) and cystic fibrosis transmembrane conductance regulator interaction. *Proteins* **77**:253-261.
16. **Ball, G., E. Durand, A. Lazdunski, and A. Filloux.** 2002. A novel type II secretion system in *Pseudomonas aeruginosa*. *Mol. Microbiol.* **43**:475-485.
17. **Belete, B., H. Lu, and D. J. Wozniak.** 2008. *Pseudomonas aeruginosa* AlgR regulates type IV pilus biosynthesis by activating

transcription of the fimU-pilVWXY1Y2E operon. J. Bacteriol. **190**:2023-2030.

18. **Bernard, C. S., C. Bordi, E. Termine, A. Filloux, and S. de Bentzmann.** 2009. Organization and PprB-dependent control of the *Pseudomonas aeruginosa tad* Locus, involved in Flp pilus biology. J. Bacteriol. **191**:1961-1973.
19. **Berry, J.-L., and V. Pelicic.** 2015. Exceptionally widespread nanomachines composed of type IV pilins: the prokaryotic Swiss Army knives. FEMS Microbiol. Rev. **39**:1-21.
20. **Bitter, W., M. Koster, M. Latijnhouwers, H. de Cock, and J. Tommassen.** 1998. Formation of oligomeric rings by XcpQ and PilQ, which are involved in protein transport across the outer membrane of *Pseudomonas aeruginosa*. Mol. Microbiol. **27**:209-219.
21. **Bleves, S., R. Voulhoux, G. Michel, A. Lazdunski, J. Tommassen, and A. Filloux.** 1998. The secretion apparatus of *Pseudomonas aeruginosa*: identification of a fifth pseudopilin, XcpX (GspK family). Mol. Microbiol. **27**:31-40.
22. **Bodey, G. P., R. Bolivar, V. Fainstein, and L. Jadeja.** 1983. Infections caused by *Pseudomonas aeruginosa*. Reviews of infectious diseases **5**:279-313.

23. **Bohn, Y. S., G. Brandes, E. Rakhimova, S. Horatzek, P. Salunkhe, A. Munder, A. van Barneveld, D. Jordan, F. Bredenbruch, S. Haussler, K. Riedel, L. Eberl, P. O. Jensen, T. Bjarnsholt, C. Moser, N. Hoiby, B. Tummler, and L. Wiehlmann.** 2009. Multiple roles of *Pseudomonas aeruginosa* TBCF10839 PilY1 in motility, transport and infection. *Mol. Microbiol.* **71**:730-747.
24. **Bradley, D. E.** 1974. The adsorption of *Pseudomonas aeruginosa* pilus-dependent bacteriophages to a host mutant with nonretractile pili. *Virology* **58**:149-163.
25. **Bradley, D. E.** 1980. A function of *Pseudomonas aeruginosa* PAO polar pili: twitching motility. *Can J Microbiol* **26**:146-154.
26. **Brissac, T., G. Mikaty, G. Dumenil, M. Coureuil, and X. Nassif.** 2012. The meningococcal minor pilin PilX is responsible for type IV pilus conformational changes associated with signaling to endothelial cells. *Infect. Immun.* **80**:3297-3306.
27. **Brown, D. R., S. Helaine, E. Carbonnelle, and V. Pelicic.** 2010. Systematic functional analysis reveals that a set of seven genes is involved in fine-tuning of the multiple functions mediated by type IV pili in *Neisseria meningitidis*. *Infect. Immun.* **78**:3053-3063.
28. **Burrows, L. L.** 2008. A nice return on the "stalk" exchange. *Structure (London, England : 1993)* **16**:19-20.

29. **Burrows, L. L.** 2012. Prime time for minor subunits of the type II secretion and type IV pilus systems. *Mol. Microbiol.* **86**:765-769.
30. **Burrows, L. L.** 2012. *Pseudomonas aeruginosa* twitching motility: type IV pili in action. *Annu. Rev. Microbiol.* **66**:493-520.
31. **Cachia, P. J., L. M. Glasier, R. R. Hodgins, W. Y. Wong, R. T. Irvin, and R. S. Hodges.** 1998. The use of synthetic peptides in the design of a consensus sequence vaccine for *Pseudomonas aeruginosa*. *The journal of peptide research : official journal of the American Peptide Society* **52**:289-299.
32. **Cachia, P. J., and R. S. Hodges.** 2003. Synthetic peptide vaccine and antibody therapeutic development: prevention and treatment of *Pseudomonas aeruginosa*. *Biopolymers* **71**:141-168.
33. **Campbell, A. P., W. Y. Wong, M. Houston, Jr., F. Schweizer, P. J. Cachia, R. T. Irvin, O. Hindsgaul, R. S. Hodges, and B. D. Sykes.** 1997. Interaction of the receptor binding domains of *Pseudomonas aeruginosa* pili strains PAK, PAO, KB7 and P1 to a cross-reactive antibody and receptor analog: implications for synthetic vaccine design. *J. Mol. Biol.* **267**:382-402.
34. **Campos, M., O. Francetic, and M. Nilges.** 2011. Modeling pilus structures from sparse data. *Journal of structural biology* **173**:436-444.

35. **Campos, M., M. Nilges, D. A. Cisneros, and O. Francetic.** 2010. Detailed structural and assembly model of the type II secretion pilus from sparse data. Proceedings of the National Academy of Sciences of the United States of America **107**:13081-13086.
36. **Carbonnelle, E., S. Helaine, X. Nassif, and V. Pelicic.** 2006. A systematic genetic analysis in *Neisseria meningitidis* defines the Pil proteins required for assembly, functionality, stabilization and export of type IV pili. Mol. Microbiol. **61**:1510-1522.
37. **Carter, M. Q., J. Chen, and S. Lory.** 2010. The *Pseudomonas aeruginosa* Pathogenicity Island PAPI-1 is transferred via a novel Type IV pilus. J. Bacteriol.
38. **Castric, P.** 1995. *pilO*, a gene required for glycosylation of *Pseudomonas aeruginosa* 1244 pilin. Microbiology (Reading, England) **141 ( Pt 5)**:1247-1254.
39. **Castric, P., F. J. Cassels, and R. W. Carlson.** 2001. Structural characterization of the *Pseudomonas aeruginosa* 1244 pilin glycan. J. Biol. Chem. **276**:26479-26485.
40. **Castric, P. A., and C. D. Deal.** 1994. Differentiation of *Pseudomonas aeruginosa* pili based on sequence and B-cell epitope analyses. Infect. Immun. **62**:371-376.

41. **Castric, P. A., H. F. Sidberry, and J. C. Sadoff.** 1989. Cloning and sequencing of the *Pseudomonas aeruginosa* 1244 pilin structural gene. *Molecular & general genetics* : MGG **216**:75-80.
42. **Cehovin, A., P. J. Simpson, M. A. McDowell, D. R. Brown, R. Noschese, M. Pallett, J. Brady, G. S. Baldwin, S. M. Lea, S. J. Matthews, and V. Pelicic.** 2013. Specific DNA recognition mediated by a type IV pilin. *Proceedings of the National Academy of Sciences of the United States of America* **110**:3065-3070.
43. **Cisneros, D. A., P. J. Bond, A. P. Pugsley, M. Campos, and O. Francetic.** 2011. Minor pseudopilin self-assembly primes type II secretion pseudopilus elongation. *The EMBO journal* **31**:1041-1053.
44. **Cisneros, D. A., G. Pehau-Arnaudet, and O. Francetic.** 2012. Heterologous assembly of type IV pili by a type II secretion system reveals the role of minor pilins in assembly initiation. *Mol. Microbiol.* **86**:805-818.
45. **Collins, R. F., L. Davidsen, J. P. Derrick, R. C. Ford, and T. Tonjum.** 2001. Analysis of the PilQ secretin from *Neisseria meningitidis* by transmission electron microscopy reveals a dodecameric quaternary structure. *J. Bacteriol.* **183**:3825-3832.
46. **Collins, R. F., S. A. Frye, A. Kitmitto, R. C. Ford, T. Tonjum, and J. P. Derrick.** 2004. Structure of the *Neisseria meningitidis* outer

membrane PilQ secretin complex at 12 Å resolution. *The Journal of biological chemistry* **279**:39750-39756.

47. **Coureuil, M., H. Lecuyer, M. G. Scott, C. Boularan, H. Enslin, M. Soyer, G. Mikaty, S. Bourdoulous, X. Nassif, and S. Marullo.** 2010. Meningococcus Hijacks a beta2-adrenoceptor/beta-Arrestin pathway to cross brain microvasculature endothelium. *Cell* **143**:1149-1160.
48. **Craig, L., and J. Li.** 2008. Type IV pili: paradoxes in form and function. *Curr. Opin. Struct. Biol.* **18**:267-277.
49. **Craig, L., M. E. Pique, and J. A. Tainer.** 2004. Type IV pilus structure and bacterial pathogenicity. *Nat.Rev.Microbiol.* **2**:363-378.
50. **Craig, L., R. K. Taylor, M. E. Pique, B. D. Adair, A. S. Arvai, M. Singh, S. J. Lloyd, D. S. Shin, E. D. Getzoff, M. Yeager, K. T. Forest, and J. A. Tainer.** 2003. Type IV pilin structure and assembly: X-ray and EM analyses of *Vibrio cholerae* toxin-coregulated pilus and *Pseudomonas aeruginosa* PAK pilin. *Mol. Cell* **11**:1139-1150.
51. **Craig, L., N. Volkmann, A. S. Arvai, M. E. Pique, M. Yeager, E. H. Egelman, and J. A. Tainer.** 2006. Type IV pilus structure by cryo-electron microscopy and crystallography: implications for pilus assembly and functions. *Mol. Cell* **23**:651-662.

52. **de Bentzmann, S., M. Aurouze, G. Ball, and A. Filloux.** 2006. FppA, a novel *Pseudomonas aeruginosa* prepilin peptidase involved in assembly of type IVb pili. *J. Bacteriol.* **188**:4851-4860.
53. **DeLano, W. L.** 2002. *The PyMOL User's Manual.* DeLano Scientific, Palo Alto, CA, USA.
54. **Douzi, B., E. Durand, C. Bernard, S. Alphonse, C. Cambillau, A. Filloux, M. Tegoni, and R. Voulhoux.** 2009. The XcpV/Gspl pseudopilin has a central role in the assembly of a quaternary complex within the T2SS pseudopilus. *The Journal of biological chemistry* **284**:34580-34589.
55. **Durand, E., A. Bernadac, G. Ball, A. Lazdunski, J. N. Sturgis, and A. Filloux.** 2003. Type II protein secretion in *Pseudomonas aeruginosa*: the pseudopilus is a multifibrillar and adhesive structure. *J. Bacteriol.* **185**:2749-2758.
56. **Durand, E., G. Michel, R. Voulhoux, J. Kurner, A. Bernadac, and A. Filloux.** 2005. XcpX controls biogenesis of the *Pseudomonas aeruginosa* XcpT-containing pseudopilus. *The Journal of biological chemistry* **280**:31378-31389.
57. **Edgar, R. C.** 2004. MUSCLE: multiple sequence alignment with high accuracy and high throughput. *Nucleic Acids Res.* **32**:1792-1797.

58. **Emsley, P., and K. Cowtan.** 2004. Coot: model-building tools for molecular graphics. *Acta crystallographica. Section D, Biological crystallography* **60**:2126-2132.
59. **Folkhard, W., D. A. Marvin, T. H. Watts, and W. Paranchych.** 1981. Structure of polar pili from *Pseudomonas aeruginosa* strains K and O. *J. Mol. Biol.* **149**:79-93.
60. **Forest, K. T.** 2008. The type II secretion arrowhead: the structure of GspI-GspJ-GspK. *Nat. Struct. Mol. Biol.* **15**:428-430.
61. **Forest, K. T., S. A. Dunham, M. Koomey, and J. A. Tainer.** 1999. Crystallographic structure reveals phosphorylated pilin from *Neisseria*: phosphoserine sites modify type IV pilus surface chemistry and fibre morphology. *Mol. Microbiol.* **31**:743-752.
62. **Francetic, O., N. Buddelmeijer, S. Lewenza, C. A. Kumamoto, and A. P. Pugsley.** 2007. Signal recognition particle-dependent inner membrane targeting of the PulG Pseudopilin component of a type II secretion system. *J. Bacteriol.* **189**:1783-1793.
63. **Fussenegger, M., T. Rudel, R. Barten, R. Ryll, and T. F. Meyer.** 1997. Transformation competence and type-4 pilus biogenesis in *Neisseria gonorrhoeae*--a review. *Gene* **192**:125-134.
64. **Giltner, C. L., M. Habash, and L. L. Burrows.** 2010. *Pseudomonas aeruginosa* minor pilins are incorporated into the type IV pilus. *J. Mol. Biol.* **398**:444-461.

65. **Giltner, C. L., M. Habash, and L. L. Burrows.** 2010.  
*Pseudomonas aeruginosa* minor pilins are incorporated into type IV pili. *J. Mol. Biol.* **398**:444-461.
66. **Giltner, C. L., Y. Nguyen, and L. L. Burrows.** 2012. Type IV pilin proteins: versatile molecular modules. *Microbiology and molecular biology reviews* : MMBR **76**:740-772.
67. **Giltner, C. L., N. Rana, M. N. Lunardo, A. Q. Hussain, and L. L. Burrows.** 2011. Evolutionary and functional diversity of the *Pseudomonas* type IVa pilin island. *Environ. Microbiol.* **13**:250-264.
68. **Giltner, C. L., E. J. van Schaik, G. F. Audette, D. Kao, R. S. Hodges, D. J. Hassett, and R. T. Irvin.** 2006. The *Pseudomonas aeruginosa* type IV pilin receptor binding domain functions as an adhesin for both biotic and abiotic surfaces. *Mol. Microbiol.* **59**:1083-1096.
69. **Hartung, S., A. S. Arvai, T. Wood, S. Kolappan, D. S. Shin, L. Craig, and J. A. Tainer.** 2011. Ultrahigh resolution and full-length pilin structures with insights for filament assembly, pathogenic functions, and vaccine potential. *The Journal of biological chemistry* **286**:44254-44265.
70. **Harvey, H., M. Habash, F. Aidoo, and L. L. Burrows.** 2009.  
Single-residue changes in the C-terminal disulfide-bonded loop of

- the *Pseudomonas aeruginosa* type IV pilin influence pilus assembly and twitching motility. *J. Bacteriol.* **191**:6513-6524.
71. **Hazes, B., P. A. Sastry, K. Hayakawa, R. J. Read, and R. T. Irvin.** 2000. Crystal structure of *Pseudomonas aeruginosa* PAK pilin suggests a main-chain-dominated mode of receptor binding. *J. Mol. Biol.* **299**:1005-1017.
72. **Hegge, F. T., P. G. Hitchen, F. E. Aas, H. Kristiansen, C. Lovold, W. Egge-Jacobsen, M. Panico, W. Y. Leong, V. Bull, M. Virji, H. R. Morris, A. Dell, and M. Koomey.** 2004. Unique modifications with phosphocholine and phosphoethanolamine define alternate antigenic forms of *Neisseria gonorrhoeae* type IV pili. *Proceedings of the National Academy of Sciences of the United States of America* **101**:10798-10803.
73. **Heiniger, R. W., H. C. Winther-Larsen, R. J. Pickles, M. Koomey, and M. C. Wolfgang.** 2010. Infection of human mucosal tissue by *Pseudomonas aeruginosa* requires sequential and mutually dependent virulence factors and a novel pilus-associated adhesin. *Cell. Microbiol.* **12**:1158-1173.
74. **Helaine, S., E. Carbonnelle, L. Prouvensier, J. L. Beretti, X. Nassif, and V. Pelicic.** 2005. PilX, a pilus-associated protein essential for bacterial aggregation, is a key to pilus-facilitated

- attachment of *Neisseria meningitidis* to human cells. *Mol. Microbiol.* **55**:65-77.
75. **Helaine, S., D. H. Dyer, X. Nassif, V. Pelicic, and K. T. Forest.** 2007. 3D structure/function analysis of PilX reveals how minor pilins can modulate the virulence properties of type IV pili. *Proceedings of the National Academy of Sciences of the United States of America* **104**:15888-15893.
76. **Hobbs, M., and J. S. Mattick.** 1993. Common components in the assembly of type 4 fimbriae, DNA transfer systems, filamentous phage and protein-secretion apparatus: a general system for the formation of surface-associated protein complexes. *Mol. Microbiol.* **10**:233-243.
77. **Holm, L., and P. Rosenstrom.** 2010. Dali server: conservation mapping in 3D. *Nucleic Acids Res.* **38**:W545-549.
78. **Holm, L., and C. Sander.** 1993. Protein structure comparison by alignment of distance matrices. *J. Mol. Biol.* **233**:123-138.
79. **Imam, S., Z. Chen, D. S. Roos, and M. Pohlschroder.** 2011. Identification of surprisingly diverse type IV pili, across a broad range of gram-positive bacteria. *PLoS one* **6**:e28919.
80. **Imhaus, A. F., and G. Dumenil.** 2014. The number of *Neisseria meningitidis* type IV pili determines host cell interaction. *EMBO J.* **33**:1767-1783.

81. **Jacobs, M. A., A. Alwood, I. Thaipisuttikul, D. Spencer, E. Haugen, S. Ernst, O. Will, R. Kaul, C. Raymond, R. Levy, L. Chun-Rong, D. Guenther, D. Bovee, M. V. Olson, and C. Manoil.** 2003. Comprehensive transposon mutant library of *Pseudomonas aeruginosa*. Proceedings of the National Academy of Sciences of the United States of America **100**:14339-14344.
82. **Johnson, M. D., C. K. Garrett, J. E. Bond, K. A. Coggan, M. C. Wolfgang, and M. R. Redinbo.** 2011. *Pseudomonas aeruginosa* PilY1 binds integrin in an RGD- and calcium-dependent manner. PloS one **6**:e29629.
83. **Jonsson, A. B., J. Pfeifer, and S. Normark.** 1992. *Neisseria gonorrhoeae* PilC expression provides a selective mechanism for structural diversity of pili. Proceedings of the National Academy of Sciences of the United States of America **89**:3204-3208.
84. **Jude, B. A., and R. K. Taylor.** 2011. The physical basis of type 4 pilus-mediated microcolony formation by *Vibrio cholerae* O1. Journal of structural biology **175**:1-9.
85. **Kachlany, S. C., P. J. Planet, R. Desalle, D. H. Fine, D. H. Figurski, and J. B. Kaplan.** 2001. *flp-1*, the first representative of a new pilin gene subfamily, is required for non-specific adherence of *Actinobacillus actinomycetemcomitans*. Mol. Microbiol. **40**:542-554.

86. **Kao, D. J., M. E. Churchill, R. T. Irvin, and R. S. Hodges.** 2007. Animal protection and structural studies of a consensus sequence vaccine targeting the receptor binding domain of the type IV pilus of *Pseudomonas aeruginosa*. *J. Mol. Biol.* **374**:426-442.
87. **Kao, D. J., and R. S. Hodges.** 2009. Advantages of a synthetic peptide immunogen over a protein immunogen in the development of an anti-pilus vaccine for *Pseudomonas aeruginosa*. *Chemical biology & drug design* **74**:33-42.
88. **Karimova, G., J. Pidoux, A. Ullmann, and D. Ladant.** 1998. A bacterial two-hybrid system based on a reconstituted signal transduction pathway. *Proceedings of the National Academy of Sciences of the United States of America* **95**:5752-5756.
89. **Karimova, G., A. Ullmann, and D. Ladant.** 2001. Protein-protein interaction between *Bacillus stearothermophilus* tyrosyl-tRNA synthetase subdomains revealed by a bacterial two-hybrid system. *J. Mol. Microbiol. Biotechnol.* **3**:73-82.
90. **Keizer, D. W., C. M. Slupsky, M. Kalisiak, A. P. Campbell, M. P. Crump, P. A. Sastry, B. Hazes, R. T. Irvin, and B. D. Sykes.** 2001. Structure of a pilin monomer from *Pseudomonas aeruginosa*: implications for the assembly of pili. *J. Biol. Chem.* **276**:24186-24193.

91. **Kelley, L. A., and M. J. Sternberg.** 2009. Protein structure prediction on the Web: a case study using the Phyre server. *Nature protocols* **4**:363-371.
92. **Kennan, R. M., O. P. Dhungyel, R. J. Whittington, J. R. Egerton, and J. I. Rood.** 2001. The type IV fimbrial subunit gene (*fimA*) of *Dichelobacter nodosus* is essential for virulence, protease secretion, and natural competence. *J. Bacteriol.* **183**:4451-4458.
93. **Kohler, R., K. Schafer, S. Muller, G. Vignon, K. Diederichs, A. Philippsen, P. Ringler, A. P. Pugsley, A. Engel, and W. Welte.** 2004. Structure and assembly of the pseudopilin PulG. *Mol. Microbiol.* **54**:647-664.
94. **Kolappan, S., J. Roos, A. S. Yuen, O. M. Pierce, and L. Craig.** 2012. Structural characterization of CFA/III and Longus type IVb pili from enterotoxigenic *Escherichia coli*. *J. Bacteriol.* **194**:2725-2735.
95. **Korotkov, K. V., M. D. Gray, A. Kreger, S. Turley, M. Sandkvist, and W. G. Hol.** 2009. Calcium is essential for the major pseudopilin in the type 2 secretion system. *J. Biol. Chem.* **284**:25466-25470.
96. **Korotkov, K. V., and W. G. Hol.** 2008. Structure of the GspK-GspL-GspJ complex from the enterotoxigenic *Escherichia coli* type 2 secretion system. *Nat. Struct. Mol. Biol.* **15**:462-468.
97. **Kuchma, S. L., A. E. Ballok, J. H. Merritt, J. H. Hammond, W. Lu, J. D. Rabinowitz, and G. A. O'Toole.** 2010. Cyclic-di-GMP-

- mediated repression of swarming motility by *Pseudomonas aeruginosa*: the pilY1 gene and its impact on surface-associated behaviors. *J. Bacteriol.* **192**:2950-2964.
98. **Kuchma, S. L., E. F. Griffin, and G. A. O'Toole.** 2012. Minor pilins of the type IV pilus system participate in the negative regulation of swarming motility. *J. Bacteriol.* **194**:5388-5403.
99. **Kuo, W. W., H. W. Kuo, C. C. Cheng, H. L. Lai, and L. Y. Chen.** 2005. Roles of the minor pseudopilins, XpsH, XpsI and XpsJ, in the formation of XpsG-containing pseudopilus in *Xanthomonas campestris* pv. *campestris*. *J. Biomed. Sci.* **12**:587-599.
100. **Kus, J. V., J. Kelly, L. Tessier, H. Harvey, D. G. Cvitkovitch, and L. L. Burrows.** 2008. Modification of *Pseudomonas aeruginosa* Pa5196 type IV Pilins at multiple sites with D-Araf by a novel GT-C family Arabinosyltransferase, TfpW. *J. Bacteriol.* **190**:7464-7478.
101. **Kus, J. V., E. Tullis, D. G. Cvitkovitch, and L. L. Burrows.** 2004. Significant differences in type IV pilin allele distribution among *Pseudomonas aeruginosa* isolates from cystic fibrosis (CF) versus non-CF patients. *Microbiology (Reading, England)* **150**:1315-1326.
102. **Larkin, M. A., G. Blackshields, N. P. Brown, R. Chenna, P. A. McGettigan, H. McWilliam, F. Valentin, I. M. Wallace, A. Wilm, R. Lopez, J. D. Thompson, T. J. Gibson, and D. G. Higgins.**

2007. Clustal W and Clustal X version 2.0. *Bioinformatics* (Oxford, England) **23**:2947-2948.
103. **Laskowski, R. A., M. W. MacArthur, D. S. Moss, and J. M. Thornton.** 1993. PROCHECK: A program to check the stereochemical quality of protein structures. *J. Appl. Cryst.* **26**:283-291.
104. **Lautrop, H.** 1961. *Bacterium anitratum* transferred to the genus *Cytophaga*. *Int.Bull.Bacteriol.Nomenclature* **11**::107-108.
105. **Lee, K. K., H. B. Sheth, W. Y. Wong, R. Sherburne, W. Paranchych, R. S. Hodges, C. A. Lingwood, H. Krivan, and R. T. Irvin.** 1994. The binding of *Pseudomonas aeruginosa* pili to glycosphingolipids is a tip-associated event involving the C-terminal region of the structural pilin subunit. *Mol. Microbiol.* **11**:705-713.
106. **Leighton, T. L., R. Buensuceso, P. L. Howell, and L. L. Burrows.** 2015. Biogenesis of *Pseudomonas aeruginosa* type IV pili and regulation of their function. *Environ. Microbiol.*
107. **Leighton, T. L., N. Dayalani, L. M. Sampaleanu, P. L. Howell, and L. L. Burrows.** 2015. A novel role for PilNO in type IV pilus retraction revealed by alignment subcomplex mutations. *J. Bacteriol.*
108. **Lewenza, S., J. L. Gardy, F. S. Brinkman, and R. E. Hancock.** 2005. Genome-wide identification of *Pseudomonas aeruginosa*

- exported proteins using a consensus computational strategy combined with a laboratory-based PhoA fusion screen. *Genome Res.* **15**:321-329.
109. **Li, J., E. H. Egelman, and L. Craig.** 2012. Structure of the *Vibrio cholerae* Type IVb Pilus and stability comparison with the *Neisseria gonorrhoeae* type IVa pilus. *J. Mol. Biol.* **418**:47-64.
110. **Li, J., M. S. Lim, S. Li, M. Brock, M. E. Pique, V. L. Woods, Jr., and L. Craig.** 2008. *Vibrio cholerae* toxin-coregulated pilus structure analyzed by hydrogen/deuterium exchange mass spectrometry. *Structure (London, England : 1993)* **16**:137-148.
111. **Lim, M. S., D. Ng, Z. Zong, A. S. Arvai, R. K. Taylor, J. A. Tainer, and L. Craig.** 2010. *Vibrio cholerae* El Tor TcpA crystal structure and mechanism for pilus-mediated microcolony formation. *Mol. Microbiol.* **77**:755-770.
112. **Lizewski, S. E., J. R. Schurr, D. W. Jackson, A. Frisk, A. J. Carterson, and M. J. Schurr.** 2004. Identification of AlgR-regulated genes in *Pseudomonas aeruginosa* by use of microarray analysis. *J. Bacteriol.* **186**:5672-5684.
113. **Lu, H. M., S. T. Motley, and S. Lory.** 1997. Interactions of the components of the general secretion pathway: role of *Pseudomonas aeruginosa* type IV pilin subunits in complex

- formation and extracellular protein secretion. *Mol. Microbiol.* **25**:247-259.
114. **Luo, Y., K. Zhao, A. E. Baker, S. L. Kuchma, K. A. Coggan, M. C. Wolfgang, G. C. Wong, and G. A. O'Toole.** 2015. A Hierarchical Cascade of Second Messengers Regulates *Pseudomonas aeruginosa* Surface Behaviors. *mBio* **6**.
115. **Lyczak, J. B., C. L. Cannon, and G. B. Pier.** 2000. Establishment of *Pseudomonas aeruginosa* infection: lessons from a versatile opportunist. *Microbes and infection / Institut Pasteur* **2**:1051-1060.
116. **Lyczak, J. B., C. L. Cannon, and G. B. Pier.** 2002. Lung infections associated with cystic fibrosis. *Clin. Microbiol. Rev.* **15**:194-222.
117. **Maier, B., L. Potter, M. So, H. S. Seifert, and M. P. Sheetz.** 2002. Single pilus motor forces exceed 100 pN. *Proceedings of the National Academy of Sciences of the United States of America* **99**:16012-16017.
118. **Mattick, J. S.** 2002. Type IV pili and twitching motility. *Annu. Rev. Microbiol.* **56**:289-314.
119. **Mattick, J. S., C. B. Whitchurch, and R. A. Alm.** 1996. The molecular genetics of type-4 fimbriae in *Pseudomonas aeruginosa*-- a review. *Gene* **179**:147-155.
120. **McCoy, A. J., R. W. Grosse-Kunstleve, P. D. Adams, M. D. Winn, L. C. Storoni, and R. J. Read.** 2007. Phaser

- crystallographic software. *Journal of applied crystallography* **40**:658-674.
121. **Melville, S., and L. Craig.** 2013. Type IV pili in Gram-positive bacteria. *Microbiology and molecular biology reviews : MMBR* **77**:323-341.
122. **Merz, A. J., M. So, and M. P. Sheetz.** 2000. Pilus retraction powers bacterial twitching motility. *Nature* **407**:98-102.
123. **Mignot, T., and J. R. Kirby.** 2008. Genetic circuitry controlling motility behaviors of *Myxococcus xanthus*. *Bioessays* **30**:733-743.
124. **Mikaty, G., M. Soyer, E. Mairey, N. Henry, D. Dyer, K. T. Forest, P. Morand, S. Guadagnini, M. C. Prevost, X. Nassif, and G. Dumenil.** 2009. Extracellular bacterial pathogen induces host cell surface reorganization to resist shear stress. *PLoS Path.* **5**:e1000314.
125. **Morand, P. C., P. Tattevin, E. Eugene, J. L. Beretti, and X. Nassif.** 2001. The adhesive property of the type IV pilus-associated component PilC1 of pathogenic *Neisseria* is supported by the conformational structure of the N-terminal part of the molecule. *Mol. Microbiol.* **40**:846-856.
126. **Murray, T. S., M. Egan, and B. I. Kazmierczak.** 2007. *Pseudomonas aeruginosa* chronic colonization in cystic fibrosis patients. *Current opinion in pediatrics* **19**:83-88.

127. **Nassif, X., J. L. Beretti, J. Lowy, P. Stenberg, P. O'Gaora, J. Pfeifer, S. Normark, and M. So.** 1994. Roles of pilin and PilC in adhesion of *Neisseria meningitidis* to human epithelial and endothelial cells. Proceedings of the National Academy of Sciences of the United States of America **91**:3769-3773.
128. **Ng, S. Y., J. Wu, D. B. Nair, S. M. Logan, A. Robotham, L. Tessier, J. F. Kelly, K. Uchida, S. Aizawa, and K. F. Jarrell.** 2011. Genetic and mass spectrometry analyses of the unusual type IV-like pili of the archaeon *Methanococcus maripaludis*. J. Bacteriol. **193**:804-814.
129. **Nguyen, Y., S. G. Jackson, F. Aidoo, M. Junop, and L. L. Burrows.** 2010. Structural characterization of novel *Pseudomonas aeruginosa* type IV pilins. J. Mol. Biol. **395**:491-503.
130. **Nguyen, Y., S. Sugiman-Marangos, H. Harvey, S. D. Bell, C. L. Charlton, M. S. Junop, and L. L. Burrows.** 2015. *Pseudomonas aeruginosa* Minor Pilins Prime Type IVa Pilus Assembly and Promote Surface Display of the PilY1 Adhesin. J. Biol. Chem. **290**:601-611.
131. **Nunn, D., S. Bergman, and S. Lory.** 1990. Products of three accessory genes, *pilB*, *pilC*, and *pilD*, are required for biogenesis of *Pseudomonas aeruginosa* pili. J. Bacteriol. **172**:2911-2919.

132. **Nunn, D. N., and S. Lory.** 1993. Cleavage, methylation, and localization of the *Pseudomonas aeruginosa* export proteins XcpT, -U, -V, and -W. *J. Bacteriol.* **175**:4375-4382.
133. **Nunn, D. N., and S. Lory.** 1991. Product of the *Pseudomonas aeruginosa* gene pilD is a prepilin leader peptidase. *Proceedings of the National Academy of Sciences of the United States of America* **88**:3281-3285.
134. **O'Toole, G. A., and R. Kolter.** 1998. Flagellar and twitching motility are necessary for *Pseudomonas aeruginosa* biofilm development. *Mol. Microbiol.* **30**:295-304.
135. **Orans, J., M. D. Johnson, K. A. Coggan, J. R. Sperlazza, R. W. Heiniger, M. C. Wolfgang, and M. R. Redinbo.** 2010. Crystal structure analysis reveals *Pseudomonas* PilY1 as an essential calcium-dependent regulator of bacterial surface motility. *Proceedings of the National Academy of Sciences of the United States of America* **107**:1065-1070.
136. **Ottow, J. C.** 1975. Ecology, physiology, and genetics of fimbriae and pili. *Annu. Rev. Microbiol.* **29**:79-108.
137. **Otwinowski, Z., and W. Minor.** 1997. Processing of X-ray diffraction data collected in the oscillation mode. *Methods Enzymol.* **276**:307.

138. **Parge, H. E., K. T. Forest, M. J. Hickey, D. A. Christensen, E. D. Getzoff, and J. A. Tainer.** 1995. Structure of the fibre-forming protein pilin at 2.6 Å resolution. *Nature* **378**:32-38.
139. **Pasloske, B. L., A. M. Joffe, Q. Sun, K. Volpel, W. Paranchych, F. Eftekhar, and D. P. Speert.** 1988. Serial isolates of *Pseudomonas aeruginosa* from a cystic fibrosis patient have identical pilin sequences. *Infect. Immun.* **56**:665-672.
140. **Pasloske, B. L., D. G. Scraba, and W. Paranchych.** 1989. Assembly of mutant pilins in *Pseudomonas aeruginosa*: formation of pili composed of heterologous subunits. *J. Bacteriol.* **171**:2142-2147.
141. **Pellicic, V.** 2008. Type IV pili: e pluribus unum? *Mol. Microbiol.* **68**:827-837.
142. **Petersen, T. N., S. Brunak, G. von Heijne, and H. Nielsen.** 2011. SignalP 4.0: discriminating signal peptides from transmembrane regions. *Nat. Methods* **8**:785-786.
143. **Piepenbrink, K. H., G. A. Maldarelli, C. F. de la Pena, G. L. Mulvey, G. A. Snyder, L. De Masi, E. C. von Rosenvinge, S. Gunther, G. D. Armstrong, M. S. Donnenberg, and E. J. Sundberg.** 2014. Structure of *Clostridium difficile* PilJ exhibits unprecedented divergence from known type IV pilins. *J. Biol. Chem.* **289**:4334-4345.

144. **Piepenbrink, K. H., G. A. Maldarelli, C. F. Martinez de la Pena, T. C. Dingle, G. L. Mulvey, A. Lee, E. von Rosenvinge, G. D. Armstrong, M. S. Donnenberg, and E. J. Sundberg.** 2015. Structural and Evolutionary Analyses Show Unique Stabilization Strategies in the Type IV Pili of *Clostridium difficile*. *Structure* **23**:385-396.
145. **Pugsley, A. P.** 1993. The complete general secretory pathway in gram-negative bacteria. *Microbiol Rev* **57**:50-108.
146. **Pugsley, A. P.** 1993. Processing and methylation of PulG, a pilin-like component of the general secretory pathway of *Klebsiella oxytoca*. *Mol. Microbiol.* **9**:295-308.
147. **Qutyan, M., M. Henkel, J. Horzempa, M. Quinn, and P. Castric.** 2010. Glycosylation of pilin and nonpilin protein constructs by *Pseudomonas aeruginosa* 1244. *J. Bacteriol.* **192**:5972-5981.
148. **Raghunathan, K., F. S. Vago, D. Grindem, T. Ball, W. J. Wedemeyer, M. Bagdasarian, and D. N. Arvidson.** 2014. The 1.59Å resolution structure of the minor pseudopilin EpsH of *Vibrio cholerae* reveals a long flexible loop. *Biochimica et biophysica acta* **1844**:406-415.
149. **Ramboarina, S., P. J. Fernandes, S. Daniell, S. Islam, P. Simpson, G. Frankel, F. Booy, M. S. Donnenberg, and S. Matthews.** 2005. Structure of the bundle-forming pilus from

- enteropathogenic *Escherichia coli*. J. Biol. Chem. **280**:40252-40260.
150. **Reardon, P. N., and K. T. Mueller.** 2013. Structure of the type IVa major pilin from the electrically conductive bacterial nanowires of *Geobacter sulfurreducens*. J. Biol. Chem. **288**:29260-29266.
151. **Reguera, G., K. D. McCarthy, T. Mehta, J. S. Nicoll, M. T. Tuominen, and D. R. Lovley.** 2005. Extracellular electron transfer via microbial nanowires. Nature **435**:1098-1101.
152. **Rudel, T., D. Facius, R. Barten, I. Scheuerpflug, E. Nonnenmacher, and T. F. Meyer.** 1995. Role of pili and the phase-variable PilC protein in natural competence for transformation of *Neisseria gonorrhoeae*. Proceedings of the National Academy of Sciences of the United States of America **92**:7986-7990.
153. **Rudel, T., I. Scheuerpflug, and T. F. Meyer.** 1995. *Neisseria* PilC protein identified as type-4 pilus tip-located adhesin. Nature **373**:357-359.
154. **Russell, M. A., and A. Darzins.** 1994. The *pilE* gene product of *Pseudomonas aeruginosa*, required for pilus biogenesis, shares amino acid sequence identity with the N-termini of type 4 prepilin proteins. Mol. Microbiol. **13**:973-985.

155. **Saiman, L., K. Ishimoto, S. Lory, and A. Prince.** 1990. The effect of piliation and exoproduct expression on the adherence of *Pseudomonas aeruginosa* to respiratory epithelial monolayers. *J. Infect. Dis.* **161**:541-548.
156. **Sali, A., and T. L. Blundell.** 1993. Comparative protein modelling by satisfaction of spatial restraints. *J. Mol. Biol.* **234**:779-815.
157. **Sastry, P. A., B. B. Finlay, B. L. Pasloske, W. Paranchych, J. R. Pearlstone, and L. B. Smillie.** 1985. Comparative studies of the amino acid and nucleotide sequences of pilin derived from *Pseudomonas aeruginosa* PAK and PAO. *J. Bacteriol.* **164**:571-577.
158. **Sauvonnet, N., G. Vignon, A. P. Pugsley, and P. Gounon.** 2000. Pilus formation and protein secretion by the same machinery in *Escherichia coli*. *EMBO J.* **19**:2221-2228.
159. **Schmidt, S. A., D. Bieber, S. W. Ramer, J. Hwang, C. Y. Wu, and G. Schoolnik.** 2001. Structure-function analysis of BfpB, a secretin-like protein encoded by the bundle-forming-pilus operon of enteropathogenic *Escherichia coli*. *J. Bacteriol.* **183**:4848-4859.
160. **Semmler, A. B., C. B. Whitchurch, and J. S. Mattick.** 1999. A re-examination of twitching motility in *Pseudomonas aeruginosa*. *Microbiology (Reading, England)* **145 ( Pt 10)**:2863-2873.

161. **Siryaporn, A., S. L. Kuchma, G. A. O'Toole, and Z. Gitai.** 2014. Surface attachment induces *Pseudomonas aeruginosa* virulence. Proceedings of the National Academy of Sciences of the United States of America **111**:16860-16865.
162. **Skerker, J. M., and H. C. Berg.** 2001. Direct observation of extension and retraction of type IV pili. Proceedings of the National Academy of Sciences of the United States of America **98**:6901-6904.
163. **Smedley, J. G., 3rd, E. Jewell, J. Roguskie, J. Horzempa, A. Syboldt, D. B. Stolz, and P. Castric.** 2005. Influence of pilin glycosylation on *Pseudomonas aeruginosa* 1244 pilus function. Infect. Immun. **73**:7922-7931.
164. **Spangenberg, C., R. Fislage, W. Sierralta, B. Tummler, and U. Romling.** 1995. Comparison of type IV-pilin genes of *Pseudomonas aeruginosa* of various habitats has uncovered a novel unusual sequence. FEMS Microbiol. Lett. **125**:265-273.
165. **Stephens, D. S., A. M. Whitney, J. Rothbard, and G. K. Schoolnik.** 1985. Pili of *Neisseria meningitidis*. Analysis of structure and investigation of structural and antigenic relationships to gonococcal pili. J. Exp. Med. **161**:1539-1553.

166. **Stone, B. J., and Y. A. Kwaik.** 1999. Natural competence for DNA transformation by *Legionella pneumophila* and its association with expression of type IV pili. *J. Bacteriol.* **181**:1395-1402.
167. **Strom, M. S., and S. Lory.** 1991. Amino acid substitutions in pilin of *Pseudomonas aeruginosa*. Effect on leader peptide cleavage, amino-terminal methylation, and pilus assembly. *J. Biol. Chem.* **266**:1656-1664.
168. **Strom, M. S., and S. Lory.** 1993. Structure-function and biogenesis of the type IV pili. *Annu. Rev. Microbiol.* **47**:565-596.
169. **Strom, M. S., D. Nunn, and S. Lory.** 1991. Multiple roles of the pilus biogenesis protein pilD: involvement of pilD in excretion of enzymes from *Pseudomonas aeruginosa*. *J. Bacteriol.* **173**:1175-1180.
170. **Strom, M. S., D. N. Nunn, and S. Lory.** 1993. A single bifunctional enzyme, PilD, catalyzes cleavage and N-methylation of proteins belonging to the type IV pilin family. *Proceedings of the National Academy of Sciences of the United States of America* **90**:2404-2408.
171. **Szabo, Z., A. O. Stahl, S. V. Albers, J. C. Kissinger, A. J. Driessen, and M. Pohlschroder.** 2007. Identification of diverse archaeal proteins with class III signal peptides cleaved by distinct archaeal prepilin peptidases. *J. Bacteriol.* **189**:772-778.

172. **Takahashi, H., T. Yanagisawa, K. S. Kim, S. Yokoyama, and M. Ohnishi.** 2012. Meningococcal PilV potentiates *Neisseria meningitidis* type IV pilus-mediated internalization into human endothelial and epithelial cells. *Infect. Immun.* **80**:4154-4166.
173. **Tinsley, C. R., R. Voulhoux, J. L. Beretti, J. Tommassen, and X. Nassif.** 2004. Three homologues, including two membrane-bound proteins, of the disulfide oxidoreductase DsbA in *Neisseria meningitidis*: effects on bacterial growth and biogenesis of functional type IV pili. *J. Biol. Chem.* **279**:27078-27087.
174. **Tweedy, J. M., R. W. Park, and W. Hodgkiss.** 1968. Evidence for the presence of fimbriae (pili) on *Vibrio* species. *Journal of general microbiology* **51**:235-244.
175. **Varga, J. J., V. Nguyen, D. K. O'Brien, K. Rodgers, R. A. Walker, and S. B. Melville.** 2006. Type IV pili-dependent gliding motility in the Gram-positive pathogen *Clostridium perfringens* and other *Clostridia*. *Mol. Microbiol.* **62**:680-694.
176. **Vargas, M., N. S. Malvankar, P. L. Tremblay, C. Leang, J. A. Smith, P. Patel, O. Snoeyenbos-West, K. P. Nevin, and D. R. Lovley.** 2013. Aromatic amino acids required for pili conductivity and long-range extracellular electron transport in *Geobacter sulfurreducens*. *mBio* **4**:e00105-00113.

177. **Vignon, G., R. Kohler, E. Larquet, S. Giroux, M. C. Prevost, P. Roux, and A. P. Pugsley.** 2003. Type IV-like pili formed by the type II secretin: specificity, composition, bundling, polar localization, and surface presentation of peptides. *J. Bacteriol.* **185**:3416-3428.
178. **Voisin, S., J. V. Kus, S. Houliston, F. St-Michael, D. Watson, D. G. Cvitkovitch, J. Kelly, J. R. Brisson, and L. L. Burrows.** 2007. Glycosylation of *Pseudomonas aeruginosa* strain Pa5196 type IV pilins with mycobacterium-like alpha-1,5-linked d-Araf oligosaccharides. *J. Bacteriol.* **189**:151-159.
179. **Weiss, R. L.** 1971. The structure and occurrence of pili (fimbriae) on *Pseudomonas aeruginosa*. *Journal of general microbiology* **67**:135-143.
180. **Whitchurch, C. B., M. Hobbs, S. P. Livingston, V. Krishnapillai, and J. S. Mattick.** 1991. Characterisation of a *Pseudomonas aeruginosa* twitching motility gene and evidence for a specialised protein export system widespread in eubacteria. *Gene* **101**:33-44.
181. **Wiehlmann, L., G. Wagner, N. Cramer, B. Siebert, P. Gudowius, G. Morales, T. Kohler, C. van Delden, C. Weinel, P. Slickers, and B. Tummeler.** 2007. Population structure of *Pseudomonas aeruginosa*. *Proceedings of the National Academy of Sciences of the United States of America* **104**:8101-8106.

182. **Winsor, G. L., D. K. Lam, L. Fleming, R. Lo, M. D. Whiteside, N. Y. Yu, R. E. Hancock, and F. S. Brinkman.** 2011. *Pseudomonas* Genome Database: improved comparative analysis and population genomics capability for *Pseudomonas* genomes. *Nucleic Acids Res.* **39**:D596-600.
183. **Winther-Larsen, H. C., F. T. Hegge, M. Wolfgang, S. F. Hayes, J. P. van Putten, and M. Koomey.** 2001. *Neisseria gonorrhoeae* PilV, a type IV pilus-associated protein essential to human epithelial cell adherence. *Proceedings of the National Academy of Sciences of the United States of America* **98**:15276-15281.
184. **Winther-Larsen, H. C., M. Wolfgang, S. Dunham, J. P. van Putten, D. Dorward, C. Lovold, F. E. Aas, and M. Koomey.** 2005. A conserved set of pilin-like molecules controls type IV pilus dynamics and organelle-associated functions in *Neisseria gonorrhoeae*. *Mol. Microbiol.* **56**:903-917.
185. **Wolfgang, M., H. S. Park, S. F. Hayes, J. P. van Putten, and M. Koomey.** 1998. Suppression of an absolute defect in type IV pilus biogenesis by loss-of-function mutations in pilT, a twitching motility gene in *Neisseria gonorrhoeae*. *Proceedings of the National Academy of Sciences of the United States of America* **95**:14973-14978.

186. **Wolfgang, M., J. P. van Putten, S. F. Hayes, and M. Koomey.**  
1999. The *comP* locus of *Neisseria gonorrhoeae* encodes a type IV prepilin that is dispensable for pilus biogenesis but essential for natural transformation. *Mol. Microbiol.* **31**:1345-1357.
187. **Xu, X. F., Y. W. Tan, L. Lam, J. Hackett, M. Zhang, and Y. K. Mok.** 2004. NMR structure of a type IVb pilin from *Salmonella typhi* and its assembly into pilus. *The Journal of biological chemistry* **279**:31599-31605.
188. **Yanez, M. E., K. V. Korotkov, J. Abendroth, and W. G. Hol.**  
2008. The crystal structure of a binary complex of two pseudopilins: EpsI and EpsJ from the type 2 secretion system of *Vibrio vulnificus*. *J. Mol. Biol.* **375**:471-486.
189. **Yanez, M. E., K. V. Korotkov, J. Abendroth, and W. G. Hol.**  
2008. Structure of the minor pseudopilin EpsH from the Type 2 secretion system of *Vibrio cholerae*. *J. Mol. Biol.* **377**:91-103.
190. **Zhang, H. Z., and M. S. Donnenberg.** 1996. DsbA is required for stability of the type IV pilin of enteropathogenic *Escherichia coli*. *Mol. Microbiol.* **21**:787-797.